CLARIFYING THE ROLE OF WILDFIRES AND PERMAFROST THAW IN THE BROWNIFICATION OF A SHALLOW BOREAL LAKE USING PALEOLIMNOLOGICAL ANALYSES OF DIATOM ASSEMBLAGE CHANGE

THOMAS WU

A THESIS SUBMITTED TO THE FACULTY OF GRADUATE STUDIES IN PARTIAL FULFILLMENT OF THE REQUIREMENTS FOR THE DEGREE OF MASTER OF SCIENCE

GRADUATE PROGRAM IN GEOGRAPHY
YORK UNIVERSITY
TORONTO, ONTARIO

September 2025

Abstract:

Permafrost thaw in discontinuous permafrost peatlands has been linked to enhanced export of chromophoric dissolved organic matter (cDOM) into lakes, reducing water clarity through 'lake brownification'. In the Dehcho region (Northwest Territories, Canada), diatom (siliceous algae, Class Bacillariophyceae) assemblages in small, shallow lakes have been shown to be structured along a cDOM gradient, indicating that lake brownification can be inferred from subfossil diatoms in lake sediment cores. This thesis presents the results of a diatom-based paleolimnological study of a small, shallow Dehcho lake covering the last ~300 years. Results indicate a shift beginning circa ~1920s from epiphytic and large-sized diatom taxa characteristic of low cDOM lakes (*Denticula kuetzingii*, *Navicula*) towards increased abundance of *Pseudostaurosira brevistriata* and *Stauroforma exiguiformis* associated with higher cDOM. The timing of this shift coincided with an anomalous sediment geochemical signature potentially indicative of a drought or wildfire that likely initiated an accelerated loss of permafrost.

Acknowledgements:

The development of this graduate thesis involved a series of unfortunate events, equipment malfunctions, and health challenges that would be dismissed by most editors as being too absurd for the most fantastical novels, and its completion could not have occurred without many people to whom I would like to thank for their support. Firstly, I would like to thank my supervisor Dr. Jennifer B. Korosi for her support and encouragement, as well as her patience, which surpasses that of most saints, and I am not certain if there are any words to describe how grateful I am for the many opportunities you have provided me to expand my skills academically and scientifically. While our experiences might not have always resulted in the ideal outcome, they are a reminder that even the non-successes are an important part of science.

I would also like to extend my gratitude to Dr. Joshua Thienpont, and Dr. Sapna Sharma, who both provided incredibly insightful advice and feedback, not only during my graduate journey, but throughout my academic career in general. This thesis would not have been possible without Dr. Thienpont's mentorship in the practical applications of paleolimnology, which previously had been wholly theoretical to me. It would also not have been possible without Dr. Sharma, as my understanding of statistics and data management, and my presentation and visualisation skills are a direct product of her teachings.

I would also like to acknowledge the support given to me from past and current members of the Limnology and Paleoenvironmental Research Group (LPRG). The very premise behind this thesis is that it is a continuation of the work previously published by two former lab colleagues, Dr. Kristen Coleman, and Rachael Abulu, as part of their doctoral dissertation and M.Sc. respectively, and thus includes and references data from their research. Special thanks should also be given to Amanda Little, Rachel Pelligrino, Victori Carroll, Sorin Gruia, and Asli Yusuf, as without your help I surely would not have survived the agony of 10+ hours of waiting for my samples to finish reacting to their treatments, nor would I have understood the vast mysteries of applying heat to permanently seal my microscopy slides. I would also like to acknowledge the support from fellow colleagues, and the staff and faculty members at York University, such as Aman Basu, Ratiba Munir, Patrick Mojdehi, Anne Ralph, Dr. Kathy Young, Dr. Richard Bello, Dr. Tarmo Remmel, Dr. Adeyemi Olusola, who made my academic journey possible. I hope all of you are granted everything you ever wanted in your – and more!

Additionally, I would like to extend my heartfelt gratitude towards the Tthets'éhk'edélî (Jean Marie River) and Łíídlįį Kų́ę́ (Fort Simpson) First Nations, as it is on their traditional lands and territories that the materials and data used in this thesis were obtained, and analysis of which was done in the spirit of peaceably caretaking Turtle Island together. I look forward to the day on which I will have the opportunity to share what we've learned, to return that knowledge to where its true home has always been. Similarly, I recognize that York University, the institution with which I am affiliated with, and under which I conducted this thesis project, sits on the traditional territories that were and still are home to, many First Nations groups, including the Anishinabek Nation, the Haudenosaunee Confederacy, and the Huron-Wendat, and who continue to take care of the Great Lakes region together.

Last but not least, I must thank my family, who are currently driving me insane, but I could not have done any of this without you.

Table of Contents

List of Figures

List of Tables

CHAPTER ONE: INTRODUCTION

1.1. Background

Between 1979 – 2021, the circumpolar north has warmed ~0.73°C decade^{-1} on average, 3-4 times faster than the average global rate (~0.19°C decade^{-1}) over the same time frame (Rantanen et al., 2022). As temperatures rise, environments across northern Canada will experience altered precipitation patterns and increased lightning strikes (Bintanja, 2019; Bintanja & Andry, 2017; Veraverbeke et al., 2017), reduced seasonal snow cover (Chasmer & Hopkinson, 2017), and changes in vegetation cover (Vitt, et al., 2000; Box et al., 2019). These recent climate and environmental changes have increased the frequency and severity of wildfires (Wang et al., 2015; Veraverbeke et al., 2017; Hanes et al., 2019), and together, may be driving accelerations in permafrost thaw across northern Canada (Gibson et al., 2018; 2021; Wright et al., 2022).

Among the areas considered especially vulnerable to widespread permafrost thaw are the discontinuous permafrost peatlands of the Dehcho region, Northwest Territories, which straddle the boundary between sporadic and extensive discontinuous permafrost in northwestern Canada (AMAP, 2017), as well as being host to globally significant carbon stocks via vast peat deposits (Hugelius et al. 2020). Here, temperatures are relatively warm (~0 °C), with the discontinuous permafrost persisting (Halsey et al., 1995; Quinton et al., 2018), largely only due to the insulating provided by the peat-rich terrain (Du et al., 2021; Holloway & Lewkowicz, 2020). However, climate-warming since the 1970s, combined with environmental changes like increased wildfires, may be accelerating rates of permafrost thaw (Gibson et al., 2018; Helbig et al., 2016; Quinton et al., 2018). Decreases in areal of permafrost patches by 55% - 36% have already been reported throughout the southern boreal subarctic over the last half century

(Holloway et al., 2020; Quinton et al., 20158), with some projections suggesting much of the discontinuous permafrost peatlands of the Dehcho could be permafrost-free by 2050 (Kurylyk et al., 2016; Chasmer et al., 2017; Spence et al., 2020; Gibson et al., 2021).

Rapid permafrost degradation throughout the Dehcho region will intensify thermokarst (i.e. thawing of ice-rich permafrost) processes, resulting in the subsidence of forested peat plateaus and the expansion of adjacent wetlands and lakes (Olefeldt et al., 2021; Carpino et al., 2021). This can enhance hydrological connectivity and drainage across the watershed (Connon et al., 2014; Chasmer et al., 2017), increase runoff (Connon et al., 2014; Haynes et al., 2018) and groundwater flow (Kurylyk et al., 2016), and potentially mobilize carbon and nutrients stored in the peat-rich terrain by permafrost into nearby aquatic ecosystems (Olefeldt et al., 2013; Burd et al., 2020; Heffernan et al., 2024). Elsewhere, increased in-lake concentrations of terrestrially derived dissolved organic matter (DOM) and iron (Fe), have been implicated as the cause behind recent increases in water colour (brownification) in many lakes across the northern hemisphere (Weyhenmeyer et al., 2014; de Wit et al., 2016; Björnerås et al. 2017; Wauthy et al., 2018).

Lake brownification is of considerable interest to conservation and ecological management as it can alter water quality and critical ecosystem services in affected lakes in a variety of interacting pathways (Horppila et al., 2024; Blanchet et al., 2022). For example, reduced light availability in brownified lakes can limit primary production (Karlsson et al. 2009; Stetler et al., 2021), which can impact the quantity and quality of nutrition at higher trophic levels (Creed et al., 2018; Taipale et al., 2016; 2018). Reduced light penetration can also enhance stratification and contribute to hypoxia on the lake bottom, further impacting lake productivity and biogeochemical function (Brothers et al., 2014; Williams et al., 2016). Additionally, as DOM can often form complexes with contaminants (Oni et al., 2013; Al-Amin et al., 2024), brownification may increase in-lake concentrations of heavy metals and other toxins, which can create challenges for drinking water treatment (Oni et al., 2013; Wällstedt et al., 2010; Lavonen et al., 2013; Ritson et al., 2014). Increases in in-lake DOM may also impact carbon cycling, specifically enhancing rates of carbon mineralization, which may have globally significant consequences (Lapierre et al., 2013; Cory et al., 2014; Allesson et al., 2018). However, the precise drivers of brownification often vary regionally, and its dynamics remain uncertain in small boreal wetlands and lakes such as those of the Dehcho (Kritzberg et al., 2020; Coleman et al., 2023; 2025). Climate-driven permafrost thaw in boreal peat-rich landscapes, and the resultant increased downstream export of DOM may increase instances of brownification in small lakes across the Dehcho, significantly impacting local water resources, and their associated ecosystems and communities (Christensen, 2015), necessitating continued monitoring and study.

Brownification and other water quality changes which impact light availability in lakes can be tracked using paleolimnological techniques (Korosi et al., 2015; Tichá et al., 2023; Coleman et al., 2023; 2025). Paleolimnology refers to a broad range of multi-disciplinary scientific tools that analyze geophysical, chemical, and biological proxies preserved in lake sediments to reconstruct past trends in climates and environments (Watson et al., 2021). Diatoms are a type of microalgae widely used in paleolimnology as bioindicators due to their siliceous cell walls that preserve well (Battarbee et al., 2001), as well as their high sensitivity to environmental changes like changes in water clarity and light availability due to brownification (Rühland et al., 2015; Gushulak & Cumming, 2020). Shifts in the abundance of diatom taxa sensitive to water clarity changes may thus be useful in reconstructing historical water quality trends and could help identify the drivers potentially responsible for brownification in the small lakes of the Dehcho.

1.2. Study Rationale and Significance

This thesis focused on a small (~1.17 km^2) shallow (~1.9 m depth) lake unofficially referred to as SC11 (61°20'25.1"N, 120°57'48.3"W) located northeast of Tthets'éhk'e' (McGill Lake), the westernmost of the Five Fish Lakes (Łue Túé Sųlái) of the Dehcho region in the traditional territory of the Tthets'éhk'edélî First Nation (Figure 1). SC11 is close to the southern boundary of extensive discontinuous permafrost (AMAP, 2017; Figure 1B.), and adjacent to the Scotty Creek Basin, a site of active long-term research on permafrost thaw and wetland thermokarst landscape changes (Quinton et al., 2018).

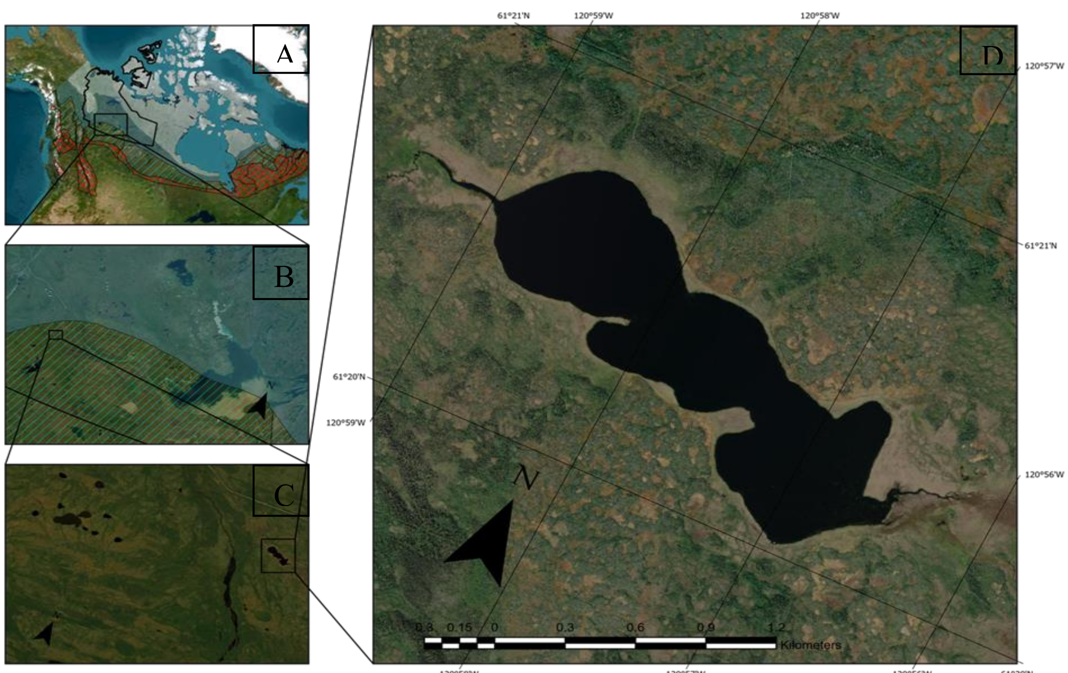

Figure 1. (A): Approximate position of SC11 within Canada with the territorial morphology of the Northwest Territories indicated by a black border, overlaid with the extent of permafrost, according to the 5th edition of the National Atlas of Canada, surveyed from 1978 to 1995. Regions with isolated patches of permafrost (<10%), are indicated in red 10% crosshatching; regions with sporadic discontinuous permafrost (10 – 50%) are in blue 10% simple hatching; regions with extensive discontinuous permafrost (50 – 90%) are in light blue; regions with continuous permafrost (90 – 100%) are in pale blue; (B): Approximate location of SC11 within the southern Northwest Territories, Canada, relative to Great Slave Lake, close to the boundary between sporadic (blue 10% simple hatching) and extensive permafrost (blue); (C): Location of SC11 relative to Scotty Creek Basin, and McGill Lake of the Five Fish Lakes; (D): SC11, Dehcho region, Northwest Territories, Canada, in true colour imagery provided by World Imagery in ArcGIS Pro with 2021 census boundary divisions from Statistics Canada.

In an earlier "top-bottom" (i.e., 1850 versus present-day; see Cumming et al., 1992) assessment of diatom assemblage changes in the Dehcho region, SC11 was identified as one of only a few known lakes that exhibited an increase in the abundance of small benthic *Fragilariaceae* diatoms, which have been previously identified as potentially indicative of lake browning (Korosi et al., 2015; Coleman et al., 2025). An analysis of the sediment geochemistry of SC11 identified a period of anomalously low concentrations of percent organic carbon in the 8.25 cm depth (Abulu 2024), which may correspond to a historical forest fire in the region spoken of by Dehcho Elders *circa* 1920 (J. Korosi, personal communication). I hypothesize that the anomalous decrease in organic carbon concentrations, may be linked to this historical wildfire, the occurrence of which, also immediately preceded the increase in benthic *Fragilariaceae*. As it is well established that forest fires accelerate permafrost thaw in the Dehcho (Gibson et al., 2018), the long-term landscape change effects may have eventually precipitated in the potential brownification and associated reduced water clarity observed at SC11 (Wauthy et al., 2018).

My MSc research tests this hypothesis by examining diatom subfossil assemblage changes at high temporal resolution in a dated sediment core from SC11. Reconstructing a paleoenvironmental record of brownification at SC11 will help to contextualize how lakes in the Dehcho region are responding to fire-stimulated permafrost thaw and landscape changes relative to pre-industrial historical trends. This will provide a more complete history of water quality changes at SC11, continuing efforts by Coleman et al., (2025) and complement the results of Abulu, (2024), to understand how permafrost thaw may be altering water quality and carbon cycling pathways in the small shallow boreal lakes of the Dehcho.

1.3. Research Questions

My research questions are:

1) What is the paleoenvironmental history of diatom assemblages and diversity at SC11 over the past few hundred years; when did assemblage shifts occur, and which taxa were the primary drivers of assemblage shifts and differences between assemblages? In particular, when and how did the diatom assemblage at SC11 evolve towards greater dominance by low-clarity tolerant diatom taxa such as small benthic *Fragilariaceae*.
2) How does the timing of shifts in diatom assemblage composition at SC11 compare to previously established trends in organic carbon and C:N ratios; more specifically did the shift towards low-clarity diatom taxa, coincide with the timing of the low-carbon anomaly *circa* 1920?

CHAPTER TWO: LITERATURE REVIEW

2.1. Carbon cycling and climate change in a rapidly warming northern Canada

As of 2023, global average atmospheric concentrations of carbon dioxide (CO_2) reached 419.3 ppm (~888.92 Pg C), ~50% greater than pre-industrial (i.e. prior to 1750) levels (~278 ppm; ~589.36 Pg C) (Friedlingstein et al., 2023). Increasing concentrations of greenhouse gases due to human activities, particularly CO_2, have led to ever larger proportions of longwave radiation being retained by the Earth's geophysical systems (Lacis et al., 2010), an atmospheric warming phenomenon known as the greenhouse effect, due to its similarities with how the glass surfaces of a greenhouse trap heat (Arrhenius, 1897). This relatively rapid increase in CO_2 and other greenhouse gases (over the past ~250 years), and the associated temperature increases, are comparatively massive and abrupt changes on a geological scale, as current concentrations of CO_2 and other greenhouse gases, have not occurred on Earth for millions of years (Lear et al., 2021; IPCC, 2021). Though there have been similar historical phases of elevated CO_2 concentrations and temperatures throughout the geological record, almost all such periods reached these states gradually over multiple millennia, as opposed to current anthropogenic warming at decadal to centennial timescales (Lear et al., 2021; Judd et al., 2024). As past conditions with comparable levels of CO_2 are associated with environments radically different to modern conditions (e.g. substantially smaller ice caps, sea levels 6 – 20 m higher than current levels, and more severe wildfire activity; Miller et al. 2012; Dumitru et al. 2019; Gaboriau et al., 2020), unprecedented levels of carbon inputs in modern times (Friedlingstein et al., 2023), will lead to rapid and extreme changes to many ecosystems across the globe (IPCC, 2021).

Although climate change is a global phenomenon, rapid climate warming and its associated impacts are not occurring uniformly across the globe, with regions in the circumpolar north experiencing the fastest rates of surface temperature warming compared to anywhere else on Earth (Post et al., 2019; IPCC, 2021). For example, one estimate by Rantanen et al., (2022) suggested that between 1979 – 2021, different regions of the Arctic (i.e. anywhere above > 60°N), were warming anywhere from 3 – 7 times faster than the mean global rate (~0.19 °C/decade). These geographical disparities in warming generally intensified along a latitudinal gradient, with the northernmost regions (i.e. those directly adjacent to the Arctic Ocean like the archipelago of Novaya Zemlaya), found to be warming much faster than more southerly regions (Rantanen et al., 2022). Notably these are also substantially faster rates compared to previous estimates of climate warming in the Arctic (e.g. ~2x the global average), with warming projected to further accelerate in the next few decades (Post et al., 2019; Rantanen et al., 2022).

This substantial difference in magnitude of current rates of warming in the north compared to rates in lower latitudes is referred to as the recent Arctic amplification effect and is controlled by multiple processes (Rantanen et al., 2022), with some of the most important ones being inefficiencies in radiative cooling to space due to lapse-rate feedback effects (Pithan & Mauritsen, 2014; Stuecker et al., 2018), albedo-feedback effects (Dai et al., 2019; Brown et al., 2010), seasonal temperature inversions (Bintanja et al., 2011), and oceanic and atmospheric heat transport (Serreze et al., 2011; Walsh et al., 2014). However, there has yet to be full consensus on the precise contribution of each mechanism to the Arctic amplification effect, due to disagreements over which areas are considered part of the Arctic, and the relevancy of each mechanism across different regions (Rantanen et al., 2022).

The especially rapid rate of warming in circumpolar regions is due to these processes and feedback mechanisms being enhanced by the effects of the recent increases in atmospheric CO_2 concentrations; the most well-known mechanism being impacted in this manner are albedo climate-feedback effects, in which climate warming induces long-term declines in highly-reflective sea ice extent and thickness and terrestrial snow cover by extending the melt season during summer and autumn while shortening the growth season during winter (Serreze et al., 2011; Brown et al., 2010; Chasmer et al., 2017). This then exposes the comparatively darker open ocean and terrain to even greater insolation, resulting in a positive feedback loop of increased energy retention and melting of sea ice and snow cover with each passing year (Perovich et al., 2007). A significant portion of the heat driving recent declines in sea ice and snow cover is also from non-local sources; as atmospheric CO_2 concentrations increase, more climate-warmed parcels of air and seawater from more equatorial latitudes are being advected northwards via horizontal (i.e. as opposed to vertical heat transport like convection through the atmosphere) poleward transport (Yang et al., 2010; Ting et al., 2009), and has been a major cause of much of the recent losses in sea ice (Bengtsson et al., 2004). More recent research has also shown that CO_2 driven warming is also enhancing evaporative processes and altering atmospheric currents, leading to intensified storms and more extreme weather that may be carrying more water vapour polewards which could further drive increased warming and other climatic and environmental changes in the north (Francis et al., 2012; Saha et al., 2023).

As large parts of the circumpolar north also serve as a substantial sink for atmospheric carbon and thus have over millennia accrued a vast reserve of soil carbon preserved only by the cold climate and the unique geographical characteristics of the permafrost-rich landscape (Hugelius et al., 2020; Holloway et al., 2020), there is substantial concern that the recent amplified warming could jeopardize this store of paleo-carbon, and release it to the atmosphere as greenhouse gases emissions, potentially further accelerating climate warming (Harris et al., 2022). In this thesis, we focused on the impacts of recent rapid climate warming and its environmental impacts like increased wildfire activity on the forested permafrost peatlands of the Canadian boreal subarctic, which may be at particular risk of undergoing rapid widespread permafrost thaw and associated landscape changes (Quinton et al., 2018; Gibson et al., 2018; Carpino et al., 2018; 2021; Wright et al., 2022), and the potential consequences for the carbon cycling of this region. More specifically, we focused on one particular aspect of the carbon cycling of this region; the potential for much of that terrestrial carbon to be exported into downstream lakes and other water bodies (Wauthy et al., 2018; Heffernan, et al., 2024), where it could have significant ecological and water quality effects (Vonk et al., 2015; Campeau et al., 2022; Xing et al, 2024; Räike et al., 2024), including possibly being an important driver of the recent brownification of several lakes (Wauthy et al., 2018; Blanchet et al., 2022; Coleman et al., 2023), which can enhance in-lake carbon mineralization and outgassing of potent greenhouse gases like CO_2 and methane (CH_4) (Lapierre et al., 2013; Saros et al., 2025). This necessitates understanding how the potential mobilization of one of the largest carbon reservoirs on Earth could affect carbon processing in northern lakes if there is to be effective action tackling climate change and its effects on water quality in the north (Harris et al., 2022; Blanchet et al., 2022).

2.2. Climate change in the permafrost peatlands of the Canadian boreal subarctic

2.2.1. What is the Canadian boreal subarctic

The boreal subarctic, or boreal zone refers to a vast circumpolar region roughly occupying the 50° – 70°N latitudes of the northern hemisphere, representing a transitional zone between the more temperate latitudes to the south, and the true, or High Arctic to the north (Brandt et al., 2009). One of Earth's largest biomes (~1.89 billion ha), the global boreal zone stretches across multiple circumpolar polities (e.g. Norway, Sweden, Finland, Russia, Canada; Brandt et al., 2009), and includes a broad range of landcovers, including grasslands, wetlands, and lakes, a large portion of which is also underlain by permafrost (Brandt et al., 2009; Price et al., 2013). However, the boreal subarctic is principally characterized by its extensive forests (primarily coniferous) and woodland (i.e. forest cover with mixed-use covers like farmland) landcovers (Brandt et al., 2009), as well as subarctic climate (i.e. short, moderately warm and humid summers with long snowy winters; Baldocchi et al., 2000). Hence, the boreal subarctic is also often referred to as the boreal forest, snow forest, or taiga (Hoffmann, 1958; Viereck, 1975).

The boreal forest is one of the most important biomes on Earth, providing a variety of ecosystem services, such as raw materials (e.g. lumber), as well as being host to many important sources of water for local communities (Brandt et al., 2009; Vonk et al., 2015; Christensen, 2015). However, in the context of climate change, the most important service provided by the global boreal forest is its role as an immense carbon sink making it an important regulator of the global climate system (Chapin III et al., 2000; Kurz et al., 2013; Bradshaw & Warkentin, 2015; Pan et al., 2024). This is because the boreal forest generally intakes more atmospheric carbon by photosynthesis than is released via plant respiration and heterotrophy, which then becomes part of its biomass and soils. Due to the cold subarctic climate, and often anoxic soils, decomposition is significantly slowed, preventing this accumulated carbon from being released back to the atmosphere, and over millennia, this has resulted in certain areas of the boreal forest developing substantial carbon accumulations (Kurz et al., 2013; Potapov et al., 2017; Harris et al., 2022), though estimates have varied widely for exactly how much carbon is stored in the boreal forest and its soils in literature (e.g. 264.9 – 1715.8 Pg C; Bradshaw & Warkentin, 2015; Pan et al., 2024). However, rapid climate warming and its environmental consequences, particularly increased wildfires are leading to significant decreases in the functioning of the boreal subarctic as a carbon sink; for example, Pan et al., 2024 estimated that between 1990 – 2019, annual rates of sequestration dropped from 508 ± 63 Tg C year^{-1} to 324 ± 41 Tg C yr^{-1}. Moreover, this decrease in carbon sequestration capacity has been occurring geographically unevenly, with the boreal forests of North America recently being declared a carbon source and thus in need of substantial monitoring (Bond-Laberty et al., 2007; Turetsky et al., 2011; Pan et al., 2024).

The North American component of the boreal forest represents a substantial portion (~28%) of the global boreal zone (Brandt et al., 2013). Most of it lies within Canada, where it constitutes ~55% (552 million ha) of the nation's total surface area, from the border between Alaska and the Yukon Territories in the west, to Newfoundland and Labrador on the east coast (Gros et al., 2023). Despite the vast extent of the Canadian boreal subarctic, its ecological diversity is limited to only a few species, owing to its relative youth, and having begun to develop only within the past 15 – 16 000 years ago, as the glacial ice caps that once covered most of North America began to retreat (Brandt et al., 2009). More specifically, these species are those that migrated northwards from refugia south of the retreating Laurentide sheet, as well as those that can survive the harsh subarctic conditions (Gauthier et al., 2015; Liang et al., 2022).

These include primarily conifers but also a few cold tolerant (i.e. able to survive 40 °C or lower) deciduous species (Brandt et al., 2009; Williams et al., 2004). Common conifers in the North American boreal forest include the white (*Picea glauca*), and black spruces (*P. mariana*), firs (*Abies balsamea, A. lasiocarpa* etc.), tamarack (*Larix laricina*), and various pine (*Pinus*) species (Brandt et al., 2009). Studies of pollen macrofossils indicate that *P. glauca* and *P. mariana*, the dominant conifers of the North American boreal forest, are thought to have expanded to their current transcontinental ranges from Pleistocene refugia located in New England (Lindbladh et al., 2007; Payette et al., 2022). Similarly, the Jack Pine (*Pinus banksiana*), was once originally limited to refugia located in central and southeastern USA (i.e. Missouri and Georgia), during the Pleistocene, but has since expanded its range northwards to their current distributions in Quebec and as far northwest as Great Bear Lake in the Northwest Territories (Payette et al., 2022). The spatial distribution of trees in the boreal forest is that of a mosaic of irregularly shaped patches or stands, often containing either only coniferous species, or only deciduous species, and only sometimes containing a mix (Weir et al., 2000). Other common species are those that can similarly survive the harsh climate, such as low growing shrubs, and ferns and fungi which produce spores that germinate only during warmer months (Robinson, 2001), as well as mosses and lichen which can self-desiccate to hibernate (Turetsky et al., 2012).

The geomorphology of the North American boreal forest is relatively young (Brandt et al., 2009), being characterized by generally undeveloped soils which are poor in key inorganic nutrients like nitrogen and phosphorus, despite being rich in organic matter from the detritus of ubiquitous coniferous trees (Maynard et al., 2014). This is partially because the cold subarctic climate strongly inhibits microbial decay (Kyaschenko et al, 2019), preventing any organic detritus from breaking down into nutrients to be returned to the forest floor (Brovkin et al., 2012;

Deluca & Boisvenue, 2012). Moreover, what few nutrients are available, are instead usually retained by fungi and microbes for their own use, rather than made accessible to larger plants and trees as typical in more temperate climates (Hensgens et al., 2020; Högberg et al., 2017; Clemmensen et al., 2014). Another reason why the soils of the Canadian boreal forest are so nutrient poor is that they are also often quite acidic, which can inhibit microbial decomposition and nutrient cycling, especially of nitrogen (Shen et al., 2021). The low soil pH was once commonly attributed to the organic acids found in coniferous needles but is now considered to be more likely derived from leachates released by *Sphagnum* spp. mosses common to the boreal forest undergrowth (Turetsky et al., 2012; Burgess-Conforti et al., 2019).

2.2.2. Fire as an ecological and environmental process in the Canadian boreal forest

Another important characteristic of the Canadian boreal forest is its frequent, and often severe forest fires (Stocks et al, 2002). On average, ~2 million hectares (Mha) are burned in the Canadian boreal forest on an annual basis due to fire activity, though the exact area varies considerably from year to year, with occasional large outliers such as in 1989, during which ~7 Mha of forest were burned (Stocks et al, 2002; Hanes et al., 2019). Most recently in 2023, a particularly devastating record high 15 Mha of forested lands in northwest Canada were burnt (Jain et al., 2024), during which in addition to the substantial loss of carbon sequestering capacity, several lives were extinguished, hundreds of homes and critical infrastructure were destroyed, and the resultant smoke reached communities as far as the east coast, causing significant health complications (Jain et al., 2024; Wang et al., 2024). However, despite its calamitous nature, fire is a necessary component to the ecology and geography of the Canadian boreal forest and has shaped its ongoing evolution since its formation began with the retreat of the Laurentide ice sheets (Anyomi et al., 2022; McLauchlan et al., 2020).

To be precise, when discussing fire in the boreal forest as an ecological and environmental process, we are referring to a type of recurring disturbance which cyclically destroys a large area of the boreal forest ecosystem every few decades (de Groot et al., 2013). We further distinguish between small (i.e. area burned <200 ha) fires, which are easily put out, as opposed to large (i.e. area burned >200 ha) fires or 'wildfires', which are often uncontrolled (Stocks et al, 2002; Shulski & Wendler, 2007). Though wildfires only make up a small fraction (~3%) of all fire activity in the boreal forest they are responsible for 90% of all areas burned (Stocks et al, 2002; Shulski & Wendler, 2007; Hanes et al., 2019), and it is wildfires which are the ecologically significant force we refer to when discussing fire in the boreal forest (Stocks et al, 2002; Hanes et al., 2019).

For example, fire is an essential catalyst in the natural cycle of succession and regeneration in the Canadian boreal landscape; periodic burns remove dead and dying trees and clear the canopy for younger and healthier saplings to recolonize recently burned areas (Anyomi et al., 2022; Figure 2.). This process is so integral to the geography of the boreal forest that it is responsible for the characteristic mosaic of stands that typifies tree spatial distributions in the Canadian boreal forest, as the result of fires burning out different areas at different times, creating patches of forests at different succession stages (Weir et al., 2000; Erni et al., 2017; Figure 2.). Some coniferous species that are common to the Canadian boreal forest, such as *Pinus banksiana*, *P. contorta var. latifolia*, and *Picea mariana* even rely upon the periodic, though infrequent (i.e. repeating at multi-decadal to multi-centurial scales) occurrence of fire to reproduce, as their seeds can only be released from the protective cone after being burned

(Sharpe et al., 2017; Edwards et al., 2015; Reid et al., 2023). The process of fire-catalyzed succession results in conifer-dominated stands that represent old-growth end-stage climax communities being cyclically replaced by a mix of younger coniferous saplings, and deciduous species (Figure 2.). The latter consist primarily of wind dispersed pioneers such as those from the genera *Betula*, *Popululus*, and *Salix*, but can also include species like *P. tremuloides* which have adapted specifically to endure fires by being able to resprout new shoots from burned stumps (Bond-Lamberty et al., 2007; Tsuyuzaki et al., 2014; Anoszko et al., 2022).

The resultant deciduous domination of the post-fire boreal stand can last for decades to centuries and can take more than a decade just to recover 10% of its previous canopy cover (Bartels et al., 2016). The relative slowness of boreal succession, and specifically the regeneration of the coniferous dominated climax community is attributable to many factors, including that the immediate and long-term post-fire conditions are usually far better suited to deciduous species than the original coniferous community (Tsuyuzaki et al., 2014; Mack et al., 2021). For example, post-fire soils are less acidic (González-Pérez et al., 2004; Certini et al., 2005; Agbeshie et al., 2022), and the microclimate is drier due to the opened canopy and more climatically polarized (up to 0.27 °C warmer in summer and 0.07 °C cooler in winter) (Wolf et al., 2021; Helbig et al., 2024). Additionally, many boreal conifers, such as *Picea mariana*, can only grow in acidic conditions which are the result of mosses like *Sphagnum* spp., that themselves can take decades to grow back to pre-fire conditions and first require a transition to shade usually provided by matured deciduous pioneer trees (Turetsky et al., 2012; Anyomi et al., 2022). Fire can also shift soil bacterial and fungal diversity (Su et al., 2022), towards species that may inhibit conifer regeneration in post-fire stands, further contributing to the length of fire recovery time (Whitman et al., 2019; Day et al., 2020).

Although delayed ecological recoveries are often viewed negatively, the relative slowness (>30 years at minimum) of secondary succession in the Canadian boreal forest is natural, and even necessary for recovering to its former conifer-dominated state (Terrier et al., 2013). For example, deciduous trees often have thicker bark and lack the characteristic flammable resins of coniferous species (Popović et al., 2021); consequently, they are substantially less flammable compared to conifers (Park et al., 2024). The comparatively more fire resistant deciduous-dominated post-fire boreal stand, has thus historically provided sufficient buffering time for emerging conifer saplings to survive and reach reproductive maturity (30 – 40 years), before the next fire outbreak (Terrier et al., 2013).

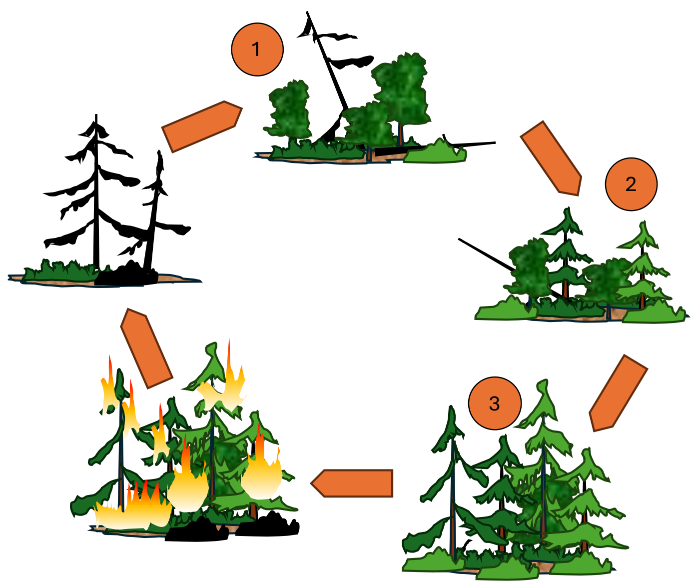

Figure 2. Mosaic cycle of fire-catalyzed succession in the Canadian boreal forest. (1) represents a stand in the boreal forest some time after a fire, in the initial stages of succession with increased deciduous cover; (2) represents a stand in the intermediate stage of succession, with deciduous pioneers beginning to give way to conifers; (3) represents a climax-stage stand, dominated by conifers and which will inevitably be disrupted by a wildfire to return to the stage of succession indicated in (1).

Wildfires also play an essential role in the biogeochemical cycling of nutrients (i.e. carbon, nitrogen, phosphorus, calcium, magnesium, potassium, and silicon), in the boreal forest (McLauchlan et al., 2020; Agbeshie et al., 2022), being a major mechanism by which they are recycled from organic detritus, and without which they would otherwise remain largely sequestered on the cold subarctic boreal forest floor (Eckdahl et al., 2023). Combustion converts still-living biomass (ex. trees, undergrowth, herbaceous plants etc.), as well as organic matter in soils like litter, detritus, and humus (i.e. decayed organic matter, usually heavily colored), into pyrogenic material (i.e. ash and charcoal; Pelligrini et al., 2018). This renders nutrients that would have otherwise been trapped in biomass much more labile and alters the environment to encourage nutrient uptake and assimilation (Agbeshie et al., 2022; Eckdahl et al., 2023).

For example, exposure to fire can mineralize organic compounds (e.g. phosphates become orthophosphate; compounds containing trace metals like calcium, magnesium, potassium, and sodium, will form oxides or exchangeable free cations), which may be comparatively more bioavailable (Souza-Alonso et al., 2024; Agbeshie et al., 2022). The resultant nutrient-enriched ash and charcoal is typically deposited as a thin (~0.5 cm) layer of finer particles (ash being particulate, and charcoal is at least more fragmented) in the soil profile, which due to its higher proportion of negatively charged binding sites, attracts the liberated cations (Bodí et al., 2014). This reduces nutrient leaching by adsorbing them to the ash-enriched soil, increasing the concentration of labile nutrients in the surficial soils relative to pre-fire conditions (Mroz et al., 1980; Granath et al., 2020), while also encouraging root growth, as the finer texture enables them to more easily access nutrients deeper in the soil profile (Lynch et al., 2021). Furthermore, because the extreme heat of a forest fire can denature the organic acids responsible for the characteristically low pH of boreal soils (González-Pérez et al., 2004; Certini et al., 2005), and the ash can contain trace metals that can neutralize H+ ions present (e.g. potassium, calcium, and magnesium), post-fire soils often become more alkaline following a fire (Bodi et al., 2014; Agbeshie et al., 2022), further encouraging microbial respiration and decay

(Shen et al., 2021), and driving nutrient accessibility and cycling (Makoto & Koike, 2021; Ibáñez et al., 2022; Agbeshie et al., 2022). However, the immediate impacts of wildfires and ash deposition on nutrient availability in the boreal forest floor, tend to last no more than one to two growing seasons (Grogan et al., 2000; Eckdahl et al., 2023). This may be due to erosion and leaching, as well as the assimilation of the influx in nutrient supply by plant growth (Caon et al., 2014; Agbeshie et al., 2022). Other fire-induced effects, such as increased alkalinity can last a few years longer (Brais et al., 2015; Su et al., 2022). Additionally, the exact impacts of changes in soil pH and nutrient availability due to ash deposition will vary for individual species according to their specific needs (Brais et al., 2015).

However, it should be noted that wildfires do not always have a positive impact on nutrient cycling in the boreal forest; it is estimated that only a fraction (ranging from 1 – 28%), of the nutrients and compounds in organic materials that are burned re-enter the ecosystem (Preston & Schmidt, 2006; Santín et al., 2015). Much of these losses are due to volatilization or vaporization, with carbon-based and nitrogen-based compounds often becoming gaseous CO_2, or NO_2 (nitrous dioxide) (Caon et al., 2014; Agbeshie et al., 2022). Other organic compounds, especially lipids or humic and or fulvic acids that are exposed to fire can also sometimes be rendered less bioavailable rather than more, by gaining a benzene ring or phenyl group (referred to as becoming ‘aromatic’), instead of mineralizing completely, typically due to incomplete combustion (González-Pérez et al., 2004). This is because benzene rings have a high degree of chemical stability due to their unusually stable molecular structure (i.e. they are composed of six carbon atoms bonded by alternating single and double bonds), and compounds that gain a phenyl group tend to be similarly conferred with a higher resistance to biodegradation (González-Pérez et al., 2004; Chebykin & Abakumov, 2022).

Additionally, just as fire can create environments more encouraging of nutrient processing, the reverse can also be true, particularly in cases of extreme (i.e. intense high temperature; > 500 °C) wildfires (Agbeshie et al., 2022). For example, fire can compact soil particles and reduce porosity, which in turn can reduce infiltration of the soil profile by rain and increase runoff that can carry off nutrients from newly deposited ash (Doerr et al., 2009; Ebel & Moody, 2016; Agbeshie et al., 2022). The compacted ground can also reduce the ability of plant roots to penetrate the soil profile and access untapped nutrients deeper in the soil profile (Certini et al., 2005; Lei et al., 2022; Agbeshie et al., 2022). Wildfires can remove important microbial, fungal, and bryophytic species on the forest floor that are essential to fixing nitrogen and other nutrients in the limited soils of the boreal forest, potentially for decades depending on the severity of the fire-driven changes to soil pH and the amount of organic matter removed by burns (Day et al., 2019, 2020; Renaudin et al, 2022; Agbeshie et al., 2022; Su et al., 2022). Additionally, while it was once thought that since wildfires can clear the boreal forest canopy, which would allow more sunlight to penetrate the undergrowth and potentially raise temperatures closer towards the optimum needed for microbial activity critical for recycling nutrients (Sariyildiz, 2008), more recent research indicates that this more often results in longer-term drying out of soils, which instead negatively impacts the enzymes needed for nutrient recycling (Monson et al., 2006; Allison & Treseder, 2008; 2011; Allison et al., 2010; Agbeshie et al., 2022). Furthermore, the reduced retainment of soil water due to the loss of vegetation cover and associated enhanced evapotranspiration (Collar et al., 2023), itself could contribute to future fires and or intensifying them (Moazeni & Cerda, 2024). As climate change and its effects continue to intensify, the non-beneficial aspects of wildfires on the ecology of the boreal forest will likely become much more common than before (Hanes et al., 2019).

2.2.3. Climate change will intensify fire activity in the boreal forests of northwestern Canada

Due to recent climate change, the boreal forests of northwest Canada are now experiencing more frequent, larger and more intense wildfires with the total area burned increasing every year since the beginning of the 21st century (Hanes et al., 2019; Jain et al., 2017; Chen et al., 2021). Fires in any given area that usually would have re-occurred only after anywhere from ~150 – 200 years (and sometimes after only 1000+ years for some wetlands in the Canadian boreal forest; de Groot et al., 2013; Sutheimer et al., 2021), are now re-occurring in less than 30 years, devastating the forest as it is repeatedly combusted faster than it can recover (Burns & Honkala, 1990). These changes have been primarily attributed to recent climate change through two primary pathways; the first is that climate change has enhanced the availability of fuel and overall flammability of the boreal forests of northwest Canada (Hanes et al., 2019).

For example, rising temperatures combined with shorter, milder winters have extended the length of the fire season; in northwest Canada, fire season normally begins in late May and June, peaks in July when the boreal forest is at its hottest and driest, and typically ends in September (Stocks et al, 2002). However, climate-driven changes to weather patterns in northwest Canada are reducing total precipitation (especially total snowfall), and leading to longer and more frequent periods of drought (Wang et al., 2014; Jain et al., 2017), allowing major fires to occur as late as October, well out of the regular fire season, which would also impact the ability for fire response and management to limit and control fires (Jain et al., 2024). The resultant drying out of the boreal forest and its soils for longer periods of time has also led to changes in the types of fires occurring, which could impact how often they may recur, and influence the severity of their impacts for the worse; whereas the wildfires of the Canadian boreal forest of the past fifty years have been almost exclusively extensive surficial crown fires (i.e. fires occurring primarily in the forest canopy; especially likely to occur when there is a high density of vegetation, as the low hanging branches can enable the fire to more rapidly climb up to the canopy and spread to adjacent trees) (de Groot et al., 2013; Watts & Kobziar et al., 2013; McLauchlan et al., 2020), increasingly frequent fires during a hotter and drier summer season (Jain et al., 2017), are also igniting ground fires (Scholten et al., 2021). Also known as subsurface fires, ground fires occur underground in areas with deep deposits of organic matter (usually peat) like wetlands, which would otherwise be somewhat resistant to ignition due to high levels of soil moisture, but which are now drying out due to climate change, and are now becoming more flammable (Huang & Rein, 2019). Ground fires are especially insidious and difficult to control, as they can smoulder for months underground with no visible flame or smoke, and can persist even through winter under the snow, making them difficult to detect and extinguish; hence they are sometimes also called 'zombie' or 'ghost' fires (Scholten et al., 2021). Climate-driven increases in subsurface fires could therefore contribute to the ignition of and spreading of even more forest fires (Huang et al., 2019; Scholten et al., 2021).

The second pathway by which climate change is increasing incidences of wildfires in the Canadian boreal forest is that altered climate and weather patterns have increased occurrences of lightning, which historically accounted for the ignition of most (70 – 90%) of the larger wildfires and total area burned in northern Canada over the past 50 years (Hanes et al., 2019; Veraverbeke et al., 2017; Janssen et al., 2023; Jain et al., 2024). Climate-driven changes to global air currents have increased transportation of water vapor and atmospheric moisture content from the Gulf of Alaska and the Arctic ocean into continental North America; as more low-pressure parcels of moisture-rich air move southeast into the Northwest Territories, they will be convected into the upper atmosphere by the unstable continental climate, where the moisture carried then forms into rapidly moving ice particles that can build up an electric charge that eventually discharges as lightning (Kochtubajda et al., 2003; Saunders, 2008). As global temperatures continue to rise, so will the amount of moisture in the atmosphere, increasing lightning occurrences, and hence also incidences of lightning-ignited fires in northwest Canada and Alaska (Veraverbeke et al., 2017; Hessilt et al., 2022), with projections suggesting that with every 1°C increase in global warming, there may be a 39 – 65% increase in lightning-ignited wildfires (Hessilt et al., 2022).

The climate-intensification of fire activity in northwestern Canada will have and is having substantial impacts on the ecology, processes, and functions of the boreal forest (Price et al., 2013). For example, increased fire frequency (e.g. having a fire once in less than 30 years, instead of once every few centuries; Burns et al., 1990), could and may already be causing changes in the composition of tree species in the boreal forest (Greene et al., 2007). Since many coniferous species, such as *Picea mariana*, take 30 – 40 years to fully mature, more fires re-occurring in the same area than they otherwise normally would, may consume young coniferous saplings and seedbeds, as well as supporting species like *Sphagnum* spp. mosses which are critical to the regeneration of *Picea mariana* stands, before they can finish their reproductive/regeneration cycle (Turetsky et al., 2012; Buma et al., 2022; Mayner et al., 2024). This limits the propagation of conifers, while deciduous pioneer species such as the fast-growing *Populus tremuloides* remain able to recolonize even remote stands (Baltzer et al., 2021; Massey et al., 2023). Combined with post-fire changes decreases in soil acidity that also disadvantages coniferous recolonization against deciduous trees (Bodi et al., 2014; Agbeshie et al., 2022), more frequent and severe fire activity in the Canadian boreal forest could facilitate a transition to a larger and more permanent state of deciduous tree cover (Greene et al., 2007; Anyomi et al., 2022). While there is some evidence that a more permanent transition to increased deciduous cover could potentially reduce fire risk due to the relatively higher moisture content of many deciduous species (Massey et al., 2023; Gaboriau et al., 2023), projections of climate trajectories show that it is more likely that any increases in fire resistance will be overwhelmed by the climate-driven increases in drought frequency and severity that originally enabled these forest fires and drove these forest composition changes (Baltzer et al., 2021; Buma et al., 2022).

More concerningly, climate-intensification of wildfires in northwest Canada are also wreaking havoc on the boreal zone's role as a carbon sink, and rather than acting as a vital mechanism of carbon and nutrient cycling, more frequent and intense fires are volatilizing the carbon stored in the surface vegetation of the boreal forest, as well as long-term soil carbon and nutrients on an unprecedentedly scale (McLauchlan et al., 2020; Walker et al., 2020). Large parts of the Canadian boreal forest have already become substantial carbon sources since the 1990s, primarily due to more frequent fires, and up to 90% of the carbon emissions emitted are directly attributable to combustion of the organic carbon stored in soils (Pan et al., 2024; Walker et al., 2020). For example, during the 2014 fires in the Northwest Territories, 2.85 Mha of forested land were burned, resulting in an estimated 94.3 Tg C of carbon emissions, nearly half the estimated mean annual net ecosystem production of the entirety of Canada alone (Walker et al., 2018). It has been suggested that a climate-driven changes towards a more deciduous dominated boreal forest may be able to offset wildfire emissions by increasing the carbon stored in soils and biomass in the long term (on a decadal scale), due to the faster growth and relative fire-resistance of deciduous trees (Mack et al., 2021), particularly in the early stages of succession when the canopy is thinnest and sapling growth is fastest (Qu et al., 2025). However, without decreases in fire activity, it is unlikely any gains in the carbon stored due to increases in deciduous cover will ever sufficiently offset emissions (Buma et al., 2022).

Though it has received less public attention by comparison, wildfires may also be substantially affecting the carbon and nutrient cycling of aquatic ecosystems in the boreal forest, though the exact impacts depend on the characteristics of each catchment (Benoy et al., 2007; Smith et al., 2011; Nunes et al., 2018; Burd et al., 2020; Grosbois et al., 2023; Caroni et al., 2024; Moazeni & Cerda, 2024). Unlike the terrestrial component of the boreal ecosystem, forest fires cannot directly affect aquatic ecosystems in boreal landscapes via combustion, but can still impact water quality by producing particulate pollution that can enter local bodies of water in fire affected catchments (e.g. ash can reduce water clarity, and choke rivers and lakes; Bodí et al., 2014), which can become stored in the sediments as an indicator of a past fire event (Smol, 2008). Ash that enters aquatic ecosystems may also contain contaminants (e.g. heavy metals, aromatic compounds, including polycyclic aromatic hydrocarbons; PAHs; Olefeldt et al., 2013; Paul et al., 2022; Sanchez-Garcia et al. 2023), and nutrient ions which can alter pH (e.g. trace metals such as calcium and phosphates can increase pH, but increases in anions like sulfates and chloride may decrease pH), which in high enough concentrations, could trigger algal blooms or eutrophication, and its associated impacts on water quality (Earl & Blinn, 2003; Bodí et al., 2014; Granath et al., 2020; Pelletier et al., 2020; Paul et al., 2022). However, these fire-driven water chemistry changes typically last for only a few years (i.e. >3 years) at most, though they may last significantly longer in lakes with higher residence times (Earl & Blinn, 2003; Granath et al., 2020; Pelletier et al., 2020). The toxicity and ecological exposure of PAHs in aquatic ecosystems following a fire, are especially short-lived compared to other contaminants due to their insolubility (and thus reduced bioavailability), and tendency to bind to sediment particles, as well as increased likelihood of mineralization via UV light in aqueous conditions despite their otherwise high aromaticity (Olefeldt et al., 2013).

Wildfires can indirectly impact aquatic ecosystems but on a longer-term scale by altering the geomorphology and ecology of fire-affected catchments which affects the rate at which carbon, nutrients and contaminants are exported to downstream rivers and lakes (Shakesby & Doerr, 2006; Nunes et al., 2018; Pelletier et al., 2020). For example, wildfires can partially denude the landscape of vegetation and bryophyte cover which would otherwise stabilize soils and intercept rainfall (Sankey et al., 2024), increasing runoff and erosion (Doerr et al., 2009; Ebel et al., 2016), and enhance the rate at which sediment, nutrients and contaminants are transported into downstream watersheds (Shakesby et al., 2006; Bladon et al., 2014). In cases of extreme heat, the soil surface may also become compacted, which can also increase runoff and erosion (Doerr et al., 2009; Ebel et al., 2016), and can eventually even shift or result in entirely new stream channels (Legleiter et al., 2003; Shakesby et al., 2006). Unlike wildfire-produced pollutants, the indirect impacts of wildfire-driven landscape changes and erosion that can enhance nutrient and carbon loading into downstream aquatic ecosystems can last for decades (Dunnette et al., 2014). Of particular concern is how wildfires may be driving widespread permafrost thaw throughout the Canadian boreal subarctic (Gibson et al., 2018), which can result in rapid and permanent changes (referred to as thermokarst) to the geomorphology and hydrology of affected areas (Connon et al., 2014; Carpino et al., 2021; Wright et al., 2022), as well as ecology (Chasmer et al., 2017; Dearborn et al., 2021), and may be increasing nutrient and carbon loading to boreal subarctic aquatic ecosystems (Wauthy et al., 2018; Fouché et al., 2020).

2.2.4. Permafrost as a foundational element of the Canadian boreal subarctic landscape

Owing to the cold subarctic climate, a large portion (estimated to be approximately 30 – 40%) of the Canadian boreal forest is also underlain by permafrost (Obu, 2021). Permafrost refers to any terrestrial substrate (i.e. soil, rock, sediment etc.) that has remained in a perennially cryotic (=< 0°C) state for at least two consecutive years (Dobiński, 2020; Obu, 2021). To be precise, permafrost is distinct from any frozen water (ground ice content) that is often but not always present within the soil pores of cryotic terrain (Permafrost Subcommittee, 1988; Devoie et al., 2024). Landscapes with permafrost are never entirely frozen through the soil profile; only a 'true' or 'isothermal' permafrost layer of the soil profile remains cryotic on a multi-year basis, which lies below a surficial 'active layer' of varying soil material and depth which seasonally thaws and refreezes, and which is the main air-ground interface where most geomorphological and biological (i.e. plant root growth, or microbial activity) processes occur (Dobiński, 2020). The isothermal permafrost layer itself caps a layer of earth that is kept unfrozen by geothermal heat (Dobiński, 2020).

Just as permafrost varies in thickness throughout the soil profile, the distribution of permafrost (and its active layer), can also vary dramatically in thickness and quality throughout the boreal subarctic, depending on the local environmental and climatic conditions (Dobiński, 2020; Figure 3.). Permafrost-rich landscapes have often been classified by the percentage of how much of the landscape is underlain by permafrost and its spatial arrangement (Obu, 2021). For example, regions where 90-100% of the terrain is underlain by contiguous permafrost are called continuous permafrost zones, whereas landscapes with 50 – 90% are considered as extensive discontinuous (Obu, 2021; Figure 3.). Landscapes where only 10 – 50% of the surface is underlain by permafrost and usually in discontinuous patches are referred to as sporadic discontinuous permafrost zones, and regions with permafrost patches that cover less than 10% of the terrain are called isolated permafrost zones (Obu, 2021; Figure 3.). Permafrost also exists underneath glaciers (Dobinski, 2011), where it is known as subglacial permafrost, though its dynamics remain comparatively understudied (Alexander et al., 2020). Permafrost can also be found underwater as subsea permafrost, which is estimated to be distributed across ~17 million km^2 of the Arctic seabed (Obu, 2021), and its dynamics are of substantial climate significance due to its potential to release huge reserves of methane should large areas of subsea permafrost continue to thaw out (Sayedi et al., 2020; Wilkensjeld et al., 2021). Neither subglacial nor subsea permafrost lie within the scope of this thesis.

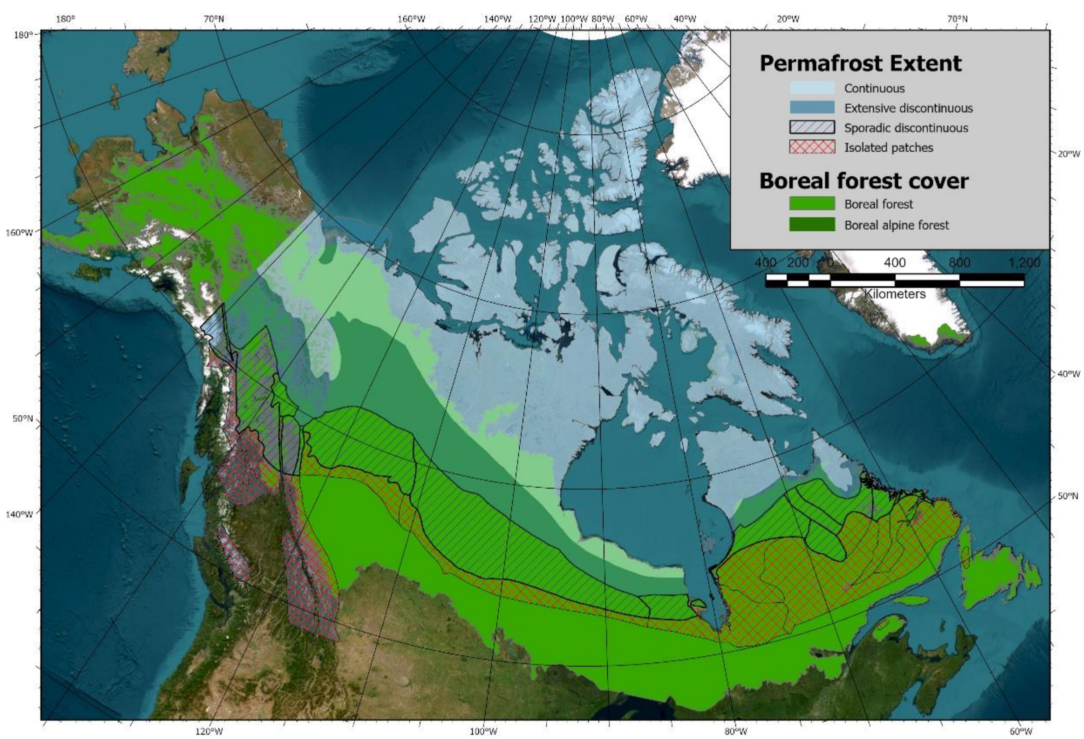

Figure 3. Distribution of permafrost extent and types (e.g. continuous, solid light blue; extensive discontinuous, solid medium blue; sporadic discontinuous, hatched in blue; and isolated, cross hatched in red) in North America relative to the extent of the Canadian boreal forest (medium green). Basemap of Canada in true colour imagery provided by World Imagery in ArcGIS Pro (Esri Inc., 2025), with permafrost geospatial data derived from boundary shapefiles from the National Atlas of Canada (5th edition) via Natural Resources Canada, while boreal forest geospatial data was derived from boundary shapefiles provided by Natural Resources Canada originally from data attached to Brandt et al., (2009).

Two main categories of factors determine the type, depth, and distribution of terrestrial permafrost for any given site: the prevailing local climate, specifically air temperatures (which roughly correlates with latitude), and the geophysical properties of that site (Dobiński, 2020). For example, in the highest latitudes (i.e. > 75°N), where even the warmest months never exceed 10 °C (Kottek et al, 2006), the permafrost is largely continuous, with some areas having isothermal permafrost layers hundreds of metres thick (Sazonova et al., 2004). In these regions, if any active layer is present, it may be seasonal, appearing only in summer and is shallow, ranging from 0.15 – 1.5 deep (Dobiński, 2020). In contrast, in the southernmost areas of the boreal subarctic, where average air temperatures may hover around 0 °C, permafrost largely occurs in discontinuous or sporadic patches generally no thicker than five metres deep (Halsey et al., 1995), and with active layers 2 – 3 m deep (Dobiński, 2020), that never truly seasonally refreeze (Kane et al., 1991). Geophysical factors that can influence the permafrost and active layer depths, include snow cover extent, structure, and volume (Gisnås et al., 2014), vegetation, local topography and hydrology (Smith, 1975), availability of geothermal heat, and local soil characteristics and textures, all of which affect how much energy from incoming insolation or warm (> 0 °C) air temperatures is applied to the ground surface and soil profile (Brown et al., 1973; Wang et al., 2021). Soil texture also impacts active layer depth; substrates composed of finer material (i.e. clay: < 2 µm, or loam: particle size ~50 µm), tend to have thinner active layers compared to coarse-grained (i.e. sand: 0.05 – 2 mm or gravel: >2 mm) materials (Dobiński, 2020). This is because coarser grained materials tend to have larger soil pores and can thus house more water, which due to its high heat capacity, can delay freezing in the active layer (Dobiński, 2020).

Since it forms a large physical component underlying much of the circumpolar landscape, permafrost is strongly involved in the processes that have and still are shaping northern geography, including in the boreal subarctic (Kokelj & Jorgenson, 2013). For example, the geologically underdeveloped and nutrient poor cryosols and histosols of the Canadian boreal forest are partially a product of the frigid conditions of permafrost-rich soils arresting soil microbial decay and other biogeochemistry processes that would otherwise advance soil development and allow nutrient recycling by microbial processes (Maynard et al., 2014; Liebmann et al., 2024). Additionally, in some regions, permafrost acts as an impermeable barrier in the soil profile which limits the depth to which plants can extend their roots, imposing an ecological filter for the common boreal conifers like *Pinus banksiana*, *Picea glauca*, and *P. mariana*, which all have horizontal rather than vertical root systems, and thus enables them to survive in the shallow soils characteristic to the boreal subarctic (Strong & Roi, 2011; Brandt et al., 2009; Ogden et al. 2023). Permafrost, and permafrost-adjacent processes have also directly shaped many of the most distinctive landforms of northern Canada; for example, patterned ground formations like ice wedges and polygons (Black, 1976), and mounds like palsas and pingos are a direct result of thermal expansion and contraction of permafrost-rich substrate as they undergo seasonally repeating cycles of freezing and thawing (Kujala et al., 2008); Mackay, 1998). Similarly, the thousands of small lakes, ponds, and wetlands scattered across the Canadian boreal subarctic are the result of rapid thawing of permafrost-rich landscapes that are especially rich in ground ice (i.e. > 30%) content, and the subsequent subsidence that produces a basin that becomes filled with formerly frozen ground water (Bouchard et al., 2016; Kokelj et al., 2013; Spence et al., 2020). This specific process of permafrost thaw and subsequent ground collapse has been an active part of the evolution of circumpolar landscapes for millennia, and is known as thermokarst (Kokelj et al., 2013; Coulombe et al., 2022).

There are several types of thermokarst processes, each of which produce specific landforms with unique features, but can generally be divided into either thermokarst processes that affect hillslopes, such as active-layer detachment slides (ALDS) and retrogressive thaw slumps, or thermokarst processes that occur on flat terrain, such as trough or pit forming thermokarst like thermal erosion gullies, as well as lake thermokarst, and wetland thermokarst (Kokelj et al., 2013). The occurrence of each thermokarst type is not mutually exclusive and some, such as lake thermokarst and wetland thermokarst often co-occur close to each other or can even cyclically transform into each other (Coulombe et al., 2022). ALDS and retrogressive thaw slumps both involve slope failure due to the loss of ground ice content that once consolidated relatively loose materials (Kokelj et al., 2013). Thermal erosion gullies and thermokarst pits and troughs are depressions and channels formed from the degradation of ice wedge polygons, which themselves are ground fissures formed by the expansion and contraction of ground during freeze-thaw cycles, and further developed by heat transferred from surface water flows (Kokelj et al., 2013). Lake thermokarst are the most widespread type of thaw-produced landform and is the formation of or the expansion of pre-existing thermokarst lakes as the ground collapses into a basin (often circular in shape) due to the underlying ground ice content thawing out and becoming liquid water (Bouchard et al., 2016; Kokelj et al., 2013). Lakes formed from thermokarst action also sometimes possess a talik underneath, a layer of thawed or unfrozen ground kept above 0 °C due to heat from the thermokarst lake above, and which can trigger further thawing of permafrost in adjacent areas (Connon et al., 2018; Devoie et al., 2019). Wetland thermokarst refers to bogs and fens formed from thaw-driven thermokarst activity, which is characterized by either permanent or seasonal waterlogging of local soils, and associated loss of prior vegetation types (typically trees or tundra shrubs) in favour of marshy sedges and or mosses like *Sphagnum* (Kokelj et al., 2013; Vitt et al., 1994). Thermokarst bogs are essentially formed in the same manner as thermokarst lakes (i.e. circular basins formed by thaw-driven ground collapse) and can even be formed from thermokarst lakes if they become drained by adjacent thermokarst features, such as gullies or even other kinds of wetland landforms like channel fens, but only have enough water to saturate the soils rather than forming an open water body (Kokelj et al., 2013; Haynes et al., 2018; Coulombe et al., 2022). Thermokarst fens (also known as collapse-scar fens or channel fens), are a subvariant of wetland thermokarst, specifically those formed from long linear (and similarly vegetated) basins through which water from adjacent thermokarst lakes and bogs drain into the watershed (Kokelj et al., 2013). As temperatures continue to rise, along with corresponding increases in the frequency of climate-driven disruptions like wildfires (Gibson et al., 2018), large portions of the permafrost underlying the Canadian boreal forest, especially in areas with highly vulnerable discontinuous permafrost such as those in the southernmost extent of permafrost-rich regions will become irreversibly degraded (Hugelius et al., 2020; Gibson et al., 2021). This could accelerate thermokarst formation, substantially altering the geomorphology and hydrology (Connon et al., 2014; Chasmer et al., 2017; Haynes et al., 2018; Quinton et al., 2018; Olefeldt et al., 2021), as well as ecology of affected areas (Price et al., 2013; Gauthier et al., 2015; Dearborn et al., 2021).

2.2.5. Permafrost thaw in the permafrost peatlands of the Dehcho region

In this thesis, we focused on one specific permafrost-rich part of the Canadian boreal subarctic, a southwestern corner of the Dehcho region in the Northwest Territories, in the wetlands of the lower Liard River valley (Quinton et al., 2018). Here, the land straddles the boundary between extensive and sporadic discontinuous permafrost, being underlain by patches of relatively shallow (< ~10 m deep) permafrost (AMAP, 2017; McClymont et al., 2013). Each permafrost patch serves as the foundation to raised (typically 1 – 3 m above the surrounding landscape) forested peat plateaus, and is interspersed by patches of permafrost-free wetlands (bogs and fens) and lakes, forming a mosaic-like landscape referred to as a permafrost peatland (Ecosystem Classification Group, 2007; Quinton et al., 2018; Wright et al., 2022). Peat refers to a type of soil-like substrate composed or partially decayed organic (usually vegetation) material, commonly found in wetlands (Vitt et al., 1994; Quinton et al., 2009). The southern Dehcho is also considered among those permafrost-rich areas of the Canadian circumpolar north most at risk of undergoing widespread accelerated permafrost thaw and its associated impacts (Quinton et al., 2018; Wright et al., 2022), owing to the already fragmented discontinuous permafrost (Devoie et al., 2021), and the relatively warm local climate, with mean annual air temperatures that hover around and above 0 °C (e.g. in January, air temperatures can range from -25.5 to -28 °C, while July temperatures can range from 15.5 to 16.5 °C), which are well above the thaw-point (Halsey et al., 1995; Ecosystem Classification Group, 2007; Quinton et al., 2009). Despite these conditions, permafrost in the southern Dehcho has been able to persist, primarily due to the rich peat deposits in the soil layers above the permafrost (Vitt et al., 1994), as peat has a relatively low thermal conductivity (~0.06 W/m·K), and which has been able to partially insulate the discontinuous permafrost (Du et al., 2021; Holloway et al., 2020).

Consequently, even small environmental disturbances can and have triggered rapid thawing and subsequent wetland and lake thermokarst in the past, though historically permafrost degradation and thermokarst have always eventually been followed by periods of permafrost aggradation, allowing the permafrost to have roughly persisted in a long-term equilibrium for millennia (Zoltai, 1993; Quinton et al., 2009; Pelletier et al., 2017; Treat & Jones, 2018). This multi-millennial cycle of permafrost degradation, thermokarst, and aggradation was what created the Dehcho region's characteristic permafrost peatlands (Zoltai, 1993; Quinton et al., 2018; Wright et al., 2022), and its vast globally significant peat deposits (Hugelius et al., 2020). When permafrost thaw is triggered and the ground ice underneath melts away, the resultant thermokarst depression becomes filled with water, forming either a wetland or shallow lake anywhere from 0.5 – 5.0 m deep (Kokelj et al., 2013; Olefeldt et al., 2021). Any flora that had previously been growing in the collapsed areas (i.e. typically black spruce, *Picea mariana*, but also white spruce, *P. glauca*; birch, *Betula* spp.; Labrador tea shrubs, *Rhododendron groenlandicum*; lichens, and *Cladina* spp. to a lesser degree; Vitt et al., 1994; Quinton et al., 2009; Alberta Biodiversity Monitoring Institute (ABMI), 2016), with the exception of any *Sphagnum* spp. mosses (e.g *S. riparium, S. angustifolium, S. fuscum*; Zoltai, 1993), will then die due to waterlogging (Zoltai, 1993). However, due to the anoxic conditions caused by the submergence, the dead vegetation will often fail to fully decompose, and together with any material produced by the *Sphagnum spp*. mosses, transforming into peat, accumulating and adding to the characteristic peat deposits of the region (Vitt et al., 1994; Quinton et al., 2009). Over time, the peat may eventually resurface due to an upward ground swelling caused by freeze-thaw cycling (called frost-heaving), and ground ice buildup (Zoltai & Tarnocai, 1975). If this underground ice and raised peat plateau can persist long enough, then the surface peat layers eventually dry out, and can be recolonized by vegetation, which can further delay thawing of the ground ice by adding another layer of insulation, and may even result in permafrost recovery (Zoltai, 1993; Kuosmanen et al., 2023). Eventually, the permafrost-rich peat plateaus suffer a disturbance, such as a forest fire, which drives rapid thaw and thermokarst eventually repeating the cycle (Zoltai, 1993; Johnston et al., 2015). This cycle of permafrost thawing, thermokarst, and eventually permafrost aggradation and peat accumulation, may take anywhere from ~450 to 1500 years to complete (Zoltai, 1993; Treat et al., 2018; Gibson et al., 2021), and has been occurring in northwest Canada since the retreat of the glaciers roughly ~9000 years ago (Loisel et al., 2014; Treat et al., 2018). Over millennia, this has eventually created deposits of peat that range from 2 – 8 m deep, which represent some of the oldest and largest known soil carbon reservoirs (Hugelius et al., 2014; Quinton et al., 2018), though the rate at which peat has accumulated varied with climate changes (Pelletier et al., 2017; Treat et al., 2016; 2018). The exact size of the carbon stocks that the Dehcho permafrost peatlands currently represent are uncertain, but one estimate by Hugelius et al., (2020) suggested that the entirety of the permafrost peatlands in the northern hemisphere may represent ~415 ± 150 Pg C and ~10 ± 7 Pg N, just under half of the amount of CO_2 estimated to currently be in the atmosphere (889.92 Pg C; Friedlingstein et al., 2023).

The high propensity for the permafrost peatlands of the southern Dehcho region to rapidly thaw out and undergo thermokarst landscape changes is due to the fragmented nature of the discontinuous permafrost, which allows multiple mechanisms of thaw (i.e. vertical vs lateral) to be acted on them at once (Kurylyk et al., 2016; Devoie et al., 2021). Vertical thaw refers to a type of permafrost thaw that is characterized by a downward transfer of heat, either by direct conduction of heat from the atmosphere on the soil profile or exposed permafrost (if any), or if a talik is present, advection as well, which eventually results in a deepening of the active layer (as much as >60% increase) over time (Devoie et al., 2021). However, vertical thaw usually occurs only seasonally, primarily during the warm summer months (Devoie et al., 2021). In contrast, lateral thaw occurs horizontally, beginning at the margins of the permafrost-rich peat plateau, as the necessary heat flux is delivered through flowing water in an adjacent wetland and or lake (Devoie et al., 2021). Unlike vertical thaw, lateral thaw can occur year-round and is the primary active thaw mechanism driving landscape change in the permafrost peatlands of the Dehcho (Kurylyk et al., 2016; Devoie et al., 2021).

However, the exact rate at which permafrost in any given area thaws is dependent on many different factors in the local environment, including vegetation cover, topography, soil moisture, ground ice content, and soil texture and composition (Hayashi et al., 2007; Wright et al., 2009; O'Neill et al., 2019; Zastruzny et al., 2023; Holloway et al., 2020). For example, thicker vegetation cover or topography that provides shade, can buffer or reduce atmospheric heat flux (Hayashi et al., 2007; Wright et al., 2009). Soil moisture and/or ground ice content are direct influences for soil thermal conductivity, and thus the rate at which permafrost is exposed to heat and thaw, and areas with drier soils and/or lower ground ice content tend to thaw slower and are less vulnerable to thermokarst (O'Neill et al., 2019; Zastruzny et al., 2023). Similarly, soil texture and composition also influence soil thermal conductivity, being a factor in soil moisture and the rate at which ground ice may accumulate underground (O'Neill et al., 2019; Holloway et al., 2020).

Recent changes in climate such as increasingly warmer air temperatures since the 19th century (Quinton et al., 2018), and in particular, increases in the frequency of climate-intensified disturbances like wildfires, may be accelerating permafrost thaw, and thermokarst and other environmental changes throughout the southern Dehcho (Gibson et al., 2018; Haynes et al., 2018; Dearborn et al., 2021; Carpino et al., 2021), and may have shifted the delicate climatic, hydrological, and ecological system of factors preserving the equilibrium of the discontinuous permafrost of the region towards a new state of potentially irreversible degraded permafrost (Gibson et al., 2021). For example, climate-driven (i.e. changes in climate towards a drier forest, and increases in lightning strikes; Hanes et al., 2019; Veraverbeke et al., 2017; Janssen et al., 2023; Jain et al., 2024), increases in forest fires can result in the formation of taliks which further fragment the already vulnerable discontinuous permafrost (Gibson et al., 2018; Ackley et al., 2021), and provide locations from which more thawing (both vertical and lateral) can develop (Gibson et al., 2018; Devoie et al., 2021). Wildfires can remove vegetation and peat that normally provide insulation to the underlying permafrost, while also depositing layers of ash which have a lower albedo, and can promote downward heat flux and vertical thawing (Ackley et al., 2021; Devoie et al., 2021). Although wildfires in wetlands like those of the southern Dehcho were historically relatively fire resistant, being restricted to crown fires on the forested peat plateaus which are comparatively much drier (Johnston et al., 2015), with centuries usually taking place between a fire for any given specific location (Zoltai, 1993), the changing climate (Wang et al., 2014), combined with fire-related related impacts on the landscape that are draining the wetlands (Connon et al., 2014; Chasmer et al., 2017; Haynes et al., 2018), and opening up the canopy to form a drier microclimate (Wolf et al., 2021; Helbig et al., 2024), may be reducing moisture content, potentially leading to a positive feedback loop that encourages the frequency of and intensifies fires (particularly incidences of ‘zombie’ or ground fires; Wilkinson et al., 2019; Huang et al., 2019; Scholten et al., 2021), and increases permafrost thaw (Kim et al., 2024).

Consequently, permafrost extent in northwest Canada has declined anywhere from ~10 – 50% over the last half century (Wright et al., 2022), with at least ~25% of the permafrost thaw and associated thermokarst landscape changes directly attributable to the impacts of disturbances like wildfires (Gibson et al., 2018), which are expected to increase in both frequency and severity (Chen et al., 2021). If these trends continue, most of the permafrost peatlands of the southern Dehcho may become irreversibly thawed out by 2100 (Gibson et al., 2021). As the permafrost peatlands of the Dehcho also represent vast carbon stocks (Hugelius et al., 2020), there has been considerable research into their continued long-term viability as a carbon sink (Hugelius et al., 2020; Turetsky et al., 2020; Heffernan et al., 2020), with one of the major concerns of rapid thawing being a high potential for the thaw-driven conversion of the landscape into much more highly connected permafrost-free bogs and fens (Connon et al., 2014; Chasmer et al., 2017; Olefeldt et al., 2021; Carpino et al., 2021), which could facilitate the export of large amounts of this paleo-carbon, including possibly chromophoric varieties into downstream aquatic ecosystems (Wauthy et al., 2018; Fouché et al., 2020). Sudden large increases in in-lake concentrations of coloured organic carbon have been attributed as one of the main drivers behind a recent phenomenon of water discolouration in many lakes across the northern hemisphere, referred to as brownification (Weyhenmeyer et al., 2014; de Wit et al., 2016; Björnerås et al. 2017), which can have a variety of water quality impacts on affected lakes, including potentially enhancing greenhouse gas emissions (Blanchet et al., 2022), which may have implications for the continued functionality of the Dehcho peatlands as a site of globally-significant carbon storage in the near future.

2.2.6. Brownification in the lakes of the permafrost peatlands of the southern Dehcho

Brownification (also known as browning), refers to a phenomenon in which a water body (including both running and standing waters), undergoes a change in water colour towards hues ranging from tea yellow to brown and darker, often accompanied by a decrease in water clarity (Kritzberg et al., 2020; Blanchet et al., 2022; Räike et al., 2024). The main cause of brownification has generally been attributed to long-term increases in aqueous natural organic matter (NOM), specifically the fraction sufficiently fine enough to pass through a ~0.45 µm (or finer) filter, which is referred to as dissolved organic matter (DOM) or carbon (DOC) (Evans et al., 2005); the remaining mass is usually referred to as particulate organic matter (POM) or carbon (POC) (Pagano et al., 2014). Indeed, at least one definition of brownification simply defines it as when a water body contains high (i.e. > 10 mg/L) concentrations of DOC (Blanchet et al., 2022). However, some cases particularly those associated with darker water colour changes, are at least partially the result of increased concentrations of iron (Fe), which can bind to organic particles present to form stable complexes, molecular entities composed of two or more compounds attached to a central typically metallic (in this case, iron) ion (Weyhenmeyer et al., 2014; Björnerås et al. 2017; Kragh et al., 2022). Although literature on brownification has used the terms DOM and DOC interchangeably, technically DOC refers specifically to only the mass of the carbon constituting dissolved organic materials, whereas DOM covers the totality of dissolved organic compounds involved (Moody et al., 2017). More recent research is also redefining brownification by clarifying that only a specific fraction of DOM/DOC may be responsible for the associated water discolouration, referred to as chromophoric dissolved organic material or carbon (cDOM or cDOC) (Blanchet et al., 2022; Rodríguez-Cardona et al., 2023; Zhao, 2024), and there are several regions in North America (e.g. Yukon, Alberta, Atlantic

Canada, and the southwestern Northwest Territories), where a distinct decoupling between DOM/DOC concentration and water colour has been observed (Johnston et al., 2020; Pugh et al., 2021; Kurek et al., 2023; Rodríguez-Cardona et al., 2023; Coleman et al., 2025).

The source of the organic material driving brownification at any given lake is generally terrestrial, usually derived from the decaying or partially decayed remains of plants and animals (Evans et al., 2005; Solomon et al., 2015; Blanchet et al., 2022; Kragh et al., 2022). Consequently, the exact composition of the materials and organic compounds driving brownification can vary widely between different water bodies and depends heavily on the characteristics of the local watershed, such as substrate composition, and vegetation cover (Blanchet et al., 2022; Rodríguez-Cardona et al., 2023; Škerlep et al., 2020; 2022; Zhao, 2024). Some of the most common materials and organic compounds associated with brownification include or are derived from decayed or partially decayed plant matter or plant-derived compounds like lignin, cellulose and hemicellulose (i.e. a polysaccharide that serves to bond cellulose and lignin in plant cells; Kaur & Sharma, 2019), particularly humic substances (i.e. humic and fulvic acids, and humin), but also various loose amino acids and proteins (Evans et al., 2005; Solomon et al., 2015; Blanchet et al., 2022; Kragh et al., 2022). It is thought that the yellow-brown hues of brownified waters are mostly due to humic substances, especially fulvic acids, as these humic compounds absorb wavelengths in the ultraviolet spectrum and the shorter ranges of the visible spectrum, while reflecting longer (i.e. yellow to red) wavelengths (Evans et al., 2005; Kubínová et al., 2021). However, the relative impact on water colour, water quality, as well as the specific degree of lability and biodegradability of most of these various organic compounds and materials remains an ongoing field of study (Blanchet et al., 2022). Quantitatively, water colour, and by extension, the severity of brownification can be measured using a platinum salt solution (units in mg Pt/l, or TCU, wherein 1 mg of Pt/L = 1 TCU; True Colour Unit; also be known as the Platinum-Cobalt or Pt-Co unit), with brownification said to occur when > 15 TCU, and can be further qualitatively graded by colour intensity (null, pale, light, dark), and hue (e.g. yellow, yellow brown, brown, dark brown) (Graneli, 2012; Kubínová et al., 2021). However, this method is now considered outdated and is increasingly being replaced with direct wavelength measurements (Graneli, 2012; Kubínová et al., 2021).

As brownification represents a substantially visible shift in water quality which can significantly impact the ecology of and alter the ecosystems services provided by affected lakes (Kritzberg et al., 2020; Blanchet et al., 2022; Anderson et al., 2023; Turunen & Aroviita, 2024; Horppila et al., 2024), there has been growing public and academic interest in brownification over the last few decades (Albrecht et al., 2023; Horppila et al., 2024). In general, the impacts of brownification can be summarized into three main types: a) the direct impacts of reduced light availability and the indirect effects, such as brownification-driven changes in thermal and stratification regimes, and oxygen availability, on a lake's ecology; b) the impacts on water quality, and availability and lability of contaminants; and c) the impacts on carbon cycling (Blanchet et al., 2022). The most visibly obvious, and primary impact of brownification is the shift towards a more light-limited environment, and the direct and indirect effects of this shift on the affected lake's ecology (Solomon et al., 2015, Strock et al., 2017; Pilla et al., 2018). An increase in DOM or cDOM can substantially reduce the depth in the water column to which light penetrates, well above the reach of benthic macrophytes and other autotrophs, significantly reducing photosynthetic efficiency and primary production and biomass (Thrane et al., 2014; Kelly et al., 2018; Stetler et al., 2021; Sherbo et al., 2023). This loss in light availability can act as a driver for species distribution changes, ecological filtering for only those few macrophytes which can adapt, such as *Elodea canadensis*, which can elongate its stems to maintain optimal light exposure (Mormul et al., 2012). The brownification-driven reduction in light availability can in turn impact the trophic structure and food webs of affected lakes in a variety of ways; for example, the reduction in primary production limits the base food supply and potential energy transferrable to higher trophic levels (Creed et al., 2018; Leech et al., 2018), while the reduced visibility can impair foraging and hunting efficiency, negatively impacting energy reserves and growth in fish despite also potential increases in supply of prey like zooplankton (Craig et al., 2017; Horppila et al., 2024). There is also evidence that brownification may reduce nutritional quality in the food web by specifically disadvantaging phytoplankton taxa that synthesize highly unsaturated fatty acids (HUFA), specifically eicosapentaenoic acid (EPA), and docosahexaenoic acid (DHA), which contain the 'omega-3' (ω-3) and 'omega-6' (ω-6) fatty acids (Taipale et al., 2016). These compounds are essential to the growth and development of many organisms, including fish, and the mammals and birds that prey upon them, (Taipale et al., 2018), and which cannot be produced by higher trophic organisms (Vance & Vance, 2008).

However, the ecological impacts of brownification on light availability in a lake are not always negative, and highly depend on the severity of the browning, as well as past environmental context of the lake prior to browning (Horppila et al., 2024). For example, moderate increases in DOC and cDOM can attenuate harmful UV radiation and provide nutrient subsidies to primary production without also impairing it; moreover, lakes that have been historically murky due to eutrophication may not necessarily be as ecologically impacted as in lakes which have historically been oligotrophic, as the species within may already be adapted to low-light conditions (Horppila et al., 2024). It should be noted, however, that the impacts of brownification in murky lakes has in general been far less studied than in oligotrophic (i.e. DOC

< 15 mg/L) lakes, and the exact ecological impact of specific concentrations of DOM/DOC, and water colour intensity remains an area of ongoing research (Horppila et al., 2024).

Brownification can also impact the ecology of affected lakes by altering lake habitat quality, through changes to the thermal regime and stratification dynamics, as well as oxygen availability (Blanchet et al., 2022). Due to the comparatively darker and or increase in opacity following brownification, uneven heating of the surface waters occurs, which results in both overall warming of the affected lake, as well as increased stratification (Solomon et al., 2015, Strock et al., 2017; Pilla et al., 2018). Combined with brownification-related reductions in primary production (both from macrophytes and phytoplankton; Thrane et al., 2014; Kelly et al., 2018; Stetler et al., 2021; Sherbo et al., 2023), and increased heterotrophy (specifically microbial respiration) (Kelly et al., 2014; Xing et al., 2024), the brownification-driven stratification may eventually result in hypoxia in the benthic layers (Brothers et al., 2014; Williams et al., 2016; Knoll et al., 2018). These habitat changes could eliminate many benthic species and may be especially problematic for many temperature-sensitive fish species that depend on the thermal refugia in the cooler waters of the lakebed (Williamson et al., 2015; Jane et al., 2024).

As brownification often represents increased in-lake concentrations of organic matter, it also represents a substantial shift in water quality and chemistry and may also enhance inputs of pollutants and contaminants entering affected lake ecosystems (Wällstedt et al., 2010; Oni et al., 2013). This is because the same property of DOC and cDOM that enables them to form stable organometallic compounds with iron, also attracts heavy metals and contaminants (e.g. mercury and arsenic); consequently, brownification and the associated increase in DOC and cDOM may increase these contaminants entering affected lakes (Oni et al., 2013; Isidorova et al., 2016; Bravo et al. 2018; Campeau et al., 2022), and in forms especially bioavailable, and vulnerable to biomagnification (Creed et al., 2018; Ahonen et al., 2018; Kozak et al., 2021). Even without considering the potential contaminants they can carry, brownified water is often considered simply unsightly or unpalatable, requiring multiple rounds of difficult and expensive treatment (e.g. chemical disinfection, coagulation and flocculation, sand and carbon filtration, UV exposure) before it will reach most drinking water quality standards (Lavonen et al., 2013; Ritson et al., 2014; Krzeminski et al., 2019; Kritzberg et al., 2020).

Lastly, brownification can impact carbon cycling in affected lakes, and can enhance lake carbon emissions (Blanchet et al., 2022). This is due in part to much of the DOC and cDOM commonly associated with brownification (e.g. humic and fulvic acids, humin etc.), although usually relatively recalcitrant, being much more easily broken down once in an aqueous environment (Lapierre et al., 2013; Allesson et al., 2018; Maavara et al., 2021), but also because increased organic matter input into lakes will also correspond to increased carbon emissions (Tranvik et al., 2009; Lapierre et al., 2013). There are two main pathways by which this occurs; the first is photodegradation; light (i.e. 'photo-', or rather specifically UV) catalyzed oxidation or mineralization, by which the DOC in a brownified lake becomes dissolved inorganic carbon (DIC; e.g. CO_2; bicarbonate, HCO_3^-; and carbonate, CO_3^{2-}), and low molecular weight carboxylic acids (e.g. oxalic, malonic, formic, and acetic acid) (Bertilsson & Tranvik, 2000). The other pathway by which brownification leads to increased emissions is by shifting the affected lake towards increased heterotrophy and microbial respiration by limiting light availability in the water column, and thereby reducing primary productivity (Lapierre et al., 2013; Kelly et al., 2014; Xing et al., 2024; Saros et al., 2025), while also providing a carbon and nitrogen subsidy to bacteria, zooplankton, and macroinvertebrates (Kelly et al., 2014; Williamson et al., 2015; Xing et al., 2024; Turunen et al., 2024). Photooxidation, and photo-mineralization generally account for less lake carbon emissions (perhaps as little as ~10% of DIC and CO_2 production), than microbial respiration (Allesson et al., 2018; Maavara et al., 2021), though there are exceptions, such as with Cory et al., (2014), which found that photooxidation accounted for ~70 – 95% of the DOC processing. Which pathway is more relevant in any given brownified lake will likely highly depend on the biogeochemistry and hydrology, particularly residence time of individual lakes and catchments (Maavara et aal., 2021; Blanchet et al., 2022).

Brownification represents a substantial water quality issue, one that has been seemingly spreading rapidly across the northern hemisphere (de Wit et al., 2016; Björnerås et al. 2017; Blanchet et al., 2022), though there is evidence that trend may have slowed recently (Eklöf et al., 2021). Consequently, there has also been considerable research in identifying, and potentially curtailing the drivers behind brownification (Kritzberg et al., 2020; Blanchet et al., 2022; Horppila et al., 2024). Despite the seemingly widespread scale of brownification, different regions may be experiencing brownification for entirely separate and unrelated reasons, necessitating individualized approaches to management (Blanchet et al., 2022; Horppila et al., 2024). For example, in some lakes in southern and eastern Canada, browning has been identified as a recovery response to acid rain in the late 20^{th} century (Monteith et al., 2007; Meyer-Jacob et al., 2019; 2020; Redden et al., 2021). In contrast, in at least one lake in central Europe, browning was found to be a response to natural climate rhythms that has cyclically recurred for millennia (Tichá et al., 2023), whereas in Finnoscandia and northern Europe, browning is not just a recovery response to late 20^{th} century acid rain and sulfate deposition in some catchments (de Wit et al., 2016), but also the result of changes in vegetation cover that are increasing export of carbon and iron (Finstad et al., 2016; Škerlep et al., 2020; 2022), that have been exacerbated by recent climate change (Björnerås et al. 2017; Blanchet et al., 2022). In the permafrost peatlands of southwestern Dehcho, rising temperatures combined with increases in extreme environmental events like wildfires, may be leading to previously unprecedentedly levels of widespread and accelerated permafrost degradation across the boreal subarctic (Chasmer et al., 2017; Gibson et al., 2018). The resultant abrupt thermokarst landscape changes and increasingly hydrologically connected landscape (Connon et al., 2014; Carpino et al., 2021), may be mobilizing globally significant stores of paleo-carbon into local lakes, potentially as cDOM (Wauthy et al., 2018; Fouché et al., 2020; Heffernan et al., 2024), which may have been responsible for the recent browning of some lakes in, around, and near the Scotty Creek Basin, though unusually, there are wide discrepancies in the severity of the brownification among individual lakes (Wauthy et al., 2018; Coleman et al., 2023; 2025). Disentangling the exact mechanisms that may be driving these differences in severity of light regime changes for different Dehcho lakes will require long-term high-resolution records of past water quality changes which can only be obtained via paleolimnological approaches (Korosi et al., 2022; Saros et al., 2023).

2.3. Paleolimnology as a tool for reconstructing past environmental states

Paleolimnology refers to a diverse suite of techniques and methodologies involving the analysis of the physical and chemical properties of lake sediments as well as any biological remains preserved within, to reconstruct past climates and environments (Smol, 2008). A still actively evolving field, paleolimnological-based approaches have been critical to the success of many environmental management strategies, being one of the few approaches able to provide environmental data on temporal scales sufficiently long (potentially centurial to multi-millennial) enough to characterise the full scope of natural rhythms and variation in ecosystems which would otherwise be too expensive or impossible to acquire (Smol, 2019; Korosi et al., 2022). For example, paleolimnological approaches have been used to reconstruct trends in pH in North American lakes from their more recent acidification due to industrial sulfate emissions in the mid to late 20th century, and back to the 1850s, before the invention of the pH scale by S. P. L. Sørensen in 1909 (Smol et al., 1998), which provided historical context critical to informing legislation for successfully resolving acid rain as an environmental crisis in North America (Smol, 2019). More relevant to this thesis, paleolimnological techniques have been used to reconstruct changes in light regimes directly due to brownification in European lakes, helping to contextualize trends on multi-millennial scales (Tichá et al., 2023), and have also contributed substantially to our understanding of how recent climate changes and permafrost thaw are impacting vulnerable shallow lake ecosystems in northern Canada (Smol et al., 2016; Anderson et al., 2019; Korosi et al., 2022; Thienpont et al., 2025). Consequently, paleolimnological approaches might also be useful in filling in the gaps in previously incomplete paleo-records for SC11 and other lakes in the rapidly warming Dehcho permafrost peatlands and help to identify the specific drivers responsible for the observed discrepancies in colour shifts among different lakes (Coleman et al., 2023; 2025; Blanchet et al., 2022).

Paleolimnological approaches generally have three basic components: sediment sample extraction, radiometric dating, and analysis of paleoenvironmental indicators and proxies (Smol, 2008). The first element, sediment sample retrieval hinges on the fundamental premise of paleolimnology, which is the tendency of lakes, being the lowest centre of gravity in their respective watersheds, to accumulate materials from within the lake, and the surrounding landscape in its sediments over time (Williamson et al., 2009). As these materials are archived in sequence as a stratigraphic record of the past, in which the age of the sediments deposited correlates positively with depth (Barker, 2009), once retrieved, they may provide easily dateable insights on past events (Smol, 2008). Sediment samples are typically extracted as cylindrical sediment cores via tube shaped corers, with many different protocols and types in different sizes and designs developed to try to minimise disrupting the structure of the sediments during the process of extraction, as any unintended alterations could skew interpretations of the paleoenvironmental information contained within (Glew et al., 2002). For example, it is recommended to extract cores from the deepest, flattest and centremost basin of the lake being studied, as that is where the sediment is expected to accumulate most evenly and is thus most likely to supply the most undisturbed records (Smol, 2008). One of the most popular types of corers, due to their mechanical simplicity and reliability, are gravity corers, so named for their mode of operation; once sunk to the lakebed, gravity corers are equipped with a line connected to the operator, along which a weight is dropped to drive the corer deep within the sediment profile, after which the corer is then sealed via trigger (Glew et al., 2002). However, gravity corers are sometimes prone to deforming the sediment layers via the movement of the corer as it penetrates the sediment profile, but this effect can be dampened by ensuring the verticality of the corer as it impacts the sediment so that the shear stress on the sediment layers is minimised (Glew et al., 2002). Once carefully retrieved, a core is then immediately (or shortly after) extruded into evenly divided samples for easier transport (Glew et al., 2002). This process is known as sectioning and is done as separating the core into equal intervals (typically ranging from 0.5 – 1.0 cm thick), allows them to be more easily assigned a rough date of deposition (Smol, 1981).

The second major element of paleolimnology is radiometric dating, which establishes a chronology (i.e. assigning a specific date of deposition to a particular sediment interval), to the sediment core. Radiometric dating is based on analyses of the quantity of certain trace radioactive elements (i.e. the unstable isotope of an element, meaning they share an atomic number or proton count with a stable element, but have differing amounts of neutrons in the nucleus, and are referred to as radioisotopes or radionuclides), that become deposited in succeeding layers of lake sediments (Appleby, 2002). Due to the imbalance in their atomic nucleus, radionuclides eventually undergo radioactive decay, releasing radioactive particles, and transform into an entirely different element which may also be radioactive (i.e. an element with a different atomic number, and is also known as a daughter isotope). Over time, this results in a loss of mass for the original radionuclide at an exponential rate, and an increase in the quantity of daughter isotopes. The rate at which each specific elemental isotope decays is unique, with the amount of time it takes for each unique radioisotope to halve its original mass referred to as the half-life. The second element of paleolimnology therefore hinges on the fact that among the materials that become incorporated into lake sediments are traces of radionuclides, both naturally occurring and from the impacts of human activities (Björck & Wohlfarth, 2002). As radionuclides become deposited in a lakebed, and are then overlain by succeeding layers of sediments, the quantities of radionuclides in the previously topmost layers cease to be replenished in mass from external sources and begin to be irreversibly decline as they decay into their daughter isotopes. Consequently, the age of any given sedimentary layer can be approximated by comparing the mass of the radionuclide material that remains, to the mass of the daughter isotopes present, and modelling the change in mass and the known half-life of the radionuclide over the sediment profile (Appleby, 2002).

The three commonly used radioisotopes used in Arctic paleolimnology (and which this thesis used) are: ^{210}Pb (lead-210; half-life 22.3 yr), a naturally occurring isotope of lead, ^{137}Cs (caesium-137; half-life 30 yr), an isotope of caesium that is most commonly produced as one of the fission products of various isotopes of uranium, and ^{14}C (carbon-14; half-life 5730 yr), a naturally occurring isotope of carbon, which is constantly created in the Earth's upper atmosphere via the interaction of cosmic rays with ^{14}N (Björck et al., 2002). Of these three radionuclides, ^{210}Pb is the most popular, due to its perceived reliability and accuracy, however due to its comparatively short half-life of ~22.3 years, it can only be used to date relatively young (~150 yr) sediments (Appleby, 2002; Jia et al., 2018). ^{210}Pb is formed by the radioactive decay of naturally occurring ^{238}U (uranium-238), which first decays into ^{230}Th (thorium-230), then ^{226}Ra (radium-226), ^{222}Rn (radon-222), and eventually ^{210}Pb; these precursor radionuclides are referred to as the parent isotopes of ^{210}Pb (Krishnaswamy et al., 1971; Appleby, 2002). ^{210}Pb itself decays into ^{210}Bi (bismuth-210), then ^{210}Po (polonium-210), and eventually back into lead, specifically the substantially more stable lead-206 or ^{206}Pb, which has a half life of ~4.5 billion years (Anokhina et al., 2008). Within the context of paleolimnology, we differentiate between ^{210}Pb of allochthonous deposition (typically of atmospheric precipitation), which is referred to as excess or unsupported ^{210}Pb, and ^{210}Pb that is autogenically produced in sediment (referred to as supported) via decay of any of its parent isotopes (primarily in-situ decay of ^{26}Ra) that are also in the lake sediments (Appleby, 2002; Barescut et al., 2011). Quantitatively, the mass of unsupported ^{210}Pb is derived by subtracting supported ^{210}Pb activity from total ^{214}Pb activity, and the ratio between unsupported and supported forms the basis of ^{210}Pb dating (Smol, 2008; Sanchez-Cabeza & Fernández, 2012; Vaikutienė et al., 2017). However, the estimates derived from ^{210}Pb dating are never used on their own, and are typically paired with estimates from ^{137}Cs dating, itself almost exclusively used only to validate ^{210}Pb based chronostratigraphies (Appleby, 2002; Björck et al., 2002). This is because although ^{137}Cs traces in sediments can sometimes be the product of naturally occurring fission of ^{238}U, the vast majority of ^{137}Cs sediment deposits are the result of anthropogenic fission of ^{235}U (uranium-235; half life 703.8 million yr), specifically as fallout from testing of thermonuclear weaponry between 1954 – 1963, which provides a distinct historical reference in the stratigraphic record from which dating estimates can be calibrated (Appleby, 2002; Barsanti et al., 2020). However, any use of ^{137}Cs estimates in radiometric dating must always consider the possibility of contamination from later incidences of substantial fallout, such as the Chernobyl accident in 1986, which may make calibrations seem younger than they really are (Appleby, 2002). ^{14}C is primarily reserved for dating of ancient (up to 40 000+ years old) deposits and organic materials (Björck et al., 2002). This is primarily due to its considerably longer half-life, but also because ^{14}C dating can be very easily skewed by the lake reservoir effect; this occurs if the lake experiences inputs of carbonates containing older, previously isolated traces of ^{14}C, which, due to the aqueous environment, may contaminate and dilute ^{14}C concentrations in lake sediments, causing them to be dated much older than they really are (Philippsen et al., 2013).

Once isotope ratios have been established for each sediment interval, an age-depth model that relates isotope ratio values with sediment depth using the known half-life can be used to estimate dates from the reference date established by ^{137}Cs (Appleby, 2002; Baud et al., 2022). The three main age-depth models commonly used by paleolimnologists are the constant flux constant sedimentation (CFCS) model, constant initial concentration (CIC) model, and constant rate of supply (CRS) model, each of which have their own flaws and assumptions and so must be carefully chosen to best accurately model the relationship between sediment depth and age on a case-by-case basis (Baud et al., 2022). The CFCS model assumes an ideal (i.e. constant but unrealistic) rate of sediment accumulation and ^{210}Pb deposition has occurred throughout the entirety of the core (Baud et al., 2022). The CIC model assumes that some unsupported ^{210}Pb is being replenished from parent isotopes in the lakebed sediments but can also account for uneven rates of sediment deposition, which makes it ideal for sediment cores which may have experienced discontinuities (Baud et al., 2022). The CRS model is the most popular of the three models, and is the one used in this thesis (Abulu, 2024). The popularity of the CRS model lies in that it realistically assumes sedimentation rates may vary over time; however, it also assumes that the amount of unsupported ^{210}Pb that becomes deposited in the lakebed over time also remains at a relatively constant rate (Baud et al., 2022).

Although radiometric dating has long been an essential element to paleolimnology, it can be affected by many factors which can distort date estimates and how we reconstruct past environmental conditions (Björck et al., 2002). Some of these, such as uneven or intermittently interrupted sedimentation rates caused by sediment focusing, a phenomenon in which sediments may be redistributed from shallow regions to deeper areas following initial deposition, and which alters how much trace radionuclides are deposited and therefore impact dating (Crusius & Anderson, 1995; Hermanns & Biester, 2013), can be mitigated by selecting an appropriate age-depth model that can account for these discrepancies (Baud et al., 2022). Others, such as improper storage of sediment samples, could lead to bacterial growth that causes atmospheric exchange of trace radionuclides with those in the sediment samples, skewing dating estimates (Björck et al., 2002). However, there are also sources of error which are not so easily remedied, including post-burial processes like bioturbation (mixing of the sediments by organisms), which may cause quantities of trace radionuclides in the sedimentary layers to no longer reflect their original deposited quantities, skewing dating efforts (Björck et al., 2002).

The third major component of a paleolimnological approach is the usage of different techniques and methodologies to qualitatively and quantitatively analyse the physical evidence (often called indicators or proxies) of the past climate, environment, and ecology of the lake (Smol, 2008; Davidson et a., 2018). These analyses can be divided into two main categories: analyses of the sediment geochemistry (organic or inorganic), and analyses of bioindicator fossils (Smol, 2008; Davidson et a., 2018). Geochemical paleolimnological analyses include a vast diversity of different techniques and methods but are defined by their focus on the chemical and physical properties of the lake sediments (Smol, 2008). Some geochemical analyses can be very simple, such as visual inspections of the colour, and texture (or particle size classifications, e.g. clay = < 0.002 mm; silt = < 0.004 mm; sand = 0.06 – 2 mm; gravel = > 2 mm), which can inform our understanding of the geomorphological history of the lake and its relative surroundings (Last, 2002; Smol, 2008). For example, fine black sediments are either basaltic tephra from a volcanic eruption, or ash indicating a wildfire (Smol, 2008), whereas a layer of sand may be evidence of a past flood (Biskaborn et al., 2013), and alternating layers of quartz-rich silt and sand may be sediment inputs from thaw slumping (Boyle, 2002). Paleolimnologists might also look out for the presence of fly-ash particles, a broad grouping of various types of particulate products emitted by the combustion of fossil fuels at very high temperatures (1750 °C), which include spheroidal carbonaceous particles (SCPs), and inorganic ash spheres (Rose, 2002). A distinctly artificial product, fly ash particles, especially SCPs are broadly useful as markers of the spatial distribution of and when a region might have started to be impacted by pollutants like heavy metals and sulfur, as byproduct of industrialisation and fossil fuel usage (Wik & Renberg, 1996). However, because fly-ash particles are extremely fine due to the high temperatures they were created under, they cannot be viewed easily with the naked eye and may require scanning electron microscopes for proper viewing (Rose, 2002).

However, other types of analyses of sediment geochemistry, particularly those focusing on specific environmental variables or parameters, and which require a quantitative aspect may require more dedicated laboratory equipment. For example, sediment water content (required to calculate bulk density for accurate sediment core dating), is derived by comparing the wet and dry weights of sediment samples from before and after drying, often in an oven, but also sometimes via freeze-dryer (Sugisaki et al., 2012; Sanchez-Cabeza & Fernández, 2012; Bertrand et al., 2024). Similarly, the organic and carbonate content of sediment samples, which may be useful indicators of productivity (see Heiri et al. 2001; Korosi et al. 2024), can be derived by comparing the weight of samples before and after combustion (a process known as 'ashing' or Loss on Ignition (LOI), typically at temperatures between 925 - 1000°C) in a special furnace (Smol, 2008; Bertrand et al., 2024). More advanced devices like X-ray fluorescence and mass spectrometers are required to identify concentrations of elements, and ratios of elements throughout the sediment profile (Boyle, 2002; Smol, 2008). Some of the most common elements studied via geochemical analyses are carbon (C), nitrogen (N), and phosphorus (P), as they are essential nutrients that drive in-lake productivity, and changes in their concentrations over time throughout the sediment profile reflect landscape and water quality changes (Smol, 2008; Moyle & Boyle, 2021). For example, the balance between carbon and nitrogen (C:N ratio) can be used to differentiate periods when the organic inputs in a lake were dominated either by allochthonous or autochthonous inputs (Smol, 2008). This is because the cells of terrestrial vascular plants often contain complex structurally supportive organic polymers like cellulose ($C_6H_{10}O_5$) so that they don't collapse under their own weight on land, whereas due to their buoyant aqueous, comparatively more nitrogen-rich medium, the cells of aquatic macrophytes and algae mostly contain just proteins (Hu et al., 2021). Consequently, terrigenous organic sediments can be identified from their relatively high (>= 20) C:N ratio values, compared to the more nitrogen-rich organic sediments produced during times when in-lake algal production is the dominant source of productivity, which are characterised by relatively low (4 – 10) C:N ratio values (Meyers & Teranes, 2001; Li et al., 2022). Analyses of C:N ratios are often additionally paired with examinations of the ratios of stable isotopes like $\delta^{13}C$ and $\delta^{15}N$ (Meyers et al., 2001). $\delta^{13}C$ is based on the ratio of concentrations between ^{13}C, and ^{12}C, and are used to distinguish the main types of vegetation (e.g. C3 vs C4) contributing to the organic sediment inputs, as well as a proxy for land use changes (i.e. clear-cutting of forests and conversion to farmland) (Meyers et al., 2001; Holtvoeth et al., 2019). Similarly, $\delta^{15}N$ is also based on the ratio of concentrations between ^{15}N, and ^{14}N, with higher $\delta^{15}N$ values known to be positively correlated with the presence of organisms that have high trophic levels (i.e. predators, and or humans) making it a useful for reconstructing changes in past food chains (Perkins et al., 2014), including historical trends in salmon populations (Dagodzo et al., 2025). As these stable isotope ratios are derived from organic residues of biological origin, some of which are relatively recalcitrant, it may be possible to analyze some of these compounds more directly, such as certain plant biomarker molecules (e.g. aliphatic hydrocarbons (n-alkanes), carboxylic acids (n-alkanoic acids), n-alkanols, and sterols), which can be unique markers for different taxa, and therefore may be able to provide further information on past changes in the ecology of the lake and surrounding watershed (Meyers, 2003).

Although sediment geochemical markers are a powerful paleolimnological tool, they can also be limited in their ability to reconstruct certain information types, such as water quality parameters like past levels DOM/DOC, which are especially tricky due to the relatively high lability of organic compounds (Hanson et al,. 2011). In general, only a fraction of the organic matter in the water column at any given time becomes incorporated into lake sediments, and the rest is either mineralized through photodegradation or microbial respiration (Peter et al., 2016; Li et al., 2019), or exported downstream (Hanson et al,. 2011). Moreover, the DOM/DOC that does becomes part of lake sediments has a propensity to diffuse back into the water column and undergo further transformations (Peter et al., 2016). One method is to simply analyze other more recalcitrant sediment organic compounds which indirectly correlate with past levels of in-lake DOC, such as chlorophyll-a (Chl a), which can be reconstructed via visible-near-infrared spectroscopy or VNIRS (Michelutti et al., 2010; Rouillard et al., 2011). Much like the mass spectrometers and X-ray fluorescence spectrometers used for analyses of elemental concentrations and elemental ratios (Boyle, 2002; Smol, 2008), VNIRS is also based upon the science of analysing the spectral signature of emissions reflected from a sediment sample, specifically light emissions in the visible to near-infrared (400 – 2500 nm) regions of the electromagnetic spectrum (Wallace et al., 2009; Rouillard et al., 2011; Favot et al., 2020), and has similarly been used to infer elemental C, N, P, as well as total phosphorus (TP), pH (Korsman et al., 1992), and even cyanobacterial abundance albeit indirectly from traces of pigments like chlorophyll-a, and various xanthophylls and carotenoids in the sediments (Favot et al., 2020). VNIRS operates on the basis that for any given lake, at time of burial, certain relatively recalcitrant organic residues (i.e. specific proteins, lipids and or pigments) become incorporated into the sediments, and have a distinctive spectral signature in the VNIR spectrum, and which have a unique correlation with total organic carbon (TOC) content in the water column which can then be mathematically modeled (i.e. a transfer function), to quantitatively infer past DOC concentrations from spectral signatures (Nilsson et al., 1996; Rosén, 2005). However, such a transfer function must be calibrated using a combination of multivariate statistics like partial least squares regression and a pre-existing dataset of the known relationship between the specific sediment NIRS signature and DOC levels of a lake(s), derived from practical data (Rosén, 2005; Rouillard et al., 2011).

While VNIRS-based analyses would be of interest to this thesis as it also focuses on the impacts of changes in in-lake organic carbon concentrations and water quality on light regimes, albeit indirectly, recent studies of DOC quality in the southern Dehcho show an unusual decoupling between the traditionally assumed positive correlation between DOC and lake colour (Coleman et al., 2025). This indicates that the transfer function, and calibration dataset (i.e. Canadian Arctic Calibration Lakes set; CAC) developed and used by Rouillard et al., (2011) for inferring past DOC in Arctic lakes, may not be applicable to SC11 and other lakes in the southern Dehcho, which would need their own calibrated transfer functions and associated lake dataset to accurately reconstruct past DOC concentrations, specifically one focusing on wavelengths shorter than 500 nm to better account for the tendency of coloured or chromophoric DOC to absorb wavelengths in VNIR region of the spectrum (Jiang et al., 2014). VNIRS-based paleolimnological approaches are relatively new (Rosén, 2005; Rouillard et al., 2011); more often, DOC has been and often continues to be analyzed by multi-proxy approaches, but these are often time-consuming and are limited by the practicalities of obtaining sufficient sediment samples (Birks & Birks, 2006). As an alternative to using multiple geochemical proxies which can be time-consuming and expensive to analyze (Birks et al., 2006), DOC is now more commonly inferred via bioindicators known to be sensitive to such water quality changes (Saros et al., 2012; Brown et al., 2017), though the reliability of such methods can sometimes be confounded by other environmental variables (Korsman and Birks 1996; Roseacute;n et al., 2000; Saros et al., 2016).

Due to these challenges in directly analyzing past changes in cDOM-driven changes in light availability, this thesis utilised the other aspect of the third element of paleolimnological approaches; the reconstruction of past environments through study of paleo-bioindicators – the parts or remains of past assemblages and or biota that once lived in and around the lake, and inferring information about past environments based on their known ecology (Smol, 2008). Organisms often have specific climatic, and environmental requirements, and respond to changes in their habitat in terms of changes in population and or presence (Smol, 2008). This ecological change then becomes similarly reflected in the stratigraphic record as shifts in the abundance of and or presence of their remains (and or other anatomical parts that preserve well in the sediments), across different strata, which can be interpreted as indirect indicators of climatic and environmental changes, and can therefore be referred to as paleo-bioindicators or bioindicators for short (Smol, 2008; Davidson et a., 2018).

However, it should be noted that although bioindicators represent an extremely powerful paleolimnological tool, it also requires carefully selecting the appropriate type or species to be used effectively to reliably reconstruct the past. Indeed, not all organisms (and their remains) are useful bioindicators; such taxa must have distinctive and easily identifiable features (which are also durable enough to survive post-burial processes), as well as very specific or sensitive ecological requirements, as that allows for discrete conclusions about select aspects of past environments (Smol, 2008). While this may limit the number of environmental variables and parameters which can be reconstructed, this can be remedied by using additional species or coupling bioindicator-based analyses with geochemical analyses to more holistically integrate a broader picture of the entire ecosystem into the reconstruction, often called a 'multi-proxy' approach (Birks et al., 2006; Davidson et a., 2018). A key assumption in the use of paleo-bioindicators is that the ecological and environmental sensitivities of the organisms whose parts or remains are used have changed little since their burial, often with little consideration for any potential adaptations or variation along environmental gradients, or the confounding effects of other factors with indirect effects; this assumption is what allows for reconstruction, as the ecological responses of their modern equivalents can be defensibly projected onto the past (Burge et al., 2018).

As with geochemical analyses, there are many kinds of bioindicators that can and have been used in paleolimnology (Smol, 2008). One of the most popular such bioindicators is pollen (Chevalier et al., 2020), a fine powder-like organic material released from male flowers for the purpose of plant reproduction which can easily be scattered on a wide scale by wind patterns due to their small size (Campbell et al., 1999; Gajewski, 2006). Each pollen grain is covered in an extremely tough biopolymer known as sporopollenin, and is ornamented with unique designs and features distinctive to each plant species, allowing individual pollen grains to preserve well in lake sediments, as well as be easily identified once extracted, allowing for reconstructions of past plant assemblages of entire regions (Brugger et al., 2019; Chevalier et al., 2020). When combined with other lines of evidence, such as geochemical markers, and data on different plant species or assemblages' environmental preferences, pollen can also be used to reconstruct past climate changes though only on a regional scale as pollen can be transported across very long distances (Peros & Gajewski, 2009; Brugger et al., 2019; Chevalier et al., 2020).

Other bioindicators consist of the remains of the living organisms that once lived within the lakes and so can provide not just insight into the climate and environmental conditions at time of burial, but also the conditions within the lake itself (Smol, 2008). For example, one of the more commonly used paleolimnological bioindicators are a genus of aquatic microcrustaceans known as water fleas or Cladocerans (of the class Branchiapoda), which can be identified in lake sediments from parts of their distinctive chitinous exoskeletons (e.g. shells, heads, abdomens, and claws; Korhola & Rautio, 2001). Individual species of cladocerans have differing environmental tolerances and preferences, and changes in the level of diversity in the cladoceran assemblage have been used as indicators of climate change, acidification, and changes in water level, food webs, and lake productivity (Korhola & Rautio, 2001; Jeppesen et al., 2001).

Another crustacean used as bioindicators are ostracods, or 'seed shrimp', so named for their extremely small (ranging from 0.2mm to slightly greater than 1mm) size (Ito, 2001). Ostracods can be identified in lake sediments from their chitinous calcium rich bivalve-like shells, which they repeatedly molt out of over the course of their life cycle (Wang et al., 2021), and which incorporate trace elements like magnesium and strontium, as well as isotopes of oxygen ($\delta^{18}O$) and carbon ($\delta^{13}C$) (Ito, 2001). Ostracods have been used to infer a variety of water quality and environmental variables, including water levels (Alivernini et al., 2018), salinity (specifically concentrations of sodium, potassium, strontium, and calcium), temperature, and pH (D'Ambrosio et l., 2017; Iwatani et al., 2018; Mischke et al., 2010). The stable isotopes of $\delta^{18}O$, and $\delta^{13}C$ that were incorporated into their exoskeletons, have even been used to extract information about the past precipitation and hydrology of sampled lakes (Ito, 2001).

Although not entirely aquatic, another kind of commonly used paleolimnological bioindicator are the remains of various insects from the order Diptera (true flies), particularly the larval remains of non-biting midges (Chironomidae). Chironomids and other members of Diptera are aquatic during their larval stage and the remnants of their chitinous head capsules both preserve well and are easily identifiable by their distinct features in lakes sediments (Walker, 2001). Additionally, different species of chironomids are highly sensitive to different water quality parameters and pollution, depending on the species and have been popularly used as proxies for the reconstruction of several water quality parameters, including lake productivity and eutrophication, oxygen concentrations, and pH, as well as past climates (Walker, 2001; Robertson et al., 2025).

The remains of freshwater fishes have also sometimes been used as paleolimnological bioindicators (Patterson & Smith, 2001), as many freshwater fish species are highly sensitive to water temperature changes, with different species having specific thermal ranges and limits (Guzzo et al., 2017), and are highly responsive to other water quality variables such as water levels, salinity, and oxygen concentrations (Patterson & Smith, 2001). Despite their strong responses to environmental changes, freshwater fish have had comparatively low popularity as bioindicators, due to the tendency for their remains to be susceptible to taphonomic processes, and so rarely leave behind subfossils of sufficient fidelity for study (Elder & Smith, 1988). For example, following death, fish carcasses can become suspended in the water column by the gases produced by decay, interrupting incorporation into the sediment, and increasing the likelihood of water currents moving the remains, and either breaking or scattering the skeleton and other relatively recalcitrant parts (i.e. scale, teeth, etc.) into fragments (Elder & Smith, 1988). As paleo-bioindicators, fish remains have either been quantitatively analysed via stable isotopes (e.g. $\delta^{18}O$ and $\delta^{13}C$) extracted from surviving fragments of remains, such as bones and otoliths (aragonitic structures found in the ‘ears’ of fish), from which water temperature or lake levels can be reconstructed (Patterson & Smith, 2001; Reinthal et al., 2011), or qualitatively analysed in terms of ecology, with the presence, disappearance, or introduction of certain species throughout the sedimentary profile itself being broadly indicative of ecological and environmental changes (Patterson & Smith, 2001). More recently, there have been growing advancements in the extraction and interpretation of environmental DNA (eDNA) from fish in lake sediment samples, primarily to perform the latter type of inference about past environments (Stager et al., 2015).

In this thesis, we focused on the usage of diatom subfossils as bioindicators. Diatoms (class Bacillariophyceae) are a grouping of unicellular microscopic algae (i.e. ranging from 20 to 200 µm; may also be referred to as microalgae) uniquely characterized by their siliceous (i.e. composed of silicon dioxide; SiO_2) cell walls, and which are found in and have adapted to a wide variety of aquatic ecosystems and conditions (Battarbee et al., 2001). Diatom taxa can often respond quickly to even small deviations from their individual environmental tolerances and preferences and due to their silicious cell walls, preserve well in lake sediments (Battarbee et al., 2001). Consequently, the remains of diatom assemblages have long been used as bioindicators to track changes in climate and water quality including in lake water pH, temperature (Battarbee et al., 2001; Smol & Douglas, 2007), as well as most relevantly to this thesis, changes in light availability such as the impacts of brownification (Korosi et al., 2015; Coleman et al., 2023; Tichá et al., 2023).

2.3.1. Diatom subfossils as indicators of light regime shifts and other environmental changes in aquatic ecosystems

Diatoms, or rather more specifically, the remains of diatom assemblages are one of the more popular bioindicators used in paleolimnology (Battarbee et al., 2001). The remains of diatom assemblages have been used to provide evidence that climate change was impacting the circumpolar north, and its lakes far earlier than previously believed (Smol et al., 2005; 2007), and they continue to be an important tool in monitoring how lake ecosystems in the Arctic are responding to recent climate change impacts (Rühland et al., 2015; Coleman et al., 2023; 2025; Korosi et al., 2022). The usage of diatoms and diatom assemblages as bioindicators of past climates and lake environmental conditions is predicated on two elements; their unique anatomy, specifically their siliceous cell walls, and their ecology, as diatom taxa are known to have strong discriminatory responses to even slight changes in the environment (Battarbee et al., 2001).

Each diatom cell is structurally supported by a rigid cell wall referred to as a frustule, and which is made up of biogenic silica, and a mix of various proteins, polyamines, and polysaccharides (i.e. carbohydrate polymers), which can be found both in the structure of the frustule, and in layers coating the surface (Le Costaouëc et al., 2017). The siliceous nature of the diatom frustule makes it relatively durable, and perhaps most critically to the needs of paleolimnology, cannot decay following burial in lake sediments, though there can be a risk of fragmentation (Battarbee et al., 2001). The process by which diatom assemble their siliceous frustule (referred to as diatom silicification), is thought to involve harvesting dissolved silicon (specifically silicic acid; SiO_2*H_2O) from the water column, which is then carefully arranged and precipitated from inside the diatom cell, though there is evidence that at least some taxa (e.g. *Chaetoceros*) build their frustules along a scaffold formed from long whisker-like appendages called seta (Mayzel et al., 2021). Each frustule is composed of two overlapping nearly identical morphological halves, referred to as valves (or thecae), joined together by a 'girdle band', though one valve is generally slightly larger (referred to as the epitheca or upper theca), with the smaller being the hypotheca or 'lower' valve (Round et al., 1990). Diatoms can reproduce both sexually and asexually, with the latter occurring via binary fission, in which the two valves split apart from each other, and grow new theca; as this process results in the original hypotheca valve becoming the new 'epitheca' valve, diatom asexual reproduction results in considerable variation in frustule size even across members of the same taxa (Schmid, 1987), which can be a source of some confusion during paleolimnological analyses.

Though diatom frustules are essentially made of glass, they can also be extremely morphologically diverse (i.e. some frustules are round like disks while others resemble seeds), and are often highly intricately patterned with pores (holes that allow for nutrient and waste exchange; also known as areolae), which can be arranged into lines (called striae), and a variety of other details like slits (called raphes), spines, and ridges (Spaulding et al. 2021). Diatom morphological diversity is the primary basis for their taxonomic classification from which can then be further distinguished based on the presence and or absence of certain ornamentation (Battarbee et al., 2001; Spaulding et al. 2021). For example, several of the main diatom classes are ‘centrics’ (round disk like diatoms with radial symmetry), ‘monoraphids’, diatoms with a single raphe running down the axis, and ‘biraphids’, diatoms with two raphes, each running down half of the axis, and which can be symmetric and asymmetric (Spaulding et al. 2021). As biogenic silica does not decompose, diatom frustules, and their ornamentation can stay relatively unchanged post-burial, which can allow the exact taxa composition of past diatom assemblages to be easily reconstructed (Battarbee et al., 2001).

The second aspect of diatoms that has made them so invaluable to paleolimnology is their extremely diverse ecology. As a form of highly adaptable photosynthetic microalgae, diatoms have colonized a wide range of freshwater and marine habitats and may account for as much as 20% of Earth’s total primary production (Malviya et al., 2016). The exact number of diatom taxa that exist is uncertain, as is their exact taxonomic interrelationships (Smol, 2008), though ~10,000 – 30,000 have been described (Guiry, 2012), with up to ~200,000 taxa estimated to potentially exist (Wang et al., 2022). Just as diatom taxonomy can be organized according to morphology, so too can they be described according to their niche; diatoms are generally divided into planktonic (i.e. diatom taxa that survive primarily suspended in the water column), and benthic (i.e. diatoms that live on or near the ocean, lake and or stream bottom, also known as the benthos), while taxa that can live in either are referred to as tychoplanktonic (Battarbee et al., 2001). Benthic diatom taxa can be further subdivided by the substrate they live on; epiphytic taxa attach themselves to macrophytes (typically via mucilaginous stalks), epilithic taxa colonize rock surfaces, and epipelic and episamnic taxa live on mud and sand respectively (Battarbee et al., 2001; Štefková, 2006; Spaulding et al. 2021; Laird et al., 2023; Coleman et al., 2023). Though diatoms are unicellular, there are even taxa (e.g. *Aulacoseira* spp., and *Fragilariaceae*) that can use their spines link together into pseudo-colonies to better float and survive (Battarbee et al., 2001). Though diatoms as a whole might be able to inhabit a diverse range of habitats, individual taxa and genera often have very specific and distinct climatic and environmental niches and tolerances, outside of which they will quickly die off; coupled with relatively short lifespans and rapid rates of reproduction, diatom assemblages can respond rapidly to even small changes in terms of shifts in the abundance of specific taxa, which become reflected in sediments with their remains as evidence from which we can reconstruct the past (Battarbee et al., 2001).

Certain diatom taxa therefore have been used extensively by paleolimnologists as biological proxies to reconstruct past changes in climate, and environmental and water quality conditions, including changes in temperature, growing season length, ice cover, thermal stability and stratification (i.e. the tendency for lakes to separate into distinct layers of differing density and temperatures owing to uneven heating), pH, and salinity which directly affect the availability of light and nutrients, which are the key limiting factors in the growth and ability for photosynthetic algae like diatoms (Smol, 2008; Rühland et al., 2015). For example, one of the most well-known diatom taxa shifts that have been observed by paleolimnologists in subarctic and temperate lakes is the classic *Cyclotella-Aulacoseira* transition which is a broadly qualitative indicator of changes in climate and mixing regimes (Rühland et al., 2015). *Cyclotella* are a type of small-celled centric planktonic species, while *Aulacoseira* are a type of large and heavy centric tychoplankton; when a lake undergoes climate warming, which can reduce ice cover duration and lead to longer periods of thermal stratification with reduced mixing, the *Aulacoseira* taxa which depend on high levels of turbulence to stay within the photic zone will sink, decreasing abundance, outcompeted by the lighter *Cyclotella* which will increase their relative abundance (Rühland et al., 2015). Diatom taxa have also been used to quantitatively reconstruct pH using transfer functions, as pH is known to strongly influence diatom growth and nutrient uptake (Birks et al., 1990; Battarbee et al., 2001), though there has been growing recognition of the limits of such quantitative transfer-function based reconstructions of past lake environmental conditions, due to the inability to separate the specific impacts of the variable(s) being reconstructed from those that are simply correlated, but non-causal, and or the confounding effects of other factors (Juggins, 2013).

In this thesis, we used diatoms as qualitative bioindicators tracking changes in light availability, to reconstruct a contextualized history of reductions in water clarity at SC11 that were potentially due to brownification. As a type of photosynthetic microalgae, diatoms are inherently highly sensitive to changes in light availability in the water column, and most diatom species, save for those few species known to be able to adapt to low light, will be negatively impacted by reductions in water clarity (Rühland et al., 2015). For example, there is considerable literature on how diatom assemblages have historically responded to seasonal changes in the extent and duration of lake ice cover, as well as their more recent response to the impacts of climate warming on like ice since the 20th century (Lotter & Bigler, 2000; Rühland et al., 2008; Zepernick et al., 2024). Lake ice cover refers the perennially re-occurring layer of ice often found in many temperate, subarctic, and arctic lakes in winter, during which the lake habitat underneath typically has limited light availability, which often favours and increases the abundances of small benthic *Fragilariaceae* taxa. *Fragilariceae* are a type of araphid bilaterally symmetrical diatom (Spaulding et al. 2021), known for being able to survive in low light conditions, which would be intolerable for most other diatom taxa (Rühland et al., 2015). Benthic *Fragilariaceae* taxa previously identified in the lakes of the Dehcho permafrost peatlands by Coleman et al., (2023) included *Pseudostaurosira brevistriata*, *P. parasitica*, *Staurosira construens*, and *S. venter*. In North American lakes, recent warming has resulted in winters with shorter ice cover durations and have led to many northern lakes experiencing decreases in small benthic *Fragilariaceae*, and concurrent increases in small-celled planktonic *Cyclotella* in the sediment record (Smol et al., 2007; Rühland et al., 2015). Similarly, lakes undergoing eutrophication (i.e. an overgrowth of in-lake algal production due to an excess of nutrients; Smith et al., 1999), also experience decreased light availability, and exhibit similar shifts towards increased *Fragilariaceae* abundance and decreased abundances of *Cyclotella* (Smol et al., 2005; Rühland et al., 2015). Increases in DOC, and brownification which may be associated with conditions of reduced clarity and light availability may therefore be analogous to incidences of limited light available during periods of increased ice cover, and thus similarly result in increases in the abundance of small benthic *Fragilariaceae* as indicators of reduced light availability and brownification (Lotter et al., 2000; Korosi et al., 2015; Brown et al., 2017; Coleman et al., 2023; 2025).

CHAPTER THREE: MATERIALS AND METHODS

3.1. Field and laboratory methods

3.1.1. Sediment core extraction and preparation

The sediment core from SC11 used in this study was originally collected on July 13, 2018, as part of a survey of sixteen small shallow lakes in or near the Scotty Creek Basin (SCB) (Coleman et al., 2023). Sampled lakes were accessed via a helicopter on pontoons, with water and sediment samples collected from the approximate centre of the lake. A sediment core was extracted from SC11 using a Uwitech gravity corer with an internal diameter of 8.6 cm. (Coleman et al., 2023). As the focus was on studying the impacts of relatively recent (i.e. ~1850 - present) changes to lakes in the Dehcho, gravity corers were used as they were considered least likely to disturb the more germane shallow sediments during the process of sampling, which were more fragile due to their higher water content (Blomqvist, 1991; Glew et al., 2001). A modified Glew (1988) extruder was used to section the collected sediment core into 0.5 cm intervals for the uppermost 20 cm of the sediment core, and then at intervals of 1 cm thickness from 20-28 cm. The sediment core was sectioned on the day of collection to minimize post-extraction sediment mixing. Sectioned sediment intervals were shipped frozen to York University in individual Whirlpak™ bags and stored frozen until analysis (Coleman et al., 2023).

3.1.3. Sediment core chronology

As this thesis examined a sediment core extracted from SC11 which was previously analyzed from the perspective of geochemical proxies (Abulu, 2024), we reused the relevant previously established chronology data for the same sediment core, using the Constant Rate of Supply (CRS) model, which is based on ratios of unsupported ^{210}Pb and supported ^{210}Pb (assumed equal to ^{214}Pb), determined using gamma spectroscopy (Appleby 2001). Freeze-dried sediment samples from the SC11 sediment core were shipped to the Paleoecological Environmental Assessment and Research Lab (PEARL) at Queen's University for analysis of radioisotopes using an Ortec High Purity Germanium Gamma Spectrometer (Oak Ridge, TN, USA), and establishment of a CRS-model chronology using ScienTissiME software (Abulu, 2024). ^{137}Cs was also measured as independent verification of the chronology of SC11 (Appleby, 2001; Abulu 2024).

3.1.4. Diatom slide preparation

Diatom-enriched slurries for the creation of microscope slides were prepared following the methodology outlined by Battarbee et al., (2001). Approximately 0.5 g of wet sediment was weighed out and placed into 20 mL labelled glass scintillation vials (one for each depth interval analyzed, from 3 - 3.5 cm to 27 - 28 cm, for a total of 26 vials). Soluble inorganic compounds such as carbonates and metallic salts and oxides were removed from the sediment samples via treatment by 10% hydrochloric acid (HCl) and allowed to settle for over 24 hours. The HCl-treated samples were then siphoned and rinsed with deionized water 7 times over several days, with the samples allowed to rest for 24 hours between each siphon-rinse cycle, until circumneutral. The neutralized vials of sediment solution were then treated with 30% hydrogen peroxide (H_2O_2) to remove the organic matter fraction of the sediment samples and partially submerged in a hot bath set at 70 °C for 8 hours, with H_2O_2 added to the samples periodically as necessary to ensure complete digestion of organic matter while being monitored to prevent overflow. Following the 8-hour digestion period, the diatom enriched slurries were again repeatedly siphoned and rinsed with deionized water 7 times over several days, the samples allowed to rest for 24 hours between each siphon-rinse cycle, until circumneutral.

The diatom slurries were gently mixed in each vial by pipette suction, before subsamples from each vial were siphoned into sterilized glass tubes. The mixing was performed so that the subsamples would not be biased toward diatoms of certain sizes and weights during the pipetting. The subsamples were then diluted with distilled water to create diatom slurry solutions of different dilutions. Slides for intervals from 3 – 3.5 cm to 19.5 – 20 cm had four different dilutions, labeled 'A', 'B', 'C', and 'D', of increasing dilution (i.e. dilution 'A' had 5 mL of water added, while dilution 'B' had 10 mL of water added etc.). Slides deeper than and including 20 – 21 cm were observed to have a high density of diatoms in the initial dilutions, resulting in overcrowding that obscured taxonomic identification. Therefore, additional dilutions made with correspondingly greater quantities of distilled water labeled 'E', and 'F' were created for the slides deeper than and including 20 – 21 cm. The diluted diatom slurries were then pipetted onto labeled coverslips and dried within a closed box at room temperature to prevent contamination from dust and other particulates over the course of a week. The slow drying process is used so that clumping of diatoms does not occur (Nagy, 2011). The coverslips with dried diatom slurry were then mounted onto glass microscope slides using a mixture of toluene and Naphrax® and heated via hot plate. Naphrax® is a synthetic resin product commonly used to mount diatoms for microscopy due to its higher refractive index (RI = ~1.7) compared to the siliceous frustules of diatoms (RI = ~1.5), which enhances the visibility of diatoms under microscopy (Nagy, 2011; Fleming, 1943, 1954). The heating serves to evaporate the toluene component, bonding the dried diatom slurry coverslip to the glass microscope slide. As toluene is a known respiratory irritant (Taylor et al., 2017), diatom slide mounting occurred within a well-ventilated fume hood.

3.1.5. Diatom valve counting

Diatoms were viewed through digital images of the diatom slides taken under an oil immersion lens at 1000x magnification, by a digital camera connected to a Leica DM2500 compound light microscope (https://www.leica-microsystems.com/). I sampled only diatoms found on continuous transects zig-zagged across the surface of the slide, to ensure a representative sample of diatom counts were collected, while minimizing size sorting effects arising from evaporation during the mounting process (Battarbee et al., 2001). Following similar protocols by Rühland & Smol (2005), if after a transect traversed the entirety of a slide but less than 400 individual diatoms were sampled, another transect would be initiated on another slide of the same interval, but different dilution, with the sampling process repeating until a minimum total of 400+ individual diatom valves was counted and imaged per sediment core interval. This minimum threshold of 400 individual diatom valves ensured statistically reliable and proportionately representative counts of the diatom assemblages of SC11 (Battarbee et al., 2001). Diatoms were identified to the species level whenever possible based on multiple reference texts (Krammer and Lange-Bertalot 1997, 1999, 2000, Fallu et al. 2002), with supplementary information on morphology from the website Diatoms of North America (https://diatoms.org/;

Spaulding et al. 2021), and updated taxonomical classification and naming from the database AlgaeBase (https://www.algaebase.org/; Guiry & Guiry, 2024). Diatom counts were logged as raw totals per taxon per interval in Microsoft Excel.

3.2. Data analysis

3.2.1. Diatom dataset processing and basic diversity analyses

Initially, a total of 172 taxa were identified, including both diatom species and genera across 25 families. Taxa from my dataset were then corrected to their most modern names and taxonomic classification based on taxonomical records from AlgaeBase (Guiry et al., 2024). For example, *Fragilaria pinnata sp. cf. var. acuminata* was reclassified as *F. pinnata var. acuminata*, *F. sp. cf. pinnata* was reclassified under *F. pinnata*, and *Caloneis undulata* was corrected to *C. undosa*, and *Pinnularia undulata* was recognized as synonymous with *C. undosa*, leaving a total of 169 taxa in the final diatom dataset. To reduce potential variation in diatom taxa counts from confounding factors such as poor preservation or changes in sediment accumulation rates, rather than true changes in diatom community production environmental shifts, all further analyses of the diatom assemblages of SC11 were conducted in percent relative abundance (Battarbee et al., 2001), calculated for each diatom taxa as a percentage relative to the sum of diatom valves counted. To examine how diatom taxon diversity and evenness changed over time at SC11, particularly before and after the low-carbon anomaly identified by Abulu, (2024) at the 8.25 cm depth, Shannon's (SDI) and Simpson's (SimpDI) Diversity Indices were calculated on raw counts for each depth-interval assemblage using built-in functions in R Studio (v4.3.3; R Core Team, 2024; v2023.9.1.494, Posit team, 2023), and plotted (Figure 5.). Diversity indices are a type of method of quantifying the number of different species in and or between communities or assemblages, which can be useful for conservation management purposes, with SDI and SimpDI being amongst the most popular (Peet, 1974). The SDI, sometimes referred to as the Shannon-Weiner Index quantifies biodiversity in a given community or assemblage and incorporates both species richness (i.e. number of species present), and evenness (i.e. the relative abundance of different species), by calculating the uncertainty of predicting the identity of a randomly sampled individual (Shannon, 1948), according to the following formula:

$$SDI = \sum_{i=1}^{S} \left(\frac{n_i}{N}\right) * ln\left(\frac{n_i}{N}\right)$$

where S is species richness, n_i is the number of individuals for a given species, N is the total number of individuals in the dataset, and ln() refers to the natural logarithm function (Shannon, 1948). The SimpDI, or Simpson's Index is a similar method of quantifying biodiversity but calculates the probability that two individuals randomly sampled from the community will be of different species as a value ranging from 0 – 1, wherein the higher the value, the more likely the sampled individuals will be of the same species (Simpson, 1949). SimpDI can be calculated according to the following formula:

$$SimpDI = \sum_{i=1}^{S} \left(\frac{n_i}{N}\right)^2$$

where S is species richness, n_i is the number of individuals for a given species, and N is the total number of individuals in the dataset (Simpson, 1949). Lastly, evenness indices (J) were also calculated for each depth-interval assemblage, derived from the previously calculated SDI values according to the formula:

$$J = \frac{SDI}{H_{max}}$$

where J is the ratio of SDI divided by H_{max}, which is the natural logarithm (ln()) of species richness (S) (Pielou, 1966), though the evenness indices were not plotted.

3.2.2. Diatom paleoenvironmental history – Stratigraphy and assemblage shifts

A stratigraphy was produced to show how abundances of identified diatoms have varied throughout the sediment profile in response to recent environmental and climatic changes at SC11, such as shifts in thermal stratification regimes and ice cover, and changes in turbidity (Rühland et al., 2015). A diatom stratigraphy is a type of microfossil record which plots the percent relative abundance of select diatom taxa against sediment depth (cm), with deeper layers corresponding to older sediments, which sometimes has a secondary axis attaching an established chronology (Smol, 1981). Since different diatom taxa have specific environmental tolerances, assemblages restructure in response to habitat changes, with changes in the abundance of specific diatom taxa in the stratigraphic record reflecting corresponding environmental and climatic changes at the time they were laid down in the sediment (Smol, 2002; 2005; 2008; Thienpont et al., 2013; Rühland et al., 2015). However, such information is only useful if contextualized with a chronology that attaches precise dates (with a degree of error), to specific sediment dates and by extension, changes in diatom assemblage (Appleby et al., 1986). As this thesis represents a continuation of previous studies on the water quality of the lakes of the southern Dehcho, which have included analyses of SC11, we reused the chronology dating (based on isotopes of ^{210}Pb, ^{214}Pb, ^{137}Cs) that had previously been established by Abulu, (2024) for the same sediment core.

To prevent overcrowding the stratigraphy of SC11's history with all 169 identified taxa, we plotted only the percent relative abundances of the most abundant (>5% relative abundance) diatom taxa identified. First, the diatom dataset was filtered for individual diatom species with >5% relative abundance. The remaining taxa were then aggregated by taxonomic classification according to AlgaeBase, of increasing rank, up to the taxonomic rank of Family, with only the taxonomic groupings with >5% relative abundance kept for stratigraphic analysis. Family ranked groupings of diatom taxa with <5% relative abundances were then regrouped with other diatom families if they shared ecologically significant traits, such as morphology, and again filtered for the >5% relative abundance threshold. Non-specific taxon groupings for the final subset of diatom taxa for the stratigraphy included the families of *Achnanthidiaceae,* and *Cymbellaceae*, the genus *Encyonema*, and the morphology-based grouping of Centrics, a category of diatoms characterized by radial symmetry (Spaulding et al. 2021), which include the *Aulacoseira* and *Cyclotella* taxa, which have notably featured in limnological studies as markers of shifts in thermal stratification regimes in lakes (Rühland et al., 2003, 2015).

Some of the individual diatom species with >5% relative abundance shared taxonomic classification with these taxonomic groupings, and if found to exhibit similar response-shifts in the stratigraphy, were combined with the appropriate taxonomic grouping. For example, the diatom species *Rossithidium pusillum*, which exhibited ~5.11% relative abundance in the 11 – 11.5 cm depth interval, and is of the family *Achnanthidiaceae*, was added to the *Achnanthidiaceae* grouping. This grouping included *Eucocconeis depressa*, *E. flexella*, *Achnanthidium minutissimum*, *R. petersenii*, and *Psammothidium ventralis*. Similarly, *Encyonema neogracile* was added to the *Encyonema* grouping, which included *E. gaeumannii*, *E. minutum*, *E. reimeri*, and *E. silesiacum*, all of which, sans *E. neogracile* did not exhibit >5%

relative abundance in any interval even when combined but showed similar patterns in changes in relative abundance through the stratigraphic profile to *E. neogracile*. Note that though the *Encyonema* grouping which corresponds to the *Encyonema* genus is part of the family *Cymbellaceae*; due to observed differences in patterns of relative abundance between these taxa, they were distinguished here as separate. Conversely, despite also having radial symmetry, *Pantocsekiella tripartita* was not added to the Centric grouping, which consisted of aggregated counts of valves identified as being from the species *Aulacoseira distans*, *Lindavia antiqua*, *L. bodanica*, *Discostella pseudostelligera*, D. *stelligera*, *Pantocsekiella tripartita*, as well as from the genera *Aulacoseira*, and *Cyclotella*. This is because *P. michiganiana* both independently exceeded the 5% relative abundance threshold in at least one interval (5 – 5.5 cm) and exhibited a different pattern of change in abundance throughout the stratigraphic profile at SC11 compared to other Centric taxa (Figure 6.).

As my dataset of diatom assemblages for SC11 began at the 3 – 3.5 cm depth (the intervals corresponding to the 0 – 3 cm sediments were not analyzed by myself due to limited sediment availability), the stratigraphy was superficially supplemented with percent relative abundance data with the same select diatom taxa from surficial sediments (0 – 0.5 cm depth) of the same sediment core previously analyzed by Coleman et al., (2023). This percent relative abundance data for the surficial sediments from Coleman et al., (2023) in our stratigraphy was necessary to contextualize our results as the endpoint diatom assemblage following recent climate-driven disruptions compared to older pre-industrial assemblages we examined, and this data was not used in the statistical analyses described further below. Note that Coleman et al., (2023) used differing diatom taxonomical standards, and did not distinguish between *Pseudostaurosira brevistriata* and *Stauroforma exiguiformis*. This may be because *P. brevistriata* and *S. exiguiformis* are superficially similar, as well as functionally similar. For example, both *P. brevistriata* and *S. exiguiformis* are relatively small (~3 µm wide, by ~26 µm long); individual frustules are lanceolate in axial view, but rectangular in girdle view, and tend to live in colonies joined along the longer sides of the frustules by spines. *P. brevistriata*, and *S. exiguiformis* are only subtly distinguishable by the shape of their connective spines, and whether their striae of pores extend across the entirety of the axial area; *P. brevistriata* exhibit spatulate spines, while S. *exiguiformis* exhibit tubular spines; striae in both species run in parallel but are restricted to the mantle in *P. brevistriata* while striae in *S. exiguiformis* run along the entirety of the axial surface, and curve towards the apices (Spaulding et al. 2021). *P. brevistriata*, and *S. exiguiformis* are also both benthic diatoms that can thrive even in low-light level conditions (technically *P. brevistriata* is tychoplanktonic), and both were historically classified within the genus *Fragilaria* (Guiry et al., 2024).

Constrained hierarchical cluster analysis was also performed on the entire diatom dataset, excluding the diatoms of the surficial sediments analyzed by Coleman et al., (2023) to identify and cluster similar diatom assemblages of adjacent intervals. Cluster analysis is a method by which objects in a group are grouped together based on their similarities such as the closeness of individual points relative to each other compared to points from other clusters (Landau, 2010). The Euclidean distance measure was used to calculate similarities between, and group diatom assemblages of different strata based on the non-transformed percent relative abundance of constituent diatom taxa following Laird et al., (2023). The constrained incremental sum of squares (CONISS) method, a subtype of constrained hierarchical cluster analysis for delineating biostratigraphic zones that restricts itself to only consider adjacent clusters, was used to construct a horizontal dendrogram showing biostratigraphic zones consisting of diatom assemblages grouped together for their compositional similarities, and identify where in the stratigraphic profile that adjacent biostratigraphic zones began to diverge from each other (Grimm, 1987). A broken stick model was then used identify which biostratigraphic zones (Figure 6.) were statistically significant by comparing the variances of the CONISS cluster analysis and a random distribution of zones generated by the broken-stick model (Bennet, 1996). Once each statistically significant biostratigraphic zone, and their exact depth-intervals were identified, the average evenness index (J) for each biostratigraphic zone was also calculated from the individual evenness indices (J) of the relevant individual depth-interval assemblages of each biostratigraphic zone and compared (Table 1.).

Following the example of Emery Boeck et al., (2023), analyses of similarity (ANOSIM) were used to confirm the statistical significance of biostratigraphic zones identified by the CONISS cluster analysis and broken stick model, while a Similarity Percentage (SIMPER) analysis was used to quantify the degree of similarity and significance between and within the biostratigraphic zones. SIMPER analysis uses the Bray-Curtis dissimilarity measure to compare the difference between pairwise combinations of diatom taxa and calculate the average contribution of each taxon to the differences between each biostratigraphic zone and relativizes it (Clarke, 1993; da Costa et al., 2018), though we reported the sum of the dissimilarity indices for each pairwise combination of biostratigraphic zones. An indicator species analysis (ISA) was additionally used to determine the indicator taxa of each identified significant biostratigraphic zone, with the SIMPER analysis used to further determine the individual contributions of diatom taxa to the differences between biostratigraphic zones. ISA analysis refers to a technique by De Cáceres & Legendre, (2009), used to identify species associated with pre-defined groups such as the biostratigraphic assemblage zones identified by the CONISS cluster analysis. The key statistic of the ISA, which ranges from 0 – 1 is the product of the specificity and the fidelity of a given taxon, i.e. the ‘uniqueness’ of a given taxon relative to its specified biostratigrapic zone with respect to its presence in others (De Cáceres et al., 2009).

The values for the diversity indices (i.e. SDI, SimpDI, and *J*), stratigraphy, CONISS dendrogram and broken stick model, ANOSIM, and SIMPER analyses were produced using the vegan (v2.6-6.1; Oksanen et al., 2024), dplyr (v1.1.4; Wickham et al., 2023), rioja (v1.0-6; Juggins, S., 2023), and riojaPlot (v0.1-20; Juggins, S., 2023) packages in R Studio (v4.3.3; R Core Team, 2024; v2023.9.1.494, Posit team, 2023). However, the diversity indices plot was produced using ggplot2 (Wickham et al., 2016). The ISA was performed using the indicspecies R package (De Cáceres et al., 2009), also in R studio. The diversity indices plot and stratigraphy were then additionally altered in Inkscape (v1.3.2; Inkscape Developers, 2023) to fit academic formatting standards that could not be executed in R studio, such as adding shading to highlight the post-low-carbon anomaly assemblage zone for the diversity indices plot, as well as add subtitles and the CONISS dendrogram to the right side of the stratigraphy plot.

3.2.3. Assemblage response to environmental triggers

3.2.3.1. Principal Component Analysis

A principal component analysis (PCA) was performed to identify the main clusters of diatom taxa driving changes in the composition of the diatom assemblages at SC11. PCA is a multivariate statistical technique that uses ordination to reduce the multidimensionality of a dataset by grouping similar, highly correlated variables into linear combinations (Abdi et al., 2010). These linear combinations can then be plotted as orthogonal variables called principal components to best capture the variation observed (Abdi et al., 2010). As many diatom taxa and groupings broadly share environmental preferences, and consequently respond accordingly to changes in their environment with observable changes in their relative abundance (Rühland et al., 2003; Kahlert et l., 2022; Weckström et al., 2023), the PCA was used to visualize and identify the main clusters of diatom taxa, and therefore indirectly identify the environmental factors they were associated with that were driving assemblage shifts throughout the sediment depth-intervals at SC11. For the PCA, we used the entire diatom dataset excluding taxa with <2% relative abundance and the diatom count data for the surficial sediments analyzed by Coleman et al., (2023). Prior to analysis, the percent relative abundance data was standardized using the Hellinger transformation (Legendre & Gallagher, 2001). Scores for the PC1 and PC2 axes were then extracted for further analysis in generalized additive models (GAMs), and Spearman's rank correlation analyses. As a PCA plot that included all of the ~169 diatom taxa we identified proved difficult to use to interpret, the diatom taxa with the top ten absolute highest PCA score contributions for each of the PC1 and PC2 axes were also identified for further re-analysis as drivers of variation from a qualitative perspective, such as habitat preference (i.e. planktonic, tychoplanktonic, benthic etc., recorded by Spaulding et al. 2021), light preference, size, and taxonomic group, as well as a quantitative perspective via Spearman's rank correlation analyses, and plotted on a modified PCA plot. The PCA was produced and plotted using the vegan package (v2.6-6.1; Oksanen et al., 2024), and base functions of R like prcomp() in R Studio (v4.3.3; R Core Team, 2024; v2023.9.1.494, Posit team, 2023).

3.2.3.2. Generalized Additive Models and Correlations

To identify if the timing of the statistically significant shifts in diatom assemblages coincided with changes to influxes of terrigenous carbon and productivity at SC11, generalized additive models (GAMs) were used to model trends in %OC, C:N, and the scores of the first two axes of the PCA, against sediment core depth (cm), following the methods of Laird et al., (2023). The data for the geochemical trends in % organic carbon (%OC) and atomic carbon-to-nitrogen ratios (C:N) was extracted from, and originally published by Abulu, (2024). GAMs refer to a variation of generalized linear models, which model a linear relation between a response and predictor variables. However, rather than fitting for a single linear regression, GAMs model for non-linear relationships, using the sum of multiple smooth functions (splines) to linearize predictor variables, and connect them to the response variables using a link function (Wood, 2017), making them ideal for modelling abrupt shifts such as ecological transitions in diatom assemblages (Lei et al., 2021). First derivatives and estimated confidence intervals of the fitted GAMs were also calculated to assess the statistical significance of changes using the gratia package (v0.9.0; Simpson, 2024). The GAMs, and adjacent analyses were produced using gaussian error distributions (k=5), and restricted maximum likelihood (REML) using the gam() function in the mgcv package (v1.9-1; Wood, 2017), in R Studio (v4.3.3; R Core Team, 2024; v2023.9.1.494, Posit team, 2023). Lastly, we quantified the relationship between %OC, C:N, and percent relative abundances of the top ten diatom taxa with the highest loadings for each of the PC1 and PC2 axes, and the scores of the PC1 and PC2 axes using Spearman's rank correlation coefficient. Due to mismatches in associated sediment interval depth (cm) between %OC and C:N compared to the PC1 and PC2 axis scores, Spearman's rank correlation analyses were performed using Past (v4.03, Hammer et al., 2001).

CHAPTER FOUR: RESULTS

4.1. Chronostratigraphic analyses of SC11

Abulu (2024) reported that ^{210}Pb radioactivity at SC11 was highest (~851.92 – 933.31 Bq/kg) in the topmost (0 – 4.75 cm) sediments, plateauing at that depth before decreasing to the background rate (~21.7 – 23.7 Bq/kg), at 10 cm depth (Figure 4.). A similar trend was found for ^{137}Cs radioactivity but at lower magnitudes (almost a quarter of ^{210}Pb), with the highest (~17.99 - 18.54 Bq/kg), also occurring in the top (0 – 4.75 cm) sediments and background (~3.85 – 2.99 Bq/kg) reached at 8 cm depth with no ^{137}Cs peak (Abulu, 2024; Figure 4.). Under the CRS age-depth model, ~2018 was represented by the 0 cm depth, with the oldest possible date of ~1845 found to correspond to the ~11.5 cm depth (Abulu, 2024).

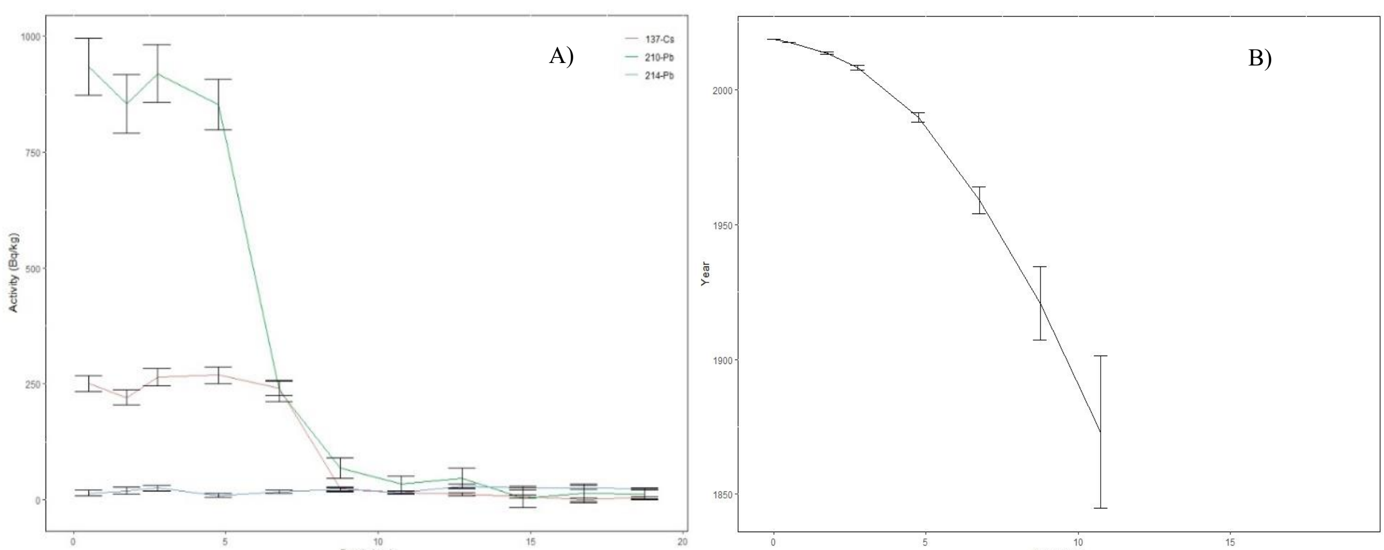

Figure 4. Chronology for SC11, recreated from data by Abulu (2024), and Coleman et al., (2023). A): Radioisotope activity for ^{210}Pb (green), ^{137}Cs (red), and ^{214}Pb (blue), plotted against sediment depth (cm); B): Date plotted against sediment depth (cm) inferred from Constant rate of supply (CRS) ^{210}Pb age-depth model.

4.2. Diatom diversity at SC11

Total diatom taxa richness throughout the core from SC11 was 169 recorded taxa from 55 genera and 26 families. 156 were species taxa, and the remaining 13 taxa could not be definitively identified beyond the genus level. Taxa richness for individual interval-assemblages was comparatively lower and fluctuated between a minimum of 54 taxa in the 5.25 cm interval to a maximum of 81 taxa in the 17.75 and 19.25 cm intervals, with an average of 69.65 taxa found per interval-assemblage. Taxa richness also decreased inversely with depth, and may have sharply decreased in more recent decades, as data from Coleman et al., (2023) for the surficial sediments (0 cm depth) recorded 48 taxa, of which only 42 were also found during sampling for this thesis. Shannon's Diversity (SDI) and Simpson's Diversity (SimpDI) Index values also fluctuated between intervals, averaging ~3.51, and 0.94 respectively. SDI and SimpDI values were only slightly smaller on average before (SDI = ~3.56, SimpDI = ~0.95), the low-carbon anomaly at the 8.25 cm depth, compared to after (SDI = ~3.27, SimpDI = ~0.93; Figure 5.).

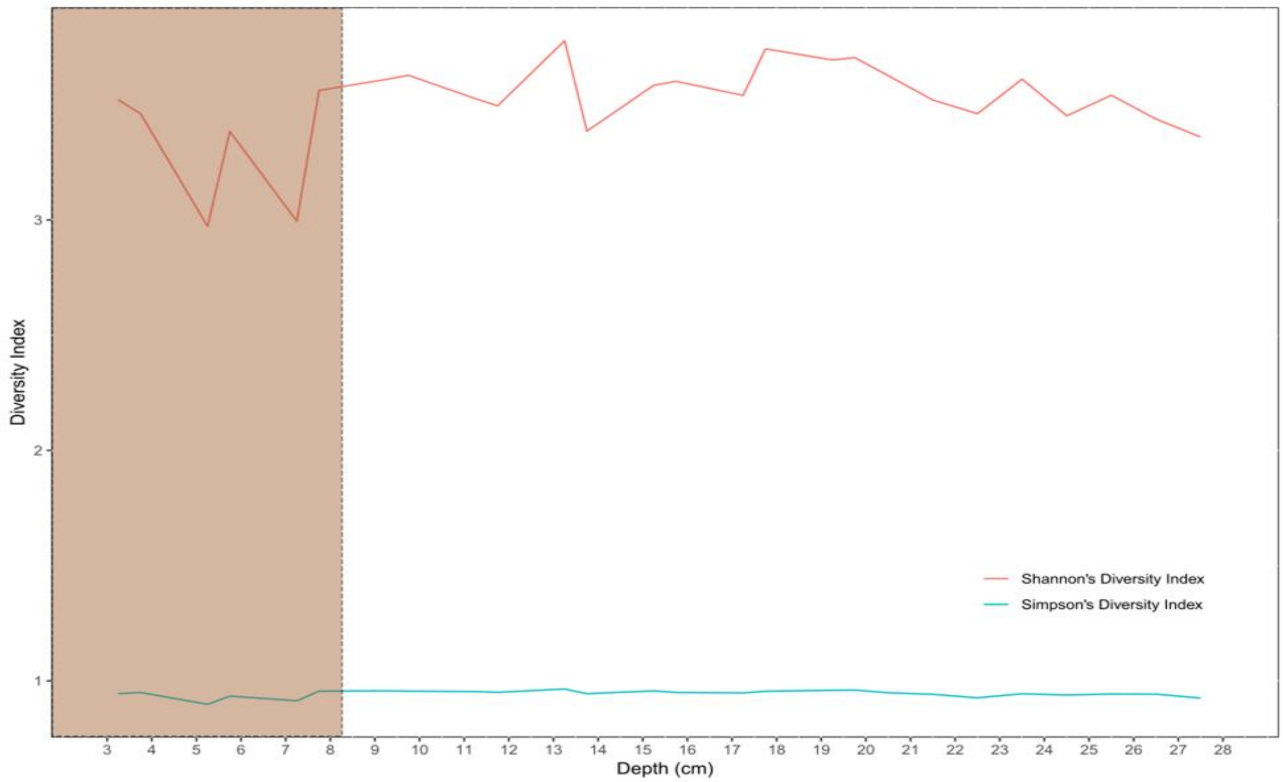

Figure 5. Shannon Diversity Index (SDI; red), and Simpson's Diversity Index (SimpDI; blue) plotted against sediment depth (cm), with sediments deposited after the low-carbon anomaly at the 8.25 cm depth shaded in grey to denote the post-low-carbon anomaly sediments.

More than half (95; 56.21%) of all the diatom taxa in our dataset were rare (<1% in any assemblage), with only 72 (~42.60%) taxa exceeding 1% relative abundance in any interval. Only a small fraction (16; 9.47%) of the recorded diatom taxa, exhibited >5% relative abundance (~5.11% – 26.88%) during any interval. Of the 169 diatom taxa identified, only 159 had a distinct known habitat, with most being benthic (139; Spaulding et al. 2021), though some taxa were further distinguished as epilithic (Štefková, 2006), epipelic (Spaulding et al. 2021), or epiphytic (Laird et al., 2023; Coleman et al., 2023). The remaining 20 non-benthic taxa were either tychoplanktonic (i.e. existing in both benthic and planktonic habitats; of which there were 9), or planktonic (Spaulding et al. 2021). No taxa classified at the genus level or higher exhibited >5% relative abundance during any interval, with the most abundant, *Pinnularia* spp., accounted for 2.61% of the assemblage during the 13.75 cm depth interval.

4.3. Diatom paleoenvironmental history – Stratigraphy and assemblage shifts

The CONISS analysis and broken-stick model identified three significantly different biostratigraphic zones of diatom assemblages throughout the core from SC11 (Figure 6.; ANOSIM R stat: 0.7277; P = 0.0001). The oldest assemblages (Zone 1), corresponding to the 27.5 - 17.5 intervals (assumed pre-1880s), were the most taxa rich ranging from 62 – 81 taxa per interval, or average of 73.36 taxa per interval, and the average evenness index (J) = ~0.83 (Table 1.). Of these, the ISA identified 22 indicator taxa for Zone 1 (Table 2.), the majority of which were benthic epilithic and epiphytic taxa, such as those of the *Encyonopsis* genus, *Denticula kuetzingii*, and/or large celled diatoms, like those of the *Epithemia* spp, and *Pinnularia maior*. However, only a small fraction (~7 taxa, two of which at maximum relative abundance, did not exceed 6%) constituted a substantial part of the Zone 1 assemblages (i.e. having >5% relative abundance in any of the assemblages constituting Zone 1). These 'dominant' taxa were not only epilithic and epiphytic, but also generally medium to large-sized (100 – 10000 µm), as well as considered moderately motile taxa. They included *Denticula kuetzingii* (~9.81 - 23.45%), and *Sellaphora pupula* (~6.68% - 12.73%), as well as diatom taxa from the families of *Achnanthidiaceae* (~5.41 - 9.76%), and *Cymbellaceae* (~4.94 – 8.90%), and the genus *Encyonema* (~4.38 - 12.63%), primarily *Encyonema neogracile* (~1.68 - 7.75%). *Navicula vulpina* (~1.20 – 5.58%), and *Pinnularia microstauron* (~3.19 – 5.45%) were also present in the Zone 1 assemblage in substantial but lesser numbers.

The second group of assemblages (Zone 2; Figure 6.) occurred within the 17.25 – 7.75 cm depth intervals (corresponding to a temporal range covering from pre ~1880s to ~1920s – 1930s). Diatom species richness ranged from 59 – 77 taxa, or an average of 68.6 taxa per interval, with an average evenness index (J) = ~0.85 (Table 1.). Despite having a lower average of number taxa per interval compared to Zone 1, the assemblages of Zone 2 were dominated by a larger and more diverse set of taxa (e.g. whereas the assemblages of Zone 1 were dominated by ~7 taxa with >5% relative abundance, 11 taxa of similar or greater relative abundance were present throughout the assemblages of Zone 2). The assemblages of Zone 2 also included diatoms of a wider range of frustule size (100 – 100000 µm). The ISA identified 8 indicator taxa for Zone 2 (Table 2.), which included almost exclusively large benthic diatoms such as *Rhopalodia* spp., and *Stauroneis* spp, but only a few of which, specifically *Navicula radiosa* (~0.32 - 6.43%), and *Neidium affine* (~2.80 - 6.43%), were found in relative abundances exceeding 5% in any of the assemblages of Zone 2. Many of the dominant taxa of Zone 2 were also those that previously characterized the assemblages of Zone 1, such as *S. pupula* (~2.17 - 16.75%), *Denticula kuetzingii* (~3.33 - 14.19%), *Pinnularia microstauron* (~5.16 - 9.77%), as well as diatom species from the *Cymbellaceae* (~1.19 - 5.37%) and *Achnanthidiaceae* families (~2.10 - 11.86%), and the *Encyonema* genus (~3.03 – 9.85%), again primarily *Encyonema neogracile* (~0.95 - 6.01%), but at smaller fractions of the assemblages than in Zone 1. The other notable diatom taxa of Zone 2 included *S. laevissima* (~3.26 - 9.22%), *Encyonopsis cesatii* (~0.48 - 7.46%), *Pinnularia mesolepta* (~0.36 - 5.45%), and *Rossithidium pusillum* (~0.64 - 5.12%). Many of these taxa previously also existed in the assemblages of Zone 1 but at smaller relative abundances and only increased their share in the assemblages during Zone 2 at the expense of some of the dominant taxa of Zone 1 (e.g. *Denticula kuetzingii* accounted for up to ~23.45% of the assemblages in Zone 1 but decreased in relative abundance in the Zone 2 assemblages (ranging from ~ 3.33 – 14.19% depending on the depth-interval).

The third group of assemblages (Zone 3) were laid down in the most recent sediments of SC11 (the 7.25 – 3.25 cm and surface depth intervals; estimated to be ~1940s – 2018), notably in the immediate sediments following the timing of the low-carbon anomaly at the 8.25 cm depth noted by Abulu, (2024). The assemblages of Zone 3 were generally the least taxa rich of the three biostratigraphic zones, with 54 – 77 taxa depending on the depth-interval, or an average of 63.6 taxa per interval (Figure 5.), and an average evenness index (J) = ~0.79 (Table 1.). The ISA analysis for Zone 3 identified 20 indicator taxa (Table 2.), mostly small to medium sized (11 – 1000 µm) benthic epilithic taxa, such as those of the family *Fragilariaceae*, as well as planktonic taxa, particularly those with a centric morphology like *Discostella stelligera*, *Pantocsekiella michiganiana*, and *Lindavia bodanica*, despite their general lack of relative abundance, save for *P. michiganiana* (~0.48% – ~7.48%). Other notable taxa indicated by the ISA analysis included *Placoneis explanata* (~1.34 - 8.17%), and *Pinnularia gigas*, which although benthic, is also exceptionally large (100001 – 1000000 µm), and was very rare (~0.17% – ~0.20%) in the assemblage. Taxa from the Zone 3 assemblage that were shared with either or both the Zone 1 and 2 assemblages occurred in substantially reduced relative abundances by comparison (e.g. *Denticula kuetzingii* went from ~5.35% to 0.826%, and the large celled *Navicula radiosa*, and *Navicula vulpina* went from >5% to near 0%). Others, increased abundance initially, but eventually also decreased in relative abundance, such as *Placoneis explanata* (from ~17.75% to ~5.62%), *S. pupula* (from ~8.29 to ~3.14%), *Pinnularia mesolepta* (from ~12.95 to 2.15%), and *Pinnularia microstauron* (~15.37 – 1.322%). By the early 2000s, they were replaced almost completely by diatom taxa that previously had little or no presence in the assemblages at SC11, primarily small benthic diatoms of the family *Fragilariaceae*, such as *Pseudostaurosira brevistriata* (~2.07 – 12.40%), *Stauroforma exiguiformis* (~3.63 – 15.70%). However, some of these new taxa also declined in relative abundance as they approached the surface, such as *Staurosira construens* which initially had 0% abundance, increased to ~5.25%, but decreased to

~3.47%), and *Pantocsekiella michiganiana*, which also initially had 0% abundance, increased to ~7.47%, and decreased to ~2.48% in the uppermost sediments.

The SIMPER analysis confirmed that all three biostratigraphic zones identified by the CONISS cluster analysis differed from each other in terms of taxa composition, but that the Zone 1 and 2 assemblages shared more similarities with each other, than with those of Zone 3 (Table 3.). Cross-referencing the significant ($p < 0.05$) diatom taxa indicated by the ISA with those highlighted by the SIMPER analysis indicates that the transition from Zone 1 to Zone 2 was marked by the loss of some the largest epiphytic diatoms in our dataset, such as *Encyonopsis descripta*, and *Epithemia argus* and *E. adnate*, in favor of the appearance of large *Naviculaceae*, and *Neideaceae*. Comparisons of the Zone 1 and 3 assemblages show that the loss of other large-sized diatoms like *Pinnularia maior*, *Navicula vulpina*, and *Stauroneidaceae*, as well as smaller diatom taxa like *D. kuetzingii,* and *Rossithidium petersenii*, which must have occurred sometime during or at the transition between Zone 2 and 3 assemblages. Comparisons of the Zone 2 and Zone 3 assemblage highlighted the appearance of low-clarity diatom taxa, like *Pseudostaurosira brevistriata*, *Stauroforma exiguiformis*, as well as some centric diatoms like *Pantocsekiella michiganiana*, *Discostella pseudostelligera*, *Lindavia bodanica*. The transition from Zone 2 to Zone 3 was also marked by the loss of large Neidiaceae that became prominent during the transition from Zone 1 to Zone 2, like *Neidium ampliatum*, and *N. affine*, as well as the loss of other larger diatoms like *Sellaphora laevissima*, and remaining taxa of the *Rhopalodiaceae* family. Exceptions to this general trend of loss in large diatoms across Zone 1 to Zone 3, include the appearance of *Placoneis explanata*, *Diploneis finnica* and *P. gigas*, which first appeared in large numbers only beginning in Zone 3.

Table 1. Average Evenness Index (J) of each biostratigraphic zone identified by the CONISS cluster analysis

Biostratigraphic zone	Evenness Index (*J*)
Zone 3	0.788474
Zone 2	0.845427
Zone 1	0.829095

Table 2. Results of ISA analysis – Indicator taxa for each biostratigraphic zone identified by CONISS analysis with species name, ISA stat, volumetric size range (in cubic micrometres; μm³), and habitat

Zone	Indicator Taxa	ISA stat	Volumetric size range (μm³)	Habitat
1	*Cymbella spp.*	0.85	101 - 10000	Assumed benthic/Epilithic
1	*Brachysira brebissonii*	0.842	101 - 1000	Benthic
1	*Fragilaria capucina*	0.836	11 - 100	Benthic/Epilithic
1	*Cymbopleura subcuspidata*	0.82	10001 - 100000	Benthic
1	*Nitzschia alpina*	0.787	101 - 1000	Benthic
1	*Denticula kuetzingii*	0.78	101 - 1000	Benthic/Epiphytic
1	*Cymbopleura incerta*	0.771	1001 - 10000	Benthic
1	*Lindavia antiqua*	0.77	101 - 1000	Planktonic
1	*Stauroneis submarginalis*	0.767	10001 - 100000	Benthic
1	*Encyonema neogracile*	0.765	101 - 1000	Benthic/Epilithic
1	*Encyonema silesiacum*	0.762	1001 - 10000	Benthic/Epilithic
1	*Encyonopsis descripta*	0.759	1001 - 10000	Benthic/Epiphytic
1	*Epithemia argus*	0.759	1001 - 10000	Benthic/Epiphytic
1	*Navicula vulpina*	0.737	1001 - 10000	Benthic
1	*Psammothidium ventrale*	0.733	11 - 100	-
1	*Eunotia praerupta*	0.72	101 - 10000	Benthic/Epilithic
1	*Stauroneis superkuelbsii*	0.713	1001 - 100000	Benthic
1	*Brachysira zellensis*	0.698	11 - 100	Benthic
1	*Pinnularia maior*	0.687	1001 - 10000	Assumed benthic/Epilithic
1	*Rossithidium petersenii*	0.683	11 - 100	Benthic
1	*Epithemia adnata*	0.674	1001 - 10000	Benthic/Epiphytic
1	*Staurosira venter*	0.607	11 - 100	Tychoplanktonic/Epilithic
2	*Neidium affine*	0.795	10001 - 100000	Assumed benthic
2	*Navicula radiosa*	0.776	101 - 1000	Benthic/Epilithic
2	*Sellaphora laevissima*	0.775	10001 - 100000	Benthic
2	*Neidium ampliatum*	0.756	10001 - 100000	Assumed benthic/Epilithic
2	*Rhopalodia spp.*	0.728	100001 - 1000000	Benthic/Epiphytic
2	*Stauroneis finlandia*	0.728	10001 - 100000	Benthic

2	*Stauroneis ancepsfallax*	0.72	1001 - 10000	Benthic
2	*Caloneis silicula*	0.706	1001 - 10000	Benthic
3	*Fragilariforma lata*	0.985	11 - 100	-
3	*Discostella pseudostelligera*	0.923	11 - 100	Planktonic
3	*Diploneis marginestriata*	0.919	101 - 1000	Benthic
3	*Placoneis explanata*	0.883	1001 - 10000	Benthic
3	*Pinnularia mesolepta*	0.871	1001 - 10000	Assumed benthic
3	*Discostella stelligera*	0.87	101 - 1000	Planktonic
3	*Pantocsekiella michiganiana*	0.866	101 - 1000	Planktonic
3	*Stauroforma exiguiformis*	0.856	101 - 100	Benthic/Epilithic
3	*Pseudostaurosira brevistriata*	0.834	11 - 100	Tychoplanktonic/Epilithic
3	*Navicula leptostriata*	0.804	101 - 1000	Benthic
3	*Lindavia bodanca*	0.787	10001 - 100000	Planktonic
3	*Neidiopsis levanderi*	0.775	101 - 1000	Benthic
3	*Staurosira construens*	0.751	11 - 100	Benthic/Epilithic
3	*Pinnularia nodosa*	0.733	101 - 10000	Benthic
3	*Navicula cryptocephala*	0.722	101 - 1000	Benthic/Epiphytic
3	*Staurosira binodis*	0.72	11 - 100	Tychoplanktonic/Epilithic
3	*Nitzschia fonticola*	0.689	101 - 1000	Benthic/Epilithic
3	*Diploneis finnica*	0.632	10001 - 100000	Benthic
3	*Chamaepinnularia mediocris*	0.632	11 - 100	Benthic
3	*Pinnularia gigas*	0.632	100001 - 1000000	Benthic

Table 3. Results of SIMPER analysis comparing the sum of the average dissimilarity indices between combinations of biostratigraphic zones identified by CONISS as calculated by the Bray-Curtis dissimilarity measure

	Zone 1	Zone 2	Zone 3
Zone 1	0	0.3808537	0.639764
Zone 2	0.380854	0	0.58194
Zone 3	0.639764	0.58194	0

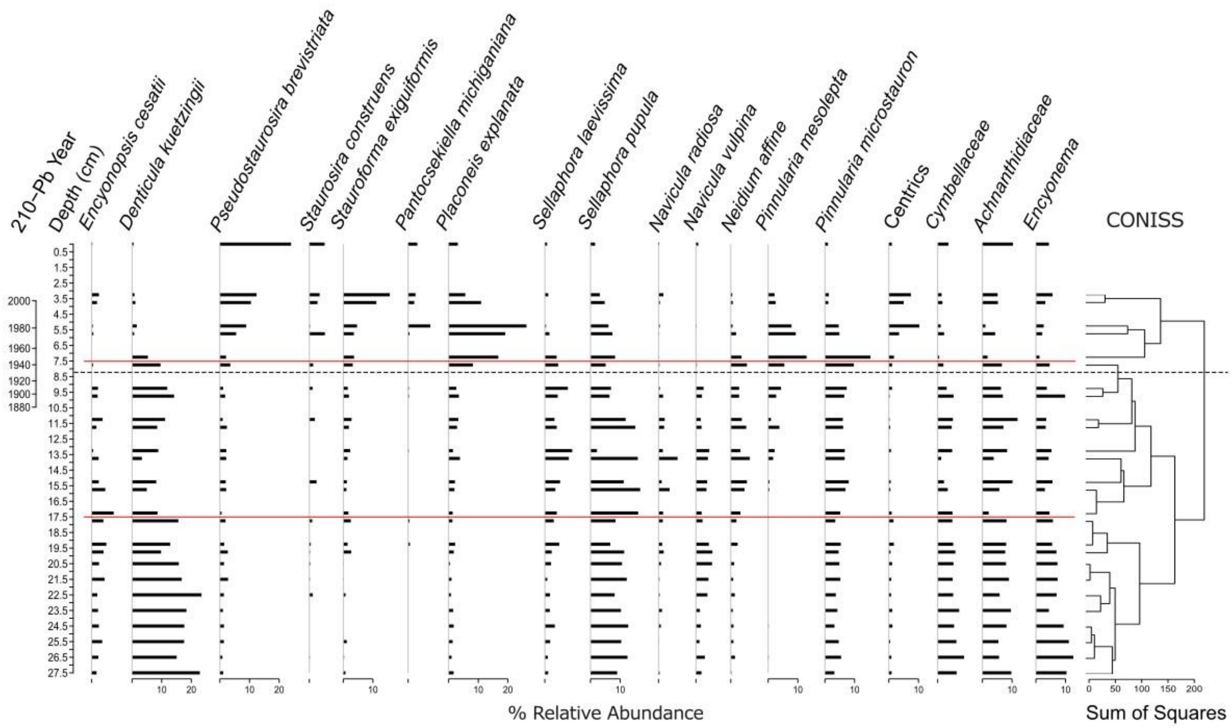

Figure 6. Stratigraphy of diatom assemblages from a sediment core collected from SC11, a small shallow lake in the Dehcho region, Northwest Territories, Canada. Sediment core depth and ^{210}Pb derived dates via CRS age-depth model prepared by Abulu, (2024), and Coleman et al., (2023), are shown on the left as the y-axis. The results of a CONISS cluster analysis are shown on the right as a horizontal dendrogram scaled to the sediment core depth. Statistically significant biostratigraphic zones indicated by the CONISS analysis and broken-stick model and confirmed by ANOSIM are indicated by red lines at the depth interval (cm) of divergence between assemblages. Approximate depth of low-carbon anomaly identified by Abulu, (2024) at the 8.25 cm depth indicated by a dashed line.

4.4. Diatom assemblage responses to environmental triggers

4.4.1. Assemblage response to environmental triggers

The PCA analysis identified 25 PC axes of variation in the diatom assemblages at SC11. The first two PC axes explained only a limited quantity of the variation in the diatom assemblages at SC11, with a cumulative proportion explained of ~49.13%. The PC1 axis accounted for a plurality of this proportion explained, roughly ~36.86% of the variation in the diatom community, while the PC2 axis explained an additional ~12.26% of the variation (Figure 8.). Eigenvalues for PC1 (λ = 0.08061) and PC2 (λ = 0.02682) were relatively low, suggesting only a fraction of the changes to the diatom community at SC11 were driven by these two specific PC axes and their associated clusters of diatom ecological niches alone.

Many of the diatom taxa with the top ten highest contributions to the PC1 and PC2 axes also exhibited some of the highest percent relative abundances in the stratigraphy and were also either highlighted by the ISA or SIMPER or by both analyses as important markers of the biostratigraphic zones identified by CONISS. Just under half of the top ten most influential diatom taxa for PC1 provided positive contributions to PC1, which included *Denticula kuetzingii* (~0.34), *N. vulpine* (~0.20), *Encyonema neogracile* (~0.15), and *Cymbopleura incerta* (~0.14), all of which were medium to large sized benthic epiphytic taxa. Except for *Pantocsekiella michiganiana* (~0.16) which is planktonic, taxa with negative loadings to PC1 were benthic epilithic taxa and included both medium sized taxa like *Placoneis explanata* (~-0.34), *Pinnularia mesolepta* (~-0.30), and *Diploneis marginestriata* (~-0.19), as well as small benthic *Fragilaria* like *Pseudostaurosira brevistriata* (-0.19), and *Stauroforma exiguiformis* (-0.24). As with PC1, less than half of the top ten diatom taxa driving the variation in the assemblage provided positive contributions to the PC2 axis. Additionally, some of the driving taxa of PC2 were found to overlap with PC1, specifically *Pinnularia microstauron*, and *Pseudostaurosira brevistriata*. Taxa with positive loadings to PC2 were exclusively small to medium sized (11 – 1000) benthic taxa, with little to moderate motility, including *Psammothidium ventrale* (~0.12), *Pseudostaurosira brevistriata var. papillosa* (~0.09), *Nitzschia fonticola* (~0.09), and *Pseudostaurosira brevistriata* (~0.08). In contrast, the diatom taxa with negative loadings to PC2 consisted exclusively of medium to large sized taxa with moderate to high motility, and included *Sellaphora laevissima* (~-0.18), *Neidium affine* (~-0.18), *Pinnularia microstauron* (~-0.16), *Pinnularia mesolepta* (~-0.15), *Neidium ampliatum* (~-0.09), and *Caloneis silicula* (~-0.08).

4.4.2. Generalized Additive Models and Correlation

%OC generally exhibited a linear increase over the entirety of the core at SC11, with a statistically significant ($p = 0.009$), increase occurring in %OC from 6.67% to 33.94% between the 21.5 cm depth and the surficial sediments (0.5 cm depth). As noted by Abulu, (2024), an anomalously low (5.69%) level of %OC, and a relative outlier was recorded as occurring at the 8.25 cm depth (Figure 7.). In contrast, C:N ratios at SC11 exhibited a statistically significant ($p = 0.003$) linear decrease from 13.65 to 12.69, also between the 21.5 cm depth and the surficial sediments (0.5 cm depth; Figure 7.).

PC1 axis scores generally decreased over the entire core, relative to the initial maximum of ~0.29 at the 27.5 cm depth, characterized by an initial phase of gradual decline followed by a more rapid decrease in score values following the 8.25 cm depth (Figure 7.). First derivatives of the GAM model for PC1 indicated two sections (22.11 – 19.42 cm; 14.03 – 3.25 cm) of the trends for PC1 were statistically significant changes in PC1 axis scores. The section covering the 22.11 – 19.42 cm depth intervals ($p = 0.004$) corresponded to the beginning of the gradual decrease in PC1 axis scores centred around the 21.5 cm depth, corresponding to a transition from a stable PC1 axis scores averaging ~0.28 to a phase of gradual decline. The second statistically significant change, corresponding to the 14.03 – 3.25 cm depth section ($p = 0.004$) covers the period of rapid decrease in PC1 axis score values around and following the low-carbon anomaly at the 8.25 cm depth. PC2 axis scores exhibited a rough U-shaped trend, characterized by an initial phase of stable values averaging ~0.20 (Figure 7.). Following the 19.75 cm depth, PC2 axis scores rapidly decreased, reaching negative values. This trend reversed following the 8.25 cm depth, until PC2 axis score values returned to equal or greater magnitudes compared to initial values (Figure 7.). First derivatives indicated two sections of statistically significant change;

during the phase of rapid decline observed from the 19.25 – 13.25 cm depth ($p = 0.002$), and during phase of rapid increase following the 8.25 cm depth ($p < 0.001$).

Spearman's rank correlations found a weak inverse relationship between %OC and the PC1 axis (Spearman's $r_s = -0.2$; $p = 0.73$), and no association between %OC and the PC2 axis (Spearman's $r_s = 0$; $p = 1.0$). A weak positive relationship between C:N and the PC1 axis (Spearman's $r_s = 0.3$; $p = 0.68$), but a strong positive association between C:N and the PC2 axis (Spearman's $r_s = 0.7$; $p = 0.23$) were identified. In contrast, correlations between the percent relative abundances of the individual top ten contributing taxa of the PC1 axis and their axis scores were moderate to high, as well as matching the sign of their loading contribution (Table 4.). Similarly, except for *Pseudostaurosira brevistriata*, which was not found to be statistically significant (Spearman's $r = \sim 0.06$; $p = 0.77$), correlations between the top ten contributing taxa of the PC2 axis and their axis scores were moderate to high (Table 4.)

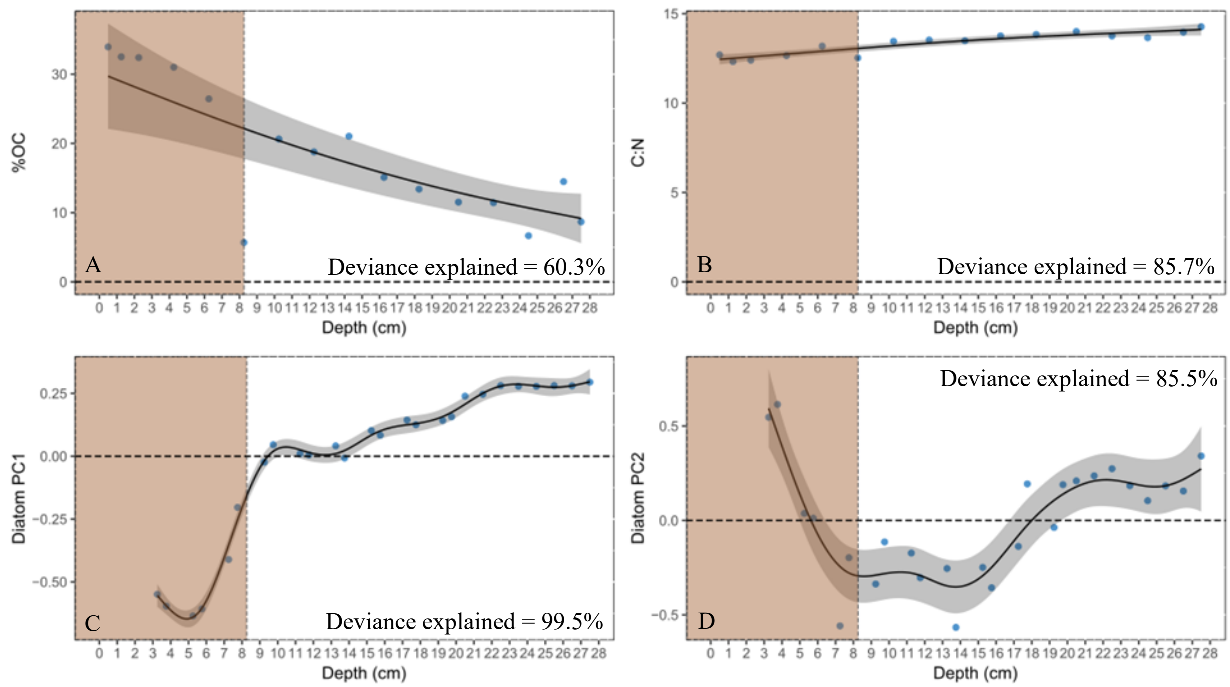

Figure 7. Results of the Generalized Additive Models (GAMs) performed for time series trends of %OC (Top left; A), C:N (Top right; B), PC1 (Bottom left; C) and PC2 (Bottom right; D) axis score values for SC11. Areas shaded in gray represent the 95% CI for each model. % of deviance for each GAM model is also listed. Wherever the trendline for each GAM model intersects with the zeroth intercept on the horizontal axis, indicated by the dotted line, is when the GAM model is not statistically significant.

Table 4. Summary of Spearman's rank correlation test with the percent relative abundance of the top ten loading contributing species of the PC1 and PC2 axes with the PC1 and PC2 axis scores, %OC, and C:N

PC axis	Species	Size range	Score	Spearman's r coefficient with PC	Spearman's r coefficient with %OC
1	*Placoneis explanata*	1001 – 10000	-0.34	-0.86	-0.60
1	*Denticula kuetzingii*	101 – 1000	0.34	0.87	-0.60
1	*Pinnularia mesolepta*	1001 – 10000	-0.30	-0.87	-0.22
1	*Stauroforma exiguiformis*	101 – 100	-0.24	-0.83	0.20
1	*Navicula vulpina*	1001 – 10000	0.20	0.46	0.70
1	*Pseudostaurosira brevistriata*	11 – 100	-0.19	-0.66	-0.30
1	*Diploneis marginestriata*	101 – 1000	-0.19	-0.80	0.34
1	*Pantocsekiella michiganiana*	101 – 1000	-0.16	-0.57	0.00
1	*Encyonema neogracile*	101 – 1000	0.15	0.81	0.20
1	*Cymbopleura incerta*	1001 – 10000	0.14	0.73	0.40
2	*Caloneis silicula*	1001 – 10000	-0.08	-0.58	0.30
2	*Neidium affine*	10001 - 100000	-0.18	-0.85	0.80
2	*Neidium ampliatum*	10001 - 100000	-0.10	-0.62	0.30
2	*Nitzschia fonticola*	101 – 1000	0.10	0.78	-0.20
2	*Pinnularia mesolepta*	1001 – 10000	-0.15	-0.52	-0.22
2	*Pinnularia microstauron*	1001 – 10000	-0.16	-0.88	0.90
2	*Psammothidium ventralis*	11 – 100	0.12	0.65	-0.30
2	*Pseudostaurosira brevistriata*	11 – 100	0.09	0.06	-0.30
2	*Pseudostaurosira brevistriata var. papillosa*	11 – 100	0.10	0.66	0.40
2	*Sellaphora laevissima*	10001 - 100000	-0.18	-0.79	-0.60

*Spearman's rank correlation coefficients with p-values < 0.05 are indicated with *

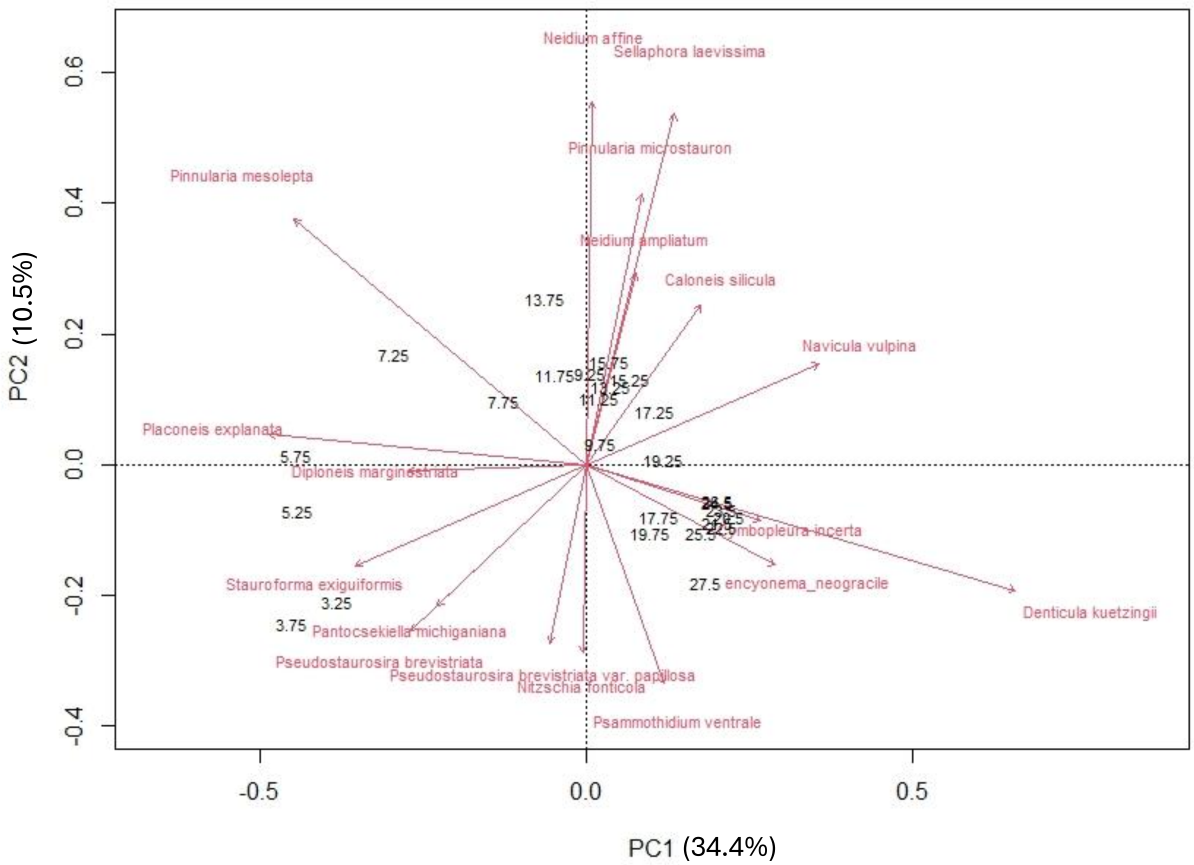

Figure 8. Principal components analysis (PCA) of the top ten contributing diatom taxa for the PC1 and PC2 axes across each of the depth-interval assemblages of SC11.

CHAPTER FIVE: DISCUSSION

At Scotty Creek Basin and adjacent areas in northwestern Canada, rapidly warming air temperatures combined with wildfires of increasing severity and frequency are accelerating permafrost degradation on a widespread scale (Gibson et al., 2018). The resultant thaw driven hydrological changes (Connon et al., 2014; Chasmer et al., 2017), combined with alterations to boreal forest vegetation cover via wetland thermokarst (Carpino et al., 2018; 2021; Haynes et al. 2018; Dearborn et al., 2020), and succession catalyzed by wildfires (Helbig et al., 2016; Chasmer et al., 2017; Haynes et al. 2018), along with climate-induced extreme drought and precipitation (Price et al., 2013; Tiwari et al., 2022), may be altering the quantity, quality, and timing of DOC and inorganic nutrients entering downstream wetlands and lakes in the southern Dehcho (Burd et al., 2020; Rodríguez-Cardona et al., 2020; Olefeldt et al., 2013; Abulu, 2024; Ackley et al., 2021). In cases involving increased chromophoric DOC influx, there may be an enhanced risk of brownification, which can impact the water quality of affected lakes, and is of substantial global concern as it could increase the rate at which CO_2 is released from northern lakes (Tranvik et al., 2009; Blanchet et al., 2022). Although previous surveys in 2018 showed that many lakes in and around Scotty Creek Basin were already exhibiting relatively high (> 10 mg/L) levels of DOC, ranging from 10.5 to 57.7 mg/L, no correlation was observed between DOC and lake colour, suggesting spatial variation in the "quality" of the DOC entering different lakes (Coleman et al., 2025), with the specific factors driving the observed differential browning unclear (Coleman et al., 2015; 2023; 2025).

This study builds on previous research on the water quality dynamics of the southern Dehcho (Korosi et al. 2015; Coleman et al., 2015; 2023; 2025; Abulu, 2024), focusing on how water colour and clarity changed over the last few centuries in a small shallow lake (SC11) near the Scotty Creek Basin. SC11 was previously identified as being one of only two lakes in the Dehcho that exhibited evidence of a potential micro-algal assemblage shift from epiphytic and periphytic diatoms (e.g. *Encyonema silesiacum*, and *E. hebridicum*), associated with high water clarity (Rühland et al., 2003), to small benthic *Fragilariaceae* taxa (e.g. *Staurosira construens*, *Staurosira venter*, *Pseudostaurosira brevistriata* etc.) associated with lower-light conditions (Coleman et al., 2025; Figure X). Small benthic *Fragilariaceae* have been reported in other lakes as indicators of reduced light availability, specifically increased ice cover (Lotter et al., 2000; Karst-Riddoch et al., 2005; Rühland et al., 2008; Dalton et al., 2018), but may also be a useful at indicating ecologically analogous conditions of limited light availability such as brownified waters (Brown et al., 2017; Coleman et al., 2023; 2025).

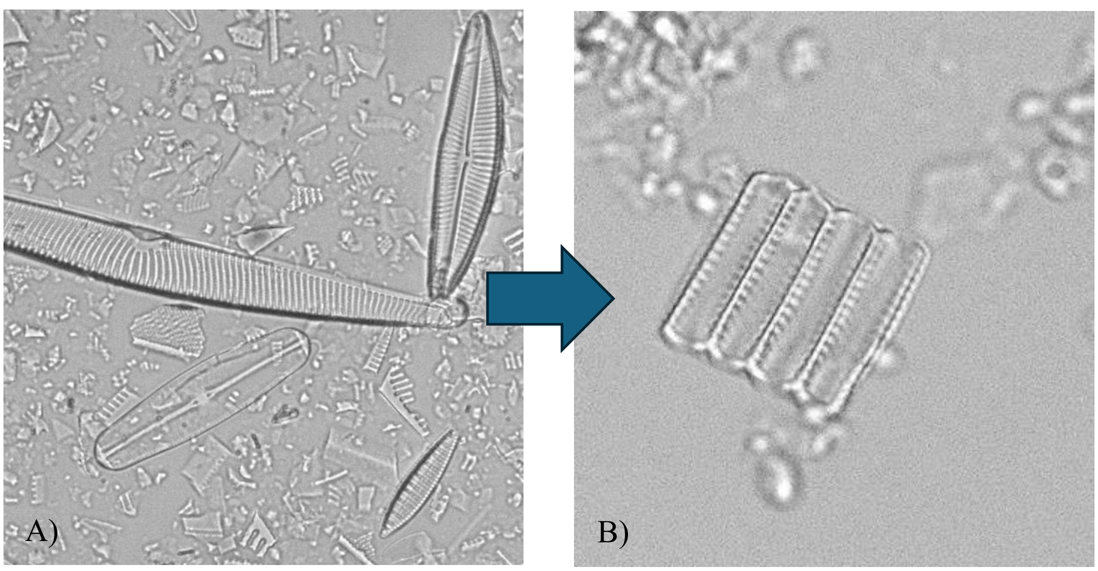

Figure 9. Examples of prominent varieties of diatom taxa in assemblages before and after the community shift observed by Coleman et al., (2025) at SC11. A): Left, a variety of epiphytic diatom taxa from the 26.5 cm depth interval of the sediment core from SC11; from top to bottom, E. hebridicum, Navicula radiosa, N. pupula, D. kuetzingii; B) Right, an example of a cluster-colony of benthic Stauroforma exiguiformis from the 3.25 cm depth interval of the sediment core.

The circumstances at SC11 thus offer an opportunity to fill research gaps on which specific drivers of brownification may be involved in the lakes of the Dehcho permafrost peatlands. To identify and better understand when and which specific environmental drivers initiated the diatom-inferred shift to conditions of lower light availability and assumed brownification at SC11 that was first identified by Coleman et al., (2025), we used paleolimnological methods to reconstruct a more comprehensive long-term (i.e. multi-centurial) record of the history of the water quality conditions at SC11, focusing on when light availability changed, as inferred from changes in the relative abundance of light-sensitive diatom subfossils in a dated sediment core spanning the last several hundred years. We identified the groups of diatom taxa most responsible for driving any observed assemblage shifts and analyzed whether their timing coincided with changes in %OC and C:N trends that marked known events in history of SC11's watershed, and which may have been a factor in SC11's differential level of brownification compared to other lakes in and around the Scotty Creek Basin (see Coleman et al., 2023). However, we did not directly analyze brownification at SC11 in terms of changes in DOC concentration or composition throughout the sediment profile of SC11 due to the challenges of reconstructing DOC from sediments, as well as limited sediment availability, nor did we directly analyze how different environmental drivers may have contributed to brownification at SC11. This study provides valuable insights into how brownification, as inferred from its impacts on in-lake diatom-assemblages may begin, and progress in a lake environment in the boreal permafrost peatlands of the southern Dehcho.

5.1 Shifts from epilithic and epiphytic to small *Fragilariaceae* dominated assemblages at SC11 indicate reductions in water clarity between the 1920s and 2000s

The paleoenvironmental history of diatom diversity at SC11 can be divided into three distinct groupings of diatom assemblages, each corresponding to a different phase of water quality at SC11 within the past 150+ years, though only the last (dated to have diverged from the others around the ~1930s), included taxa (i.e. *Fragilariaceae*) associated with lower water clarity and elevated water colour. Each assemblage grouping differed in levels of species richness, which generally decreased over time, but throughout the known history of SC11, diatom diversity remained consistently relatively low (ranging from 81 – 54 taxa depending on the interval), comparable to other shallow lakes in Scotty Creek Basin and the southern Dehcho in both richness and the variety of species present (Coleman et al., 2015; 2023). The relatively low diversity is likely the product of the cold subarctic climate (Rühland et al., 2003; Kahlert et al., 2022), though it remains comparatively higher than most lakes in the even colder High Arctic (Kahlert et al., 2022; Weckström et al., 2023).

The first and oldest diatom assemblages corresponded to the earliest part of SC11's known sedimentary records, beginning sometime prior to the 1880s, but with an otherwise uncertain date, as the accuracy for ^{210}Pb dating decreases drastically for dates older than 150 years (Appleby et al., 1986; Abulu, 2024). These assemblages were dominated by benthic epilithic and or epiphytic diatom taxa indicative of a shallow lake environment with high clarity waters. For example, these assemblages were particularly rife with *Denticula kuetzingii*, as well as diatoms from family *Cymbellaceae* (e.g. *Encyonema hebridicum*, *E. neogracile*, and *E. silesiacum*) (Rühland et al., 2003; Coleman et al., 2015), both of which are known to attach to either submerged macrophytes or benthic moss mats, and are indicative of high clarity conditions, as they require sufficient light to reach the bottom of SC11 to survive (Bahls, 2013). Additionally, *Cymbellaceae* are also associated with shallow oligotrophic lakes, which also tend to have relatively clear water conditions (Rühland et al., 2003). Similarly, other notable taxa in the pre-1880s diatom assemblages at SC11 included *Sellaphora pupula*, *Navicula vulpina*, *Pinnularia microstauron*, and those of the family *Achnanthidiacae*, are all also associated with shallow oligotrophic lakes (Krammer, 2000; Poulíčková et al., 2008; Lim et al., 2007; Zibulski et l., 2013), and their presence further corroborates that prior to the 1880s, the waters at SC11 were relatively high clarity and/or were relatively shallow.

The second grouping of diatom assemblages also corresponded to a period beginning sometime prior to the 1880s but ended between the 1920s – 1930s and likely reflects a transitional period of increasing nutrient availability and/or lengthening ice-free season. For example, these assemblages included most of the main diatoms of earlier assemblages (i.e. *D. kuetzingii*, *P. microstauron*, and diatoms of the family *Cymbellaceae*, and the genus *Encyonema*, primarily *E. neogracile*), indicating that water clarity remained similarly sufficiently transparent for benthic production during this phase of SC11's history. However, their abundances were much lower than before, and as there was also an increase in many previously rarer epilithic and epiphytic taxa, formed assemblages with a more even distribution of species. Many of these newly more abundant taxa were also known to be associated with increased DOC and nutrient availability, such as *Navicula radiosa*, *Sellaphora laevissima*, and *Rossithidium pusillum* (Rühland et al., 2003; Mohammed et al., 2021; Weckström et al., 2023). Some of the newer taxa, specifically *Rhopalodia* spp., *Stauroneis* spp., *N. radiosa*, and *Neidium affine* were also considerably larger than most taxa from previous assemblages.

In other lakes across the northern hemisphere, similar increases diatom diversity has been linked to general regional-scale climate warming and its impacts, such as decreased duration of seasonal ice cover and longer growing seasons (Smol et al., 2005; Smol & Douglas, 2007; Rühland et al. 2013; Coleman et al., 2025). *R. pusillum* has also been previously associated with fen environments in the Scotty Creek Basin (Coleman et al., 2023), and part of the increased nutrient availability may also have been the result of this inferred climate warming driving the formation or expansion of a thermokarst fen directly adjacent to or connected SC11, which could have provided an additional outlet for DOC and nutrients to enter the lake (Rydberg et al., 2010; Quinton et al., 2018; Coleman et al., 2015; 2023). The additional presence and or increase in *Rhopalodia* spp., and *P. mesolepta*, which are associated with macrophytes, may even be an indicator that the inferred increase in nutrient availability and/or a longer ice-free season may have facilitated more advanced macrophyte growth (Kelly et al., 2018; Rybak et al., 2020; Weckström et al., 2023).

However, from the 1930s – 1940s onwards, there were substantial changes in diatom assemblages at SC11, suggesting a considerable shift in water quality compared to previous conditions, specifically a decrease in clarity. Almost all major taxa from earlier 'light' assemblages, especially those associated with oligotrophy and or high clarity conditions, were greatly reduced in relative abundance, either almost immediately in the 1940s (as was the case for *D. kuetzingii*, *N. radiosa*, and *N. vulpina*), or in the decades afterwards and were replaced by a substantially fewer number of taxa, the composition of which continued to evolve over time. The new 'dark' assemblages were initially characterized by a large increase in the abundance of *Placoneis explanata*, which between the 1940s – 1980s constituted roughly a fifth of the new assemblages alone, as well as increases in *Pinnularia mesolepta*, and *P. microstauron* to a lesser extent. Beyond being an indicator of oligo-to-mesotrophic conditions, and being a benthic epilithic taxa, the autecology of *Placoneis explanata* is not well understood (Van de Vijver et al., 2024), and while both *Pinnularia mesolepta* and *P. microstauron* were part of previous 'light' assemblages, they are also considered cosmopolitan taxa that can also survive mesotrophic conditions to some degree (Lange-Bertalot et al., 2017; Van de Vijver et al., 2024). These changes are likely the continuation of previous trends of increasing nutrient availability, but the abrupt loss of so many of the taxa associated with high clarity that had characterized earlier assemblages, also strongly suggests a comparatively substantial decrease in water clarity. However, by the 2000s, the abundances of *Placoneis explanata*, *Pinnularia mesolepta*, and *P. microstauron*, had also collapsed, replaced by populations of small benthic *Fragilariaceae*, specifically *Pseudostaurosira brevistriata*, *Stauroforma exiguiformis*, *Staurosira construens*, and *Staurosira venter* that had also been steadily growing since the 1940s. This is most likely when the diatom assemblages at SC11 completely transitioned to the benthic *Fragilariaceae* dominated diatom assemblage that was described by Coleman et al., (2025) as a brownification signal. The considerable proliferation of *Fragilariaceae* (which had come to account for around a third of the assemblage by 2018) at the expense of even mesotrophic and or cosmopolitan taxa may be an indication that the shift towards decreased water clarity and increased water colour at SC11 beginning *circa* 1930s – 1940s may have intensified over time (Lotter & Bigler, 2000; Rühland et al., 2008; Brown et al., 2017; Dalton et al., 2018).

I used principal components analysis to further assess the timing of diatom assemblage shifts, and the scores of the PC1 and PC2 axes (which together accounted for ~49% of the variation in the diatom assemblages at SC11), were plotted against sediment depth in generalized additive models. From prior to the 1880s to 2018, PC1 axis scores decreased in a non-linear fashion, from positive values associated with medium to large-sized benthic epiphytic diatom taxa (e.g. *Denticula kuetzingii*), to negative values associated with benthic epilithic taxa (e.g. *Placoneis explanata*, as well as *Pinnularia mesolepta*), as well as small benthic *Fragilariaceae* taxa. The non-linear decrease in PC1 axis scores was initially gradual, consistent with the small changes between 1880 and the 1920s – 1930s, but accelerated beginning around the 8.25 cm depth, which corresponded to the 1920s – 1930s, reflecting the observed rapid shift from 'light' to 'dark' assemblages dominated by small benthic *Fragilariaceae* taxa. As PC1 accounts for a plurality (~36.86%) of the changes in diatom assemblages at SC11, this suggests that a large proportion of the observed post-1930s shifts were driven by the transition primarily from benthic epiphytes to small benthic *Fragilariaceae*, which has been identified in other lakes in the southern Dehcho as a response to a loss in light availability possibly due to brownification (Korosi et al., 2015; Coleman et al., 2015; 2023; 2025).

The PC2 axis accounted for ~12.26% of the variation in the diatom assemblages at SC11 and may be reflecting trait-based changes in diatom motility, roughly in line with the three previously identified phases of water quality history at SC11. For example, while the earliest assemblages were associated with positive values (i.e. small to medium sized benthic taxa of low motility, such as *Psammothidium ventrale*, and *Pseudostaurosira brevistriata var. papillosa*), over time they decreased towards negative scores, indicating a change towards conditions favouring diatom taxa with moderate to high motility (e.g. *Sellaphora laevissima, Neidium affine*, and *Pinnularia microstauron*), however, around the 1920s and 1930s, PC2 axis scores began to rapidly increase back towards positive values, indicating a return to conditions favouring low motility diatom taxa. As an environmental bioindicator trait, diatom motility is relatively understudied, but drought increased turbidity, as well as higher total phosphorus and conductivity has been suggested to favour diatom taxa with higher motility (Peszek et al., 2021). The period around which PC2 axis scores were negative strongly overlapped with the Zone 2 assemblages, which included taxa associated with warmer and wetter conditions, the decrease may have been related to the water quality changes associated with warming-driven wetland thermokarst activity and should be further investigated.

Unlike other lakes that have undergone changes in light availability (see Rosén et al., 2009; Gushulak et al., 2020; Emery Boeck et al., 2023; Tichá et al., 2023), the shift from 'light' to 'dark' assemblages at SC11 following the post-1930s did not include a shift from being dominated by benthic taxa to planktonic taxa. Instead, the entirety of the known history (i.e. pre 1880s to 2018) of the diatom assemblages of SC11 remained consistently dominated by benthic taxa. The only exception may be in the most recent sediments which began to be laid down around the early 2000s, in which the dominant diatom taxa were *Fragilariaceae*, which are sometimes considered tychoplanktonic instead (Velez et al., 2021). The minimal presence of planktonic diatom taxa (specifically centric diatom taxa, e.g. those of the genera *Aulacoseira* or *Cyclotella*) at SC11 in substantial (i.e. >5%) relative abundances at any point over the past 150+ years is most likely due to the relative shallowness (i.e. no more than ~1.9m deep) of SC11, resulting in sufficient mixing to inhibit stratification (Holgerson et al., 2022), despite the relatively high DOC, and or water colour, as such lakes often become stratified due to the propensity for DOC to absorb more solar radiation and heat the surface water temperatures (Strock et al., 2017; Pilla et al., 2018).

In other subarctic lakes in northwest Canada (e.g. Slipper Lake; Rühland et al., 2005), decreases in light availability such as increased ice cover normally results in the classic shift from heavy tychoplanktonic *Aulacoseira* diatoms to the lighter and smaller *Cyclotella* (Rühland et al., 2005; 2015). However, an increase in the few centric planktonic diatom taxa (e.g. *Pantocsekiella michiganiana*, *Lindavia bodanica*, *Discostella pseudostelligera*, and *D. stelligera*, with the latter two formerly classified within the genus *Cyclotella*; Rühland et al., 2005; Guiry et al., 2024) identified at SC11 did still occur only after the 1980s, along with the increase in small benthic *Fragilariaceae* (e.g. *Pseudostaurosira brevistriata*) associated with increased water colour, and therefore may have been an analogous response to changes in light availability. Of these, only *P. michiganiana* existed at SC11 in relative abundances greater than 5% in any given assemblage, and only in the most recent sediments, and its increased abundance is consistent with the observed increased abundance in *P. brevistriata*, as both prefer higher alkalinity (Rühland et al., 2003; Duda et al., 2023), as well as the pH (7.94) measurements of SC11 taken by Coleman et al., (2023).

5.2 The timing and rate of change in diatom assemblage composition at SC11 suggests that extreme environmental changes and events may be an important trigger of long-term permafrost thaw, and brownification in Dehcho lakes

Consistent with my hypothesis, the observed post-1930s transition from ‘light’ to ‘dark’ diatom assemblages, and inferred shift towards brownification at SC11, began shortly after the occurrence of an anomalous temporary decrease in %OC in the sediments at SC11 that was first identified by Abulu, (2024), and which may represent an interruption in primary production in SC11 and its watershed (Meyers & Lallier-Vergès, 1999), occurring sometime between the 1920s – 1930s. Rather than a slow gradual multi-centurial change (similar to the gradual increase in %OC temporarily interrupted by the low %OC anomaly), the post-1930s shift consisted of a comparatively more rapid decadal-scale non-linear change in diatom assemblage composition, characterized initially by the loss of most of the diatom taxa of earlier assemblages that were known to be associated with high-clarity conditions, and an increase in mesotrophic taxa associated with higher DOC, and culminated in the 2000s with the assemblage dominated by small benthic *Fragilariaceae* taxa that was previously identified by Coleman et al., (2025) as distinctly indicative of brownification. Such non-linear ecological changes in diatom assemblage composition and the inferred water quality changes at SC11 are characteristic of 'regime shifts' in which change is either gradual or negligible (e.g. the transition from Zone 1 to Zone 2 assemblages), until a critical threshold is breached, following which the ecosystem response (e.g. transition from Zone 2 to Zone 3 assemblages) is relatively rapid (Andersen et al., 2009; Randsalu-Wendrup et al., 2016).

As non-linear ecological changes also sometimes reflect extreme or abrupt environmental changes (Williams et al., 2011; Randsalu-Wendrup et al., 2013; 2016), such as extreme climate events like El Niño (see Sepúlveda-Zúñiga et al., 2024), we therefore hypothesize that a similarly extreme environmental event or perturbation also responsible for that abrupt temporary decrease in productivity sometime in the 1920s – 1930s, may have been the main trigger for the observed diatom assemblage shifts and inferred eventual transition towards brownification at SC11, by sufficiently altering the conditions at the permafrost-rich landscape surrounding SC11 past a critical threshold, resulting in a regime shift to a new state of accelerated thaw relative to prior conditions (see Chasmer et al., 2017). In other boreal wetland catchments, rapid permafrost thaw has been observed to lead to changes in the geomorphology and hydrology of affected areas as the ground subsides due to wetland thermokarst, increasing hydrological connectivity (Connon et al., 2014; Wright et al., 2022). This increase in hydrological connectivity may have facilitated long-term increases in the export of chromophoric DOC from newly waterlogged or otherwise now more leachable peat-rich organic soils (Wauthy et al., 2018), containing aromatic compounds associated with water discolouration (Olefeldt et al., 2013; Blanchet et al., 2022), and eventually leading to the inferred changes in light availability and possible brownification at SC11. However, the exact nature of the extreme event or environmental change that may have triggered the inferred acceleration in permafrost thaw at SC11 was not evident from our diatom-based reconstruction of SC11's history alone. Based on the known history of SC11's watershed, we hypothesize two non-mutually exclusive possibilities, which may even have exacerbated each other's impacts, to have been responsible for what was observed at SC11, and which should be the subject of future investigations.

The first possibility is that the inferred interruption in productivity was the result of environmental and climatic changes brought on by a severe El Niño event, one of which is known to have occurred in 1925 – 1926 (Takahashi & Martínez, 2019), which closely matches the 1920s – 1930s date assigned to the %OC anomaly identified by Abulu, (2024). El Niño (EN) refers to an irregularly recurring (once every two to seven years) climate phenomenon, during which the trade winds behind an ocean-to-atmospheric system over the Pacific Ocean that normally transport warm water from the west coast of the Americas towards Asia instead reverse resulting in extremely disruptive changes in climate and weather patterns in affected areas (Neelin et al., 1998), such as coastal Peru, where EN occurrences can cause uncharacteristically strong rainfall and flooding in a desert (Takahashi & Martínez, 2019). EN has also been observed to result in abnormal climate changes elsewhere in the Americas, including in British Columbia and Yukon (Taylor, 1998), as well as in the Dehcho region of northwestern Canada, where the resultant climate and environmental changes effected by a 1997 – 1998 EN may have led to a threshold shift towards accelerated permafrost loss (Chasmer et al., 2017).

During this 1997 – 1998 EN, the southern Dehcho region, or more specifically, the Scotty Creek Basin, experienced abnormal changes in climate and seasonal weather patterns, including increased snow precipitation during winter, significantly warmer air temperatures and earlier onset of spring, and intensified droughts during summer (Chasmer et al., 2017), which may have disrupted the fragile balance maintaining the discontinuous permafrost in this region (Halsey et al., 1995; Camill & Clark, 1998; 2000), as rates of permafrost thaw from before the 1997 – 1998 EN (0.19% loss per year), were found to have increased threefold afterwards to 0.58% loss per year (Chasmer et al., 2017). The increased snow accumulation may have insulated the ground, keeping it relatively warm even during winter, and ironically halting any seasonal permafrost aggradation (Hinkel & Hurd, 2006; Osterkamp, 2007). Combined with when the EN enhanced buildup of snow inevitably melted due to the ENN-enhanced temperatures and earlier onset of spring, this also led to increased volumes of water moving through the wetland and enhancing lateral thaw at the peat plateau margins via the heat flux of the soil-water interaction (Kurylyk et al., 2016; Devoie et al., 2021). This may have then created a positive feedback loop of wetland collapse and increased hydrological flow in the affected areas, leading to the accelerated rate of permafrost degradation observed by Chasmer et al., (2017).

However, the exact impacts of the 1925 – 1926 EN on permafrost thaw in the Dehcho region and Scotty Creek Basin are not as well understood as the 1997 – 1998 EN, as the literature has generally focused more on the impacts of the 1925 – 1926 EN in Asia and Peru (Takahashi & Martínez, 2019), and there is a lack of comprehensive climate and hydrological data from this time period owing to the relative remoteness of the region. Nevertheless, it may be reasonable to hypothesize that its impacts on the permafrost of the region were comparable, as while the 1997 – 1998 EN is considered the strongest EN event of the 20th century (the second being the 1982 – 1983 EN) in terms of environmental impact (i.e. severity of rainfall and flooding), the 1925 – 1926 EN has been classified as the third most severe (Takahashi & Martínez, 2019). As the severity of the 1997 – 1998 EN is often attributed to its coinciding with a warming event caused by the North Atlantic Oscillation (Chasmer et al., 2017), and the 1925 – 1926 EN also coincided with an abrupt warming period, though possibly related to the Pacific Decadal Oscillation instead (Varotsos et al., 2014), it may be reasonable to assume that the impacts of the 1925 – 1926 EN may have similarly severe enough to also lead to a threshold loss of permafrost, increasing hydrology connectivity throughout Scotty Creek, and facilitating an increase in chromophoric DOC influx and in-lake concentrations at SC11, leading to the inferred brownification (Coleman et al., 2025). The signal of interrupted productivity may therefore have been the result of a summer drought enhanced or induced by the 1925 – 1926 EN, as EN is known to sometimes cause in northwestern Canada (Shabbar & Khandekar, 1996; Shabbar et al., 1997; Bonsal et al., 2011), as a reflection of the negative impacts of drought on primary production (Piao et al., 2019; Tiwari et al., 2022; Jaman et al., 2024), and/or discharge (Chiu et al., 2020; Tiwari et al., 2022; Al-Kharusi et al., 2024).

Alternatively, but not mutually exclusively, the signal of interrupted productivity in the SC11 watershed that was dated to sometime between the 1920s – 1930s, may correspond to a historical forest fire. Much like the climatic and environmental changes induced by EN (Chasmer et al., 2017), forest fires are also known to be able to trigger rapid permafrost degradation in northwest Canada by removing and or altering the environmental conditions that otherwise preserve the delicate balance maintaining the discontinuous permafrost in the area (Brown et al., 2015; Gibson et al., 2018). For example, wildfires can burn trees and vegetation present (mostly black spruce in the Dehcho, but also *Sphagnum* mosses), as well peat rich soils (which can become highly flammable if dried out, such as during a drought), and their removal increases soil heat flux and irreversibly expands the active layer (Yoshikawa et al., 2003; Viereck et al., 2008). Deposition of ash can also lead to increased snowmelt during spring, which can also promote ground heat flux (Ackley et al., 2021). All of these fire-driven environmental changes can create a positive feedback loop of vertical as well as lateral thaw, once enough of the peat plateau collapses into an adjacent wetland and also becomes exposed to heat flux from adjacent water bodies via the soil-water interaction (Brown et al., 2015; Kurylyk et al., 2016; Gibson et al., 2018; Devoie et al., 2021; Ackley et al., 2021). The resultant fire-triggered accelerated permafrost thaw in the watershed surrounding SC11 may then have enhanced wetland thermokarst and associated increased hydrological connectivity (Connon et al., 2014), analogous to the EN driven threshold loss of permafrost described by Chasmer et al., (2017), and increased the quantity of chromophoric DOC entering the waters of SC11, leading to the observed diatom assemblage changes and inferred shift towards brownification (Wauthy et al., 2018; Ackley et al., 2021; Coleman et al., 2023).

Although forest fires can reduce productivity in affected watersheds via combustion of biomass, they also often result in short-term increases in nutrient influx into nearby water bodies afterwards, due to the production of nutrient-rich ash and charcoal and or increase in runoff due to post-fire changes to the landscape that favour erosion (Shakesby et al., 2006; Bladon et al., 2014; Legleiter et al., 2003). This can lead to increased in-lake production (Paul et al., 2022; Caroni et al., 2024), therefore fire-driven increases in production and sediment loads generally become reflected in lake sediments as elevations in nutrient and organic content (separate from that produced by fires) that can last for decades (Meyers et al., 1999; Pelletier et al., 2020). However, in the boreal subarctic, and especially in the specific region (Taiga Plains) of northwest Canada the Scotty Creek Basin and adjacent areas are part of, there is an unusual precedent to wildfires instead sometimes interrupting DOC exports (Olefeldt et al., 2013; Burd et al., 2018; Rodríguez-Cardona et al., 2020; Hutchins et al., 2023), though the usual rule of post-fire increases in nutrient flux has yet to be similarly contradicted (Granath et al., 2020; Paul et al., 2022). This may have been due to fire converting any organic matter present into compounds that are more readily susceptible to photodegradation once they enter the waters of SC11 and thus do become part of the lake sediments (Olefeldt et al., 2013; Rodríguez-Cardona et al., 2020; Burd et al., 2020), or a case of an unusually severe forest fire that volatilized most of the burnt carbon that would have been transported downstream into the atmosphere (Wei et al., 2021; Agbeshie et al., 2022; Bélair et al., 2025). As SC11 is a peatland lake with C:N ratios that have consistently remained above 10 throughout the entire sediment profile indicating the majority of the carbon entering SC11 has been mostly allochthonous in origin (Meyers et al., 2001), fire-related interruptions in allochthonous DOC influx to SC11 could have been responsible for the observed the low %OC anomaly and or signal of interrupted production. Unfortunately, we did not have the opportunity to examine the sediments of SC11 for traces of charcoal which are direct indicators of past forest fires (Smol, 2008), to directly test this wildfire hypothesis due to the constraints of limited sediment availability during this thesis.

However, there may be precedence for increased chromophoric DOC and brownification in at least one lake in the southern NWT that experienced thaw-driven landscape changes after a forest fire. A study by Coleman et al., (2015), compared two small shallow lakes in the southern NWT, Canada, referred to as KAK-1 (61.038056°N, 117.551111°W), and TAH-7 (60.570567°N, 116.904032°W), and how their aquatic ecosystems (specifically diatom assemblages) responded to permafrost thaw and peatland collapse. Of the two lakes, only the watershed around TAH-7 was known to have been influenced by a past forest fire, as marked by a peak in charcoal in the sediment strata that was dated to circa ~1845, and as expected, TAH-7 also exhibited far greater wetland collapse, which experienced a 44% increase in fen area over 1950 to 2012, compared to KAK-1, which experienced a 28% increase in fen area over 1970 to 2012 (Coleman et al., 2015), further lending credence to fire being able to trigger long-term changes in rates of permafrost thaw and wetland thermokarst development in the Dehcho region (see Gibson et al., 2018). Critically, TAH-7 was also the only one of the two to exhibit substantial changes in diatom assemblages, specifically a decrease in large benthic taxa such as Navicula, as well as *Sellaphora*, which occurred alongside an increase in small periphytic taxa indicating increased nutrient availability (Coleman et al., 2015; Mohammed et al., 2021; Weckström et al., 2023), which notably occurred following the aforementioned charcoal peak, and may parallel the loss of epiphytic and epilithic taxa we observed at SC11 following the ~1920s and alleged fire. The diatom assemblages at TAH-7 even exhibited a secondary shift, decades later around ~1940, which consisted of increases in small sized *Navicula* and benthic *Fragilariaceae* taxa (Coleman et al., 2015), which also similarly parallels the second post-anomaly diatom shift observed at SC11 that culminated in the *Fragilariaceae*-dominated assemblage previously identified as indicative of brownification.

However, as both fire and EN-related climate and environmental changes are relatively large scale disturbances with potentially regional-scale impacts, it is unusual that, to our knowledge, there are relatively few other instances of non-linear changes in diatom assemblages, specifically shifts towards abundances of small benthic *Fragilariaceae*, and indicating brownification, that were as severe as those observed at SC11 and TAH-7. To be clear, we do not mean to imply that other lakes in and around Scotty Creek, and the Taiga Plains are not experiencing brownification; indeed Coleman et al., (2023) noted five other lakes with similar assemblages also dominated by small benthic *Fragilariaceae* (SC1, SC2, SC3, SC5, and SC9). Water chemistry analysis of SC11 and other lakes in and around Scotty Creek by Coleman et al., (2023), even reveals that of the six lakes with the small benthic *Fragilariaceae* dominated assemblage, there are many lakes with much more intense water colour than SC11 (TCU = 195.9), with SC5 having the highest water colour (TCU = 463). There are also several lakes in and around Scotty Creek Basin which did not exhibit small benthic *Fragilariaceae* in high abundances, but also had TCU levels higher than SC11, namely SC8 (TCU = 284.9), Next Lake (TCU = 258.2), and First Lake (TCU = 249.3) (Coleman et al., 2023). TCU, however, is only an indirect indicator of light penetration to the benthic zone, and further study is needed to understand the drivers of diatom assemblages in shallow Dehcho lakes (Coleman et al. 2025).

The exact reasons for the apparent substantial spatial distribution in DOC quantity and quality, and by extension degree of brownification, among different lakes in the Scotty Creek Basin, currently remain unclear. Coleman et al., (2023) initially hypothesized that certain wetland thermokarst landforms may be sources (wetland collapse scar) of or conveyors (channel fens) of DOC leachate in the aftermath of submergence following peatland collapse, and that increased areal connection to wetland thermokarst may therefore be responsible for those water bodies exhibiting more intense browning, but found no consistent evidence for this, with some lakes (i.e. SC5 and SC8) found to have higher TCU values despite being hydrologically isolated, while others (Next Lake) had higher TCU values in spite of being hydrologically connected. Coleman et al., (2023) further postulated that the spatial variation in water colour intensity and brownification may simply be a factor of specific quirks in the hydrology of the area which are affecting residence time, and therefore rate of photobleaching of the often aromatic DOC compounds usually responsible for water discolouration, but which we do not understand yet (Olefeldt et al., 2013; Mazoyer et al., 2022; Blanchet et al., 2022). More recently, Coleman et al., (2025) demonstrated that contrary to conventional assumptions (which may remain true in other geographical jurisdictions, such as Finnoscandia; Seekell et al., 2015; Bouchard et al., 2017; Blanchet et al., 2022), there is an unusual decoupling between DOC and water colour for SC11 and other lakes in and around Scotty Creek Basin, a phenomenon seen only in a few other regions in North America, including the Yukon Flats, and boreal Alberta, (Johnston et al., 2020; Pugh et al., 2021; Kurek et al., 2023). Coleman et al., (2025) hypothesizes that this may be due to these lakes having a shared trait in longer residence times compared to other regions, and future study is needed to determine how the local hydrology of Scotty Creek Basin and how DOC, and specifically chromophoric DOC is moving through it, and what its ultimate fate is.

Increases in coniferous tree cover are also known to result in long-term increases in DOC (Sobek et al., 2007; Fredh et al., 2012; Finstad et al., 2016; Kritzberg, 2017), and therefore secondary succession post-fire may result in changes to vegetation communities that influenced downstream transport of DOC to lakes. However, almost all known studies discussing afforestation-related brownification take place in Finnoscandia and involve conifer (specifically by Norway Spruce; *Picea abies*) reforestation (Sobek et al., 2007; Fredh et al., 2012; Finstad et al., 2016; Kritzberg, 2017; Škerlep et al., 2020; 2022; Björnerås et al., 2017; 2022). Moreover, reforestation in the Scotty Creek Basin and southern NWT has been observed not to result in recolonization by the black spruce that is the predominant conifer of the region, but more commonly by eastern larch, and in those areas specifically affected by fire, by the deciduous white birch (Dearborn et al., 2021). This is tentatively supported by increases in lignin-derived phenols (specifically syringyls) associated with deciduous trees (Hedges and Mann 1979; Hu et al. 1999; Ishiwatari et al. 2006), that were reported in post-fire sediments in TAH-7 (Korosi et al., 2015). Additionally, Finnoscandia-based studies have previously found that other tree types, specifically deciduous trees like birch (i.e. silver birch, *Betula pendula*; mountain birch, *Betula pubescens*), may negatively impact DOC influx and downstream water colour (Brandtberg et al., 2000; Fröberg et al., 2011). Nevertheless, as Coleman et al., (2025) has already demonstrated, some of the traditional assumptions regarding DOC composition, and specifically that of chromophoric DOC may not be applicable to the specific situation at Scotty Creek Basin, and there is empirical evidence that DOC leachates from birches native to the Canadian boreal forest (i.e. white birch, and yellow birch), are comparable to conifer produced DOC in at least volume (Spencer et al., 2008; Helms et al., 2008; Hansen et al., 2016; Ryan et al., 2023). The difference is mostly in composition; while conifers are associated with lignin-based chromophoric DOC, deciduous trees like birch may be producing tannin-based DOC (Thieme et al., 2019), and future studies could focus on whether high concentrations of tannin-based DOC from deciduous trees native to the Canadian boreal forest can similarly discolour lakes.

CHAPTER SIX: CONCLUSIONS AND FUTURE STEPS

6.1. General Conclusions

Our results concur with those of Coleman et al., (2025), and confirm that historically (during and prior to the 1880s), water quality at SC11 was relatively clear and oligotrophic, characterized by benthic epiphytic taxa associated with high light availability. A transition to low-clarity or 'dark' conditions, as inferred by the loss of predominant epiphytic and epilithic diatoms and their eventual replacement by *Fragilariaceae* and other generalist diatom taxa associated with lake brownification began in the ~1930s – 1940s. This manifested as a relatively rapid response following a suspected environmental disturbance event, marked by anomalously low sediment organic carbon concentrations in the immediate prior decade, indicating a temporary interruption to watershed productivity. As these diatom assemblage composition shifts were accompanied by only slight changes in C:N ratios (i.e. from 13.65 to 12.69 over the core), indicating that the main source of organic carbon at SC11 remained primarily terrestrial in origin rather than algal production (though a slight increase in relative algal contribution did occur over time), the diatom inferred reduction in water clarity at SC11 is most likely a response to brownification (and not, for example, turbidity associated with algal productivity). Although there have been other lakes affected by permafrost thaw, and associated wetland thermokarst (specifically peatland collapse; see KAK-1), the observed rapid and non-linear regime shift from 'light' to 'dark' diatom assemblages following the 1930s, has only ever been found in lakes subjected to environmental disturbances like fire that can accelerate permafrost thaw (see TAH-7; Coleman et al., 2015). As climate change is expected to lead to more frequent and severe forest fires, and other environmental disturbances throughout the Canadian boreal forest (Price et al., 2013; Wang et al., 2014; Jain et al., 2017; Veraverbeke et al., 2017; Hessilt et al., 2022), which can accelerate permafrost thaw on a widespread scale, we may expect to see many more instances of brownification in the southern NWT. This may have global-scale implications for carbon cycling in the Canadian boreal subarctic, as brownified lakes may be more likely to process DOC and release it as CO_2 to the atmosphere (Lapierre et al., 2013; Blanchet et al., 2022). A better understanding of the underlying mechanism that leads to brownification is needed to be able to make more accurate projections of future lake changes across landscapes and ecozones.

6.2. Future Steps

The results of our study reinforce previous literature that diatom-based paleolimnology may be useful in tracking brownification and other changes in light availability in the Dehcho. Moreover, the dominant factor controlling brownification in lakes in the Dehcho may be external factors, specifically environmental disruptions which can trigger accelerated permafrost thaw, leading to changes in the landscape (geomorphologically, hydrologically, and perhaps even ecologically) that are changing the quantity, quality, and timing of chromophoric DOC entering lakes. However, many questions remain regarding both the nature of brownification in lakes in the southern Dehcho, as well as the factors driving it, especially those that may be responsible for the unusual spatial differentiation in browning.

For example, although the results of our diatom-based paleolimnological analysis of SC11 shows a sustained change in diatom assemblages associated with brownification, suggesting a prolonged multi-decadal browning, it is unknown whether the browning occurs year-wide, or is merely a response that now recurs seasonally because of permafrost-related changes in hydrological connectivity. It may therefore be of value to obtain even finer time-series data on the water chemistry of SC11 and other lakes in the Scotty Creek Basin using data loggers present at these sites. Additionally, as Coleman et al., (2025) demonstrated, there is considerable evidence that the quality of DOC, especially the variety of chromophoric DOC entering or present at the lakes of the southern NWT, may be very different from in other regions. Future studies should include a focus on identifying the exact composition of the DOC entering and found in the lakes of the southern Dehcho, and how it differs from the DOC entering other lakes in Canada, and across the world that are experiencing brownification.

Lastly, we still do not have a solid understanding of why there is so much spatial variation in brownification among lakes which should be somewhat uniformly impacted by the environmental perturbations we propose to be critical to driving lake brownification in the Dehcho. We propose returning to SC11 and the other lakes previously sampled by Coleman et al., (2023) to retrieve sufficient sediment samples to perform a more expanded multi-proxy paleolimnological investigation. Such an investigation should include a VNIRS-based approach similar to that devised by Rosen et al., (2005) and Rouillard et al., (2011) for reconstructing past DOC concentrations at SC11 and other lakes in and around Scotty Creek Basin (calibrating a model specific to the Dehcho region), and should also examine for traces of charcoal in the strata dated to the ~1920s – 1930s, specifically to test the wildfire hypothesis (Smol, 2008), as well as how other paleolimnological indicators (e.g. stable isotope ratios such as δ13C, δ15N, and n-alkanol ratios; $C_{30}/(C_{30} + C_{28})$), have changed throughout the sediments (see Coleman et al., 2015; Korosi et al., 2015), which may shed further light on how productivity, types of vegetation, and land covers have changed in and around SC11 and its watershed over time (Meyers et al., 2001; Meyers, 2003; Perkins et al., 2014; Holtvoeth et al., 2019). The investigation should also combine these paleolimnological approaches with GIS and remote-sensing approaches to a) model the complex hydrology of the Scotty Creek Basin, and how DOC moves through it and its ultimate fate (see Dick et al., 2015; Rankinen et al., 2023), and b) identify the impacts of fire on the watershed around SC11 if any, and determine the extent of peatland collapse (see Coleman et al., 2015; Abulu, 2024; Coleman et al., 2023; Carpino et al., 2025), as well as how fire or another environmental disturbance may have influenced vegetation cover (e.g. coniferous vs deciduous) in and around SC11 and TAH-7 (see Carpino et al., 2025; Enyetullah et al., 2022).

REFERENCES:

Abdi, Hervé, and Lynne J. Williams. "Principal component analysis." *Wiley interdisciplinary reviews: computational statistics* 2.4 (2010): 433-459.

Abulu, R. E. (2024). Carbon and Mercury Accumulation in Lake Sediments of Rapidly Thawing Discontinuous Permafrost Peatlands (Northwest Territories, Canada). [Master's Thesis, York University]. YorkSpace.

Ackley, C., Tank, S. E., Haynes, K. M., Rezanezhad, F., McCarter, C., & Quinton, W. L. (2021). Coupled hydrological and geochemical impacts of wildfire in peatland-dominated regions of discontinuous permafrost. *Science of the Total Environment*, *782*, 146841.

Agbeshie, A.A., Abugre, S., Atta-Darkwa, T. *et al.* A review of the effects of forest fire on soil properties. *J. For. Res.* 33, 1419–1441 (2022). https://doi.org/10.1007/s11676-022-01475-4

Ahonen, S. A., Hayden, B., Leppänen, J. J., & Kahilainen, K. K. (2018). Climate and productivity affect total mercury concentration and bioaccumulation rate of fish along a spatial gradient of subarctic lakes. *Science of the Total Environment*, *637*, 1586-1596.

Al-Amin, A., Ryan, R. J., & McKenzie, E. R. (2024). Effects of dissolved organic carbon on potentially toxic element desorption in stormwater bioretention systems. *Science of The Total Environment*, *912*, 168651.

Alberta Biodiversity Monitoring Institute (ABMI) (2016). Detailed Vegetation Maps. Available online at: http://www.abmi.ca/home/data-analytics/da-top/ da-product-overview/GIS-Land-Surface/Detailed-Vegetation-Maps.html (accessed January 10, 2019).

Albrecht, E., Hannonen, O., Palacín-Lizarbe, C., Suni, J., Härkönen, L. H., Soininen, N., ... & Vainikka, A. (2023). Browning of boreal lakes: Do public perceptions and governance align with the biological foundations?. *Ecological Applications*, *33*(5), e2856.

Alexander, A., Obu, J., Schuler, T. V., Kääb, A., & Christiansen, H. H. (2020). Subglacial permafrost dynamics and erosion inside subglacial channels driven by surface events in Svalbard. *The Cryosphere*, *14*(11), 4217-4231.

Alivernini, M., Lai, Z., Frenzel, P., Fürstenberg, S., Wang, J., Guo, Y., ... & Mischke, S. (2018). Late quaternary lake level changes of Taro Co and neighbouring lakes, southwestern Tibetan Plateau, based on OSL dating and ostracod analysis. *Global and Planetary Change*, *166*, 1-18.

Al-Kharusi, E. S., Hensgens, G., Abdi, A. M., Kutser, T., Karlsson, J., Tenenbaum, D. E., & Berggren, M. (2024). Drought Offsets the Controls on Colored Dissolved Organic Matter in Lakes. *Remote Sensing*, *16*(8), 1345.

Allesson, L., Koehler, B., Thrane, J. E., Andersen, T., & Hessen, D. O. (2021). The role of photomineralization for CO2 emissions in boreal lakes along a gradient of dissolved organic matter. *Limnology and Oceanography*, *66*(1), 158-170.

Allison, S. D., & Treseder, K. K. (2008). Warming and drying suppress microbial activity and carbon cycling in boreal forest soils. *Global change biology*, *14*(12), 2898-2909.

Allison, S. D., & Treseder, K. K. (2011). *Climate change feedbacks to microbial decomposition in boreal soils. Fungal Ecol 4: 362–374*.

Allison, S. D., McGuire, K. L., & Treseder, K. K. (2010). Resistance of microbial and soil properties to warming treatment seven years after boreal fire. *Soil Biology and Biochemistry*, *42*(10), 1872-1878.

AMAP. 2017. Snow, Water, Ice and Permafrost in the Arctic (SWIPA) 2017. Arctic Monitoring and Assessment Programme (AMAP), Oslo, Norway.

Andersen, T., Carstensen, J., Hernández-García, E., & Duarte, C. M. (2009). Ecological thresholds and regime shifts: approaches to identification. *Trends in Ecology & Evolution*, *24*(1), 49-57.

Anderson, L. E., DeMont, I., Dunnington, D. D., Bjorndahl, P., Redden, D. J., Brophy, M. J., & Gagnon, G. A. (2023). A review of long-term change in surface water natural organic matter concentration in the northern hemisphere and the implications for drinking water treatment. *Science of The Total Environment*, *858*, 159699.

Anderson, L., Edwards, M., Shapley, M.D., Finney, B.P., & Langdon, C. (2019). Holocene thermokarst lake dynamics in northern interior Alaska: the interplay of climate, fire, and subsurface hydrology. Frontiers in Earth Science, 7, 53.

Anokhina, A., Aoki, S., Ariga, A., Arrabito, L., Autiero, D., Badertscher, A., ... & Sirignano, C. (2008). Study of the effects induced by lead on the emulsion films of the OPERA experiment. *Journal of Instrumentation*, *3*(07), P07002.

Anoszko, E., Frelich, L. E., Rich, R. L., & Reich, P. B. (2022). Wind and fire: Rapid shifts in tree community composition following multiple disturbances in the southern boreal forest. *Ecosphere*, *13*(3), e3952.

Anyomi, K. A., Neary, B., Chen, J., & Mayor, S. J. (2022). A critical review of successional dynamics in boreal forests of North America. *Environmental Reviews*, *30*(4), 563-594.

Appleby, P.G. (2002). Chronostratigraphic Techniques in Recent Sediments. In: Last, W.M., Smol, J.P. (eds) Tracking Environmental Change Using Lake Sediments. Developments in Paleoenvironmental Research, vol 1. Springer, Dordrecht. https://doi.org/10.1007/0-306-47669-X_9

Arrhenius, S., & Holden, E. S. (1897). On the influence of carbonic acid in the air upon the temperature of the earth. *Publications of the Astronomical Society of the Pacific*, *9*(54), 14-24.

Bahls L. 2013. Encyonopsis from western North America: 31 species from Alberta, Idaho, Montana, Oregon, South Dakota, and Washington, including 17 species described as new. Northwest diatoms, Volume 5. Helena (MT): The Montana Diatom Collection; 46 p.

Baldocchi, D., Kelliher, F. M., Black, T. A., & Jarvis, P. (2000). Climate and vegetation controls on boreal zone energy exchange. *Global change biology*, *6*(S1), 69-83.

Baltzer, J. L., Day, N. J., Walker, X. J., Greene, D., Mack, M. C., Alexander, H. D., ... & Johnstone, J. F. (2021). Increasing fire and the decline of fire adapted black spruce in the boreal forest. *Proceedings of the National Academy of Sciences*, *118*(45), e2024872118.

Barescut, J., Lariviere, D., Stocki, T., Pittauerová, D., Hettwig, B., & Fischer, H. W. (2011). Pb-210 sediment chronology: Focused on supported lead. *Radioprotection*, *46*(6), S277-S282.

Barsanti, M., Garcia-Tenorio, R., Schirone, A., Rozmaric, M., Ruiz-Fernández, A. C., Sanchez-Cabeza, J. A., ... & Osvath, I. (2020). Challenges and limitations of the 210Pb sediment dating method: Results from an IAEA modelling interlaboratory comparison exercise. *Quaternary Geochronology*, *59*, 101093.

Bartels, S. F., Chen, H. Y., Wulder, M. A., & White, J. C. (2016). Trends in post-disturbance recovery rates of Canada's forests following wildfire and harvest. *Forest Ecology and Management*, *361*, 194-207.

Battarbee, R. W., V. J. Jones, N. G. Cameron, H. Bennion, L. Carvalho, and S. Juggins. 2001. Diatoms. Pages 155–202 *in* J. P. Smol, H. J. B. Birks, and W. M. Last, editors. *Tracking environmental change using lake sediments*. Volume **3**. Kluwer, Dordrecht, The Netherlands.

Baud, A., Aulard, C., Ghanbari, H., Fradette, M., Antoniades, D., Del Giorgio, P., ... & Gregory-Eaves, I. (2022). A framework for 210Pb model selection and its application to 37 cores from Eastern Canada to identify the dynamics and drivers of lake sedimentation rates. *Earth Surface Processes and Landforms*, *47*(10), 2518-2530.

Bélair, M., McCullough, I. M., Filstrup, C. T., Brentrup, J. A., & Lapierre, J. F. (2025). Wildfires mediate carbon transfer from land to lakes across boreal and temperate regions. *Communications Earth & Environment*, *6*(1), 94.

Bengtsson, L., Semenov, V. A., & Johannessen, O. M. (2004). The early twentieth-century warming in the Arctic—A possible mechanism. *Journal of Climate*, *17*(20), 4045-4057.

Bennett, K. (1996) Determination of the number of zones in a biostratigraphic sequence. *New Phytologist*, **132**, 155-170.

Benoy, G., Cash, K., McCauley, E., & Wrona, F. (2007). Carbon dynamics in lakes of the boreal forest under a changing climate. *Environmental Reviews*, *15*(NA), 175-189.

Bertilsson, S., & Tranvik, L. J. (2000). Photochemical transformation of dissolved organic matter in lakes. *Limnology and Oceanography*, *45*(4), 753-762.

Bertrand, S., Tjallingii, R., Kylander, M. E., Wilhelm, B., Roberts, S. J., Arnaud, F., ... & Bindler, R. (2024). Inorganic geochemistry of lake sediments: A review of analytical techniques and guidelines for data interpretation. *Earth-Science Reviews*, *249*, 104639.

Bintanja, R. (2018). The impact of Arctic warming on increased rainfall. *Scientific reports*, *8*(1), 16001.

Bintanja, R., & Andry, O. (2017). Towards a rain-dominated Arctic. *Nature Climate Change*, *7*(4), 263-267.

Bintanja, R., Graversen, R. G., & Hazeleger, W. (2011). Arctic winter warming amplified by the thermal inversion and consequent low infrared cooling to space. *Nature Geoscience*, *4*(11), 758-761.

Birks, H. H., & Birks, H. J. B. (2006). Multi-proxy studies in palaeolimnology. *Vegetation history and Archaeobotany*, *15*, 235-251.

Birks, H. J. B., Braak, C. T., Line, J. M., Juggins, S., & Stevenson, A. C. (1990). Diatoms and pH reconstruction. *Philosophical transactions of the royal society of London. B, Biological Sciences*, *327*(1240), 263-278.

Biskaborn, B. K., Herzschuh, U., Bolshiyanov, D. Y., Schwamborn, G., & Diekmann, B. (2013). Thermokarst processes and depositional events in a tundra lake, northeastern Siberia. *Permafrost and Periglacial Processes*, *24*(3), 160-174.

Björck, S., & Wohlfarth, B. (2001). 14 C chronostratigraphic techniques in paleolimnology. *Tracking environmental change using lake sediments: basin analysis, coring, and chronological techniques*, 205-245.

Björnerås, C., Weyhenmeyer, G. A., Evans, C. D., Gessner, M. O., Grossart, H. P., Kangur, K., ... & Kritzberg, E. S. (2017). Widespread increases in iron concentration in European and North American freshwaters. *Global Biogeochemical Cycles*, *31*(10), 1488-1500.

Björnerås, C., Weyhenmeyer, G. A., Hammarlund, D., Persson, P., & Kritzberg, E. S. (2022). Sediment records shed light on drivers of decadal iron concentration increase in a Boreal Lake. *Journal of Geophysical Research: Biogeosciences*, *127*(3), e2021JG006670.

Black, R. F. (1976). Periglacial features indicative of permafrost: ice and soil wedges. *Quaternary Research*, *6*(1), 3-26.

Bladon, K. D., Emelko, M. B., Silins, U., & Stone, M. (2014). Wildfire and the future of water supply.

Blanchet, C. C., Arzel, C., Davranche, A., Kahilainen, K. K., Secondi, J., Taipale, S., ... & Nummi, P. (2022). Ecology and extent of freshwater browning-What we know and what should be studied next in the context of global change. *Science of the Total Environment*, *812*, 152420.

Blomqvist, S. (1991). Quantitative sampling of soft-bottom sediments: problems and solutions. Marine Ecology Progress Series, 72(3), 295-304.

Bodí, M. B., Martin, D. A., Balfour, V. N., Santín, C., Doerr, S. H., Pereira, P., ... & Mataix-Solera, J. (2014). Wildland fire ash: production, composition and eco-hydro-geomorphic effects. *Earth-Science Reviews*, *130*, 103-127.

Bond-Lamberty, B., Peckham, S., Ahl, D. *et al.* Fire as the dominant driver of central Canadian boreal forest carbon balance. *Nature* 450, 89–92 (2007). https://doi.org/10.1038/nature06272

Bonsal, BR, Wheaton, EE, Chipanshi, AC, Lin, C., Sauchyn, DJ, & Wen, L. (2011). Drought research in Canada: A review. *Atmosphere-Ocean* , *49* (4), 303-319.

Bouchard, F., MacDonald, L. A., Turner, K. W., Thienpont, J. R., Medeiros, A. S., Biskaborn, B. K., ... & Wolfe, B. B. (2016). Paleolimnology of thermokarst lakes: a window into permafrost landscape evolution. *Arctic Science*, *3*(2), 91-117.

Bouchard, F., Proult, V., Pienitz, R., Antoniades, D., Tremblay, R., & Vincent, W. F. (2017). Periphytic diatom community structure in thermokarst ecosystems of Nunavik (Québec, Canada). *Arctic Science*, *4*(1), 110-129.

Box, J. E., Colgan, W. T., Christensen, T. R., Schmidt, N. M., Lund, M., Parmentier, F. J. W., ... & Olsen, M. S. (2019). Key indicators of Arctic climate change: 1971–2017. *Environmental Research Letters*, *14*(4), 045010.

Bradshaw, C. J., & Warkentin, I. G. (2015). Global estimates of boreal forest carbon stocks and flux. *Global and Planetary Change*, *128*, 24-30.

Brais, S., Bélanger, N., & Guillemette, T. (2015). Wood ash and N fertilization in the Canadian boreal forest: Soil properties and response of jack pine and black spruce. *Forest Ecology and Management*, *348*, 1-14.

Brandt, J. P. (2009). The extent of the North American boreal zone. *Environmental Reviews*, *17*(NA), 101-161.

Brandt, J. P., Flannigan, M. D., Maynard, D. G., Thompson, I. D., & Volney, W. J. A. (2013). An introduction to Canada's boreal zone: ecosystem processes, health, sustainability, and environmental issues. *Environmental Reviews*, *21*(4), 207-226.

Brandtberg, P. O., Lundkvist, H., & Bengtsson, J. (2000). Changes in forest-floor chemistry caused by a birch admixture in Norway spruce stands. *Forest Ecology and Management*, *130*(1-3), 253-264.

Bravo, A. G., Kothawala, D. N., Attermeyer, K., Tessier, E., Bodmer, P., Ledesma, J. L., ... & Amouroux, D. (2018). The interplay between total mercury, methylmercury and dissolved organic matter in fluvial systems: A latitudinal study across Europe. *Water Research*, *144*, 172-182.

Brothers, S., Köhler, J., Attermeyer, K., Grossart, H. P., Mehner, T., Meyer, N., ... & Hilt, S. (2014). A feedback loop links brownification and anoxia in a temperate, shallow lake. *Limnology and Oceanography*, *59*(4), 1388-1398.

Brovkin, V., Van Bodegom, P. M., Kleinen, T., Wirth, C., Cornwell, W. K., Cornelissen, J. H. C., & Kattge, J. (2012). Plant-driven variation in decomposition rates improves projections of global litter stock distribution. *Biogeosciences*, *9*(1), 565-576. o

Brown, D. R., Jorgenson, M. T., Douglas, T. A., Romanovsky, V. E., Kielland, K., Hiemstra, C., ... & Ruess, R. W. (2015). Interactive effects of wildfire and climate on permafrost degradation in Alaskan lowland forests. *Journal of Geophysical Research: Biogeosciences*, *120*(8), 1619-1637.

Brown, R. E., Nelson, S. J., & Saros, J. E. (2017). Paleolimnological evidence of the consequences of recent increased dissolved organic carbon (DOC) in lakes of the northeastern USA. *Journal of Paleolimnology*, *57*, 19-35.

Brown, R. J. E. (1973). Distribution of permafrost in North America and its relationship to the evironment; A reviw, 1963-1973. In *Proceedings of secound international conference on permafrost, National Academy of Sciences* (pp. 71-100).

Brown, R., Derksen, C., & Wang, L. (2010). A multi-data set analysis of variability and change in Arctic spring snow cover extent, 1967–2008. *Journal of Geophysical Research: Atmospheres*, *115*(D16).

Brugger, S. O., Gobet, E., Blunier, T., Morales-Molino, C., Lotter, A. F., Fischer, H., ... & Tinner, W. (2019). Palynological insights into global change impacts on Arctic vegetation, fire, and pollution recorded in Central Greenland ice. *The Holocene*, *29*(7), 1189-1197.

Buckley, L. B., Hurlbert, A. H., & Jetz, W. (2012). Broad-scale ecological implications of ectothermy and endothermy in changing environments. *Global Ecology and Biogeography*, *21*(9), 873-885.

Buma, B., Hayes, K., Weiss, S., & Lucash, M. (2022). Short-interval fires increasing in the Alaskan boreal forest as fire self-regulation decays across forest types. *Scientific Reports*, *12*(1), 4901.

Burd, K., Estop-Aragonés, C., Tank, S. E., & Olefeldt, D. (2020). Lability of dissolved organic carbon from boreal peatlands: interactions between permafrost thaw, wildfire, and season. *Canadian Journal of Soil Science*, *100*(4), 503-515.

Burge, D. R., Edlund, M. B., & Frisch, D. (2018). Paleolimnology and resurrection ecology: The future of reconstructing the past. *Evolutionary Applications*, *11*(1), 42-59.

Burgess-Conforti, J. R., Moore, P. A., Owens, P. R., Miller, D. M., Ashworth, A. J., Hays, P. D., ... & Anderson, K. R. (2019). Are soils beneath coniferous tree stands more acidic than soils beneath deciduous tree stands?. *Environmental Science and Pollution Research*, *26*, 14920-14929.

Burns, R.M., & Honkala B.H. Silvics of North America US Department of Agriculture, Forest Service, Ag. Handbook **654,** (1990).

Camill P, Clark JS (1998) Climate change disequilibrium of boreal permafrost peatlands caused by local processes. The American Naturalist, 151, 207–222.

Camill P, Clark JS (2000) Long-term perspectives on lagged ecosystem responses to climate change: permafrost in boreal peatlands and the grassland/woodland boundary. Ecosystems, 3, 534–544

Campbell, I. D., McDonald, K., Flannigan, M. D., & Kringayark, J. (1999). Long-distance transport of pollen into the Arctic. *Nature*, *399*(6731), 29-30.

Campeau, A., Eklöf, K., Soerensen, A. L., Åkerblom, S., Yuan, S., Hintelmann, H., ... & Zdanowicz, C. (2022). Sources of riverine mercury across the Mackenzie River Basin; inferences from a combined Hg [sbnd] C isotopes and optical properties approach.

Caon, L., Vallejo, V. R., Ritsema, C. J., & Geissen, V. (2014). Effects of wildfire on soil nutrients in Mediterranean ecosystems. *Earth-Science Reviews*, *139*, 47-58.

Caroni, R., Pinardi, M., Free, G., Stroppiana, D., Parigi, L., Tellina, G., ... & Giardino, C. (2024). Investigating the Impact of Wildfires on Lake Water Quality Using Earth Observation Satellites. *Applied Sciences*, *14*(6), 2626.

Carpino, O. A., Berg, A. A., Quinton, W. L., & Adams, J. R. (2018). Climate change and permafrost thaw-induced boreal forest loss in northwestern Canada. *Environmental Research Letters*, *13*(8), 084018.

Carpino, O., Haynes, K., Connon, R., Craig, J., Devoie, É., & Quinton, W. (2021). Long-term climate-influenced land cover change in discontinuous permafrost peatland complexes. *Hydrology and Earth System Sciences*, *25*(6), 3301-3317.

Carpino, O., Wright, S., Guo, J., van Der Sluijs, J., Connon, R., & Quinton, W. (2025). Detecting Forest-Wetland Changes in Northwestern Canada's Discontinuous Permafrost Region Using Landsat Trend Analysis. *Ecohydrology*, *18*(1), e2759.

Certini, G. (2005). Effects of fire on properties of forest soils: a review. *Oecologia*, *143*, 1-10.

Chapin iii, F. S., Mcguire, A. D., Randerson, J., Pielke, R., Baldocchi, D., Hobbie, S. E., ... & Running, S. W. (2000). Arctic and boreal ecosystems of western North America as components of the climate system. *Global Change Biology*, *6*(S1), 211-223.

Chasmer, L., & Hopkinson, C. (2017). Threshold loss of discontinuous permafrost and landscape evolution. *Global change biology*, *23*(7), 2672-2686.

Chebykina, E., & Abakumov, E. (2022). Essential role of forest fires in humic acids structure and composition alteration. *Agronomy*, *12*(12), 2910.

Chen, Y., Romps, D.M., Seeley, J.T. *et al.* Future increases in Arctic lightning and fire risk for permafrost carbon. *Nat. Clim. Chang.* **11**, 404–410 (2021). https://doi.org/10.1038/s41558-021-01011-y

Chevalier, M., Davis, B. A., Heiri, O., Seppä, H., Chase, B. M., Gajewski, K., ... & Kupriyanov, D. (2020). Pollen-based climate reconstruction techniques for late Quaternary studies. *Earth-Science Reviews*, *210*, 103384.

Chiu, C. Y., Jones, J. R., Rusak, J. A., Lin, H. C., Nakayama, K., Kratz, T. K., ... & Tsai, J. W. (2020). Terrestrial loads of dissolved organic matter drive inter-annual carbon flux in subtropical lakes during times of drought. *Science of The Total Environment*, *717*, 137052.

Christensen, L. M., Nation, L. F., & Bharadwaj, L. (2015). The accessibility, quality, and safety of the Liard First Nation's drinking water supply.

Clarke, K. R. (1993). Non-parametric multivariate analyses of changes in community structure. *Australian journal of ecology*, *18*(1), 117-143.

Clemmensen, K. E., Finlay, R. D., Dahlberg, A., Stenlid, J., Wardle, D. A., & Lindahl, B. D. (2015). Carbon sequestration is related to mycorrhizal fungal community shifts during long-term succession in boreal forests. *New Phytologist*, *205*(4), 1525-1536.

Coleman, K. A., Hoskin, G. N., Chasmer, L., Thienpont, J. R., Quinton, W. L., & Korosi, J. B. (2023). Limnology and diatom ecology of shallow lakes in a rapidly thawing discontinuous permafrost peatland. *Inland Waters*, *13*(1), 13-29.

Coleman, K. A., Palmer, M. J., Korosi, J. B., Kokelj, S. V., Jackson, K., Hargan, K. E., ... & Smol, J. P. (2015). Tracking the impacts of recent warming and thaw of permafrost peatlands on aquatic ecosystems: a multi-proxy approach using remote sensing and lake sediments. *Boreal environment research*, *20*(3).

Coleman, K. A., Palmer, M. J., Quinton, W. L., Thienpont, J. R., & Korosi, J. B. (2025). Spatiotemporal variability in chromophoric dissolved organic carbon in small, shallow lakes from discontinuous permafrost peatlands (Taiga Plains, Northwest Territories, Canada). *Canadian Journal of Fisheries and Aquatic Sciences*, *82*, 1-12.

Collar, N. M., Ebel, B. A., Saxe, S., Rust, A. J., & Hogue, T. S. (2023). Implications of fire-induced evapotranspiration shifts for recharge-runoff generation and vegetation conversion in the western United States. *Journal of Hydrology*, *621*, 129646.

Connon, R. F., Quinton, W. L., Craig, J. R., & Hayashi, M. (2014). Changing hydrologic connectivity due to permafrost thaw in the lower Liard River valley, NWT, Canada. *Hydrological Processes*, *28*(14), 4163-4178.

Connon, R., Devoie, É., Hayashi, M., Veness, T., & Quinton, W. (2018). The influence of shallow taliks on permafrost thaw and active layer dynamics in subarctic Canada. *Journal of Geophysical Research: Earth Surface*, *123*(2), 281-297.

Cory, R. M., Ward, C. P., Crump, B. C., & Kling, G. W. (2014). Sunlight controls water column processing of carbon in arctic fresh waters. *Science*, *345*(6199), 925-928.

Coulombe, S., Fortier, D., Bouchard, F., Paquette, M., Charbonneau, S., Lacelle, D., ... & Pienitz, R. (2022). Contrasted geomorphological and limnological properties of thermokarst lakes formed in buried glacier ice and ice-wedge polygon terrain. *The Cryosphere*, *16*(7), 2837-2857.

Craig, N., Jones, S. E., Weidel, B. C., & Solomon, C. T. (2017). Life history constraints explain negative relationship between fish productivity and dissolved organic carbon in lakes. *Ecology and Evolution*, *7*(16), 6201-6209.

Creed, I. F., Bergström, A. K., Trick, C. G., Grimm, N. B., Hessen, D. O., Karlsson, J., ... & Weyhenmeyer, G. A. (2018). Global change-driven effects on dissolved organic matter composition: Implications for food webs of northern lakes. *Global change biology*, *24*(8), 3692-3714.

Crusius, J., Anderson, R.F. Sediment focusing in six small lakes inferred from radionuclide profiles. *J Paleolimnol* **13**, 143–155 (1995). https://doi.org/10.1007/BF00678103

Cumming, B. F., Smol, J. P., Kingston, J. C., Charles, D. F., Birks, H. J. B., Camburn, K. E., ... & Selle, A. R. (1992). How much acidification has occurred in Adirondack region lakes (New York, USA) since preindustrial times?. *Canadian Journal of Fisheries and Aquatic Sciences*, *49*(1), 128-141.

D'Ambrosio, D. S., García, A., Díaz, A. R., Chivas, A. R., & Claps, M. C. (2017). Distribution of ostracods in west-central Argentina related to host-water chemistry and climate: implications for paleolimnology. *Journal of Paleolimnology*, *58*(2), 101-117.

da Costa, P. B., de Campos, S. B., Albersmeier, A., Dirksen, P., Dresseno, A. L. P., dos Santos, O. J. A. P., ... & Passaglia, L. M. P. (2018). Invasion ecology applied to inoculation of plant growth promoting bacteria through a novel SIMPER-PCA approach. *Plant and soil*, *422*, 467-478.

Dagodzo, D., Kimpe, L., Eickmeyer, D. C., Selbie, D., Smol, J. P., & Blais, J. M. (2025). Tracking long-term trends in Sockeye salmon (Oncorhynchus nerka) population dynamics using sterol and stanol biomarkers in lake sediments. *Authorea Preprints*.

Dai, A., Luo, D., Song, M., & Liu, J. (2019). Arctic amplification is caused by sea-ice loss under increasing CO2. *Nature communications*, *10*(1), 121.

Dalton, A. S., Patterson, R. T., Roe, H. M., Macumber, A. L., Swindles, G. T., Galloway, J. M., ... & Falck, H. (2018). Late Holocene climatic variability in Subarctic Canada: Insights from a high-resolution lake record from the central Northwest Territories. *PloS one*, *13*(6), e0199872.

Davidson, T. A., Bennion, H., Reid, M., Sayer, C. D., & Whitmore, T. J. (2018). Towards better integration of ecology in palaeoecology: from proxies to indicators, from inference to understanding. *Journal of Paleolimnology*, *60*, 109-116.

Day, N. J., Cumming, S. G., Dunfield, K. E., Johnstone, J. F., Mack, M. C., Reid, K. A., ... & Baltzer, J. L. (2020). Identifying functional impacts of heat-resistant fungi on boreal forest recovery after wildfire. *Frontiers in Forests and Global Change*, *3*, 68.

Day, N. J., Dunfield, K. E., Johnstone, J. F., Mack, M. C., Turetsky, M. R., Walker, X. J., White, A. L., & Baltzer, J. L. (2019). Wildfire severity reduces richness and alters composition of soil fungal communities in boreal forests of western Canada. *Global change biology*, *25*(7), 2310–2324. https://doi.org/10.1111/gcb.14641

Cáceres, M. D., & Legendre, P. (2009). Associations between species and groups of sites: indices and statistical inference. Ecology, 90(12), 3566-3574.

de Groot, W. J., Flannigan, M. D., & Cantin, A. S. (2013). Climate change impacts on future boreal fire regimes. *Forest Ecology and Management*, *294*, 35-44.

de Wit, H. A., Valinia, S., Weyhenmeyer, G. A., Futter, M. N., Kortelainen, P., Austnes, K., ... & Vuorenmaa, J. (2016). Current browning of surface waters will be further promoted by wetter climate. *Environmental Science & Technology Letters*, *3*(12), 430-435.

Dearborn, K. D., Wallace, C. A., Patankar, R., & Baltzer, J. L. (2021). Permafrost thaw in boreal peatlands is rapidly altering forest community composition. *Journal of Ecology*, *109*(3), 1452-1467.

Deluca, T. H., & Boisvenue, C. (2012). Boreal forest soil carbon: distribution, function and modelling. *Forestry*, *85*(2), 161-184.

Devoie, É. G., Craig, J. R., Dominico, M., Carpino, O., Connon, R. F., Rudy, A. C., & Quinton, W. L. (2021). Mechanisms of discontinuous permafrost thaw in peatlands. *Journal of Geophysical Research: Earth Surface*, *126*(11), e2021JF006204.

Devoie, É. G., Craig, J. R., Connon, R. F., & Quinton, W. L. (2019). Taliks: A tipping point in discontinuous permafrost degradation in peatlands. *Water Resources Research*, *55*(11), 9838-9857.

Devoie, É., Connon, R. F., Beddoe, R., Goordial, J., Quinton, W. L., & Craig, J. R. (2024). Disconnected active layers and unfrozen permafrost: A discussion of permafrost-related terms and definitions. *Science of The Total Environment*, *912*, 169017.

Dick, J. J., Tetzlaff, D., Birkel, C., & Soulsby, C. (2015). Modelling landscape controls on dissolved organic carbon sources and fluxes to streams. *Biogeochemistry*, *122*(2), 361-374.

Dobiński, W. (2020). Permafrost active layer. *Earth-Science Reviews*, *208*, 103301.

Doerr, S. H., Woods, S. W., Martin, D. A., & Casimiro, M. (2009). 'Natural background'soil water repellency in conifer forests of the north-western USA: its prediction and relationship to wildfire occurrence. *Journal of Hydrology*, *371*(1-4), 12-21.

Du, R., Peng, X., Wang, K., Frauenfeld, O. W., Chen, C., Sun, W., ... & Liang, B. (2021). Response of peat-rich permafrost to a warming climate on the northeast Tibetan Plateau. *Agricultural and Forest Meteorology*, *311*, 108681.

Duda, M.P., Sivarajah, B., Rühland, K.M. *et al.* Environmental optima for common diatoms from Ontario lakes along gradients of lakewater pH, total phosphorus concentration, and depth. *J Paleolimnol* **70**, 131–158 (2023). https://doi.org/10.1007/s10933-023-00288-7

Dumitru, O. A., Austermann, J., Polyak, V. J., Fornós, J. J., Asmerom, Y., Ginés, J., ... & Onac, B. P. (2019). Constraints on global mean sea level during Pliocene warmth. *Nature*, *574*(7777), 233-236.

Dunnette, P. V., Higuera, P. E., McLauchlan, K. K., Derr, K. M., Briles, C. E., & Keefe, M. H. (2014). Biogeochemical impacts of wildfires over four millennia in a R ocky M ountain subalpine watershed. *New Phytologist*, *203*(3), 900-912.

Earl, S. R., & Blinn, D. W. (2003). Effects of wildfire ash on water chemistry and biota in South-Western USA streams. *Freshwater Biology*, *48*(6), 1015-1030.

Ebel, B. A., & Moody, J. A. (2017). Synthesis of soil-hydraulic properties and infiltration timescales in wildfire-affected soils. *Hydrological Processes*, *31*(2), 324-340.

Eckdahl, J. A., Kristensen, J. A., & Metcalfe, D. B. (2023). Climate and forest properties explain wildfire impact on microbial community and nutrient mobilization in boreal soil. *Frontiers in Forests and Global Change*, *6*, 1136354.

Ecosystem Classification Group. (2007). Ecological regions of the northwest territories–Taiga Plains. *Department of Environment and Natural Resources, Government of Northwest Territories, Yellowknife, Northwest Territories, Canada*.

Edwards, M., Franklin-Smith, L., Clarke, C., Baker, J., Hill, S., & Gallagher, K. (2015). The role of fire in the mid-Holocene arrival and expansion of lodgepole pine (Pinus contorta var. latifolia Engelm. ex S. Watson) in Yukon, Canada. *The Holocene*, *25*(1), 64-78.

Eklöf, K., Von Brömssen, C., Amvrosiadi, N., Fölster, J., Wallin, M. B., & Bishop, K. (2021). Brownification on hold: What traditional analyses miss in extended surface water records. *Water Research*, *203*, 117544.

Elder, R. L., & Smith, G. R. (1988). Fish taphonomy and environmental inference in paleolimnology. *Palaeogeography, Palaeoclimatology, Palaeoecology*, *62*(1-4), 577-592.

Emery Boeck, M. A., Gaiser, E. E., Swain, H. M., Brenner, M., Curtis, J. H., & Kenney, W. F. (2023). Cyclical browning in a subtropical lake inferred from diatom records. *Frontiers in Ecology and Evolution*, *11*, 1020024.

Enayetullah, H., Chasmer, L., Hopkinson, C., Thompson, D., & Cobbaert, D. (2022). Identifying conifer tree vs. deciduous shrub and tree regeneration trajectories in a space-for-time boreal peatland fire chronosequence using multispectral lidar. *Atmosphere*, *13*(1), 112.

Erni, S., Arseneault, D., Parisien, M. A., & Bégin, Y. (2017). Spatial and temporal dimensions of fire activity in the fire-prone eastern Canadian taiga. *Global Change Biology*, *23*(3), 1152-1166.

Esri Inc. (2025). *ArcGIS Pro* (Version 3.5.3). https://www.esri.com/en-us/arcgis/products/arcgis-pro/overview

Esri. "World Imagery" [basemap]. Scale Not Given. "World Imagery". February 19, 2012. http://www.arcgis.com/home/item.html?id=30e5fe3149c34df1ba922e6f5bbf808f. (Jan 21, 2024).

Evans, C. D., Monteith, D. T., & Cooper, D. M. (2005). Long-term increases in surface water dissolved organic carbon: observations, possible causes and environmental impacts. *Environmental pollution*, *137*(1), 55-71.

Fallu, M. A., Allaire, N., & Pienitz, R. (2002). Distribution of freshwater diatoms in 64 Labrador (Canada) lakes: species environment relationships along latitudinal gradients and reconstruction models for water colour and alkalinity. *Canadian Journal of Fisheries and Aquatic Sciences*, *59*(2), 329-349.

Favot, E.J., Hadley, K.R., Paterson, A.M., Michelutti, N., Watson, S.B., Zastepa, A., Hutchinson, N.J., Vinebrooke, R.D. and Smol, J.P., 2020. Using visible near-infrared reflectance spectroscopy (VNIRS) of lake sediments to estimate historical changes in cyanobacterial production: potential and challenges. Journal of Paleolimnology, 64, pp.335-345.

Finstad, A. G., Andersen, T., Larsen, S., Tominaga, K., Blumentrath, S., De Wit, H. A., ... & Hessen, D. O. (2016). From greening to browning: Catchment vegetation development and reduced S-deposition promote organic carbon load on decadal time scales in Nordic lakes. *Scientific Reports*, *6*(1), 31944.

Fleming, W. D. (1943). V.—Synthetic mounting medium of high refractive index. *Journal of the Royal Microscopical Society*, *63*(1-2), 34-37.

Fleming, W. D. (1954). Naphrax: A synthetic mounting medium of high refractive Index new and improved methods of preparation. *Journal of the royal microscopical Society*, *74*(1), 42-44.

Fouché, J., Christiansen, C. T., Lafrenière, M. J., Grogan, P., & Lamoureux, S. F. (2020). Canadian permafrost stores large pools of ammonium and optically distinct dissolved organic matter. *Nature Communications*, *11*(1), 4500.

Francis, J. A., & Vavrus, S. J. (2012). Evidence linking Arctic amplification to extreme weather in mid-latitudes. *Geophysical research letters*, *39*(6).

Fredh, D., Broström, A., Zillén, L., Mazier, F., Rundgren, M., & Lagerås, P. (2012). Floristic diversity in the transition from traditional to modern land-use in southern Sweden AD 1800–2008. *Vegetation History and Archaeobotany*, *21*(6), 439-452.

Friedlingstein, P., O'sullivan, M., Jones, M. W., Andrew, R. M., Bakker, D. C., Hauck, J., ... & Zheng, B. (2023). Global carbon budget 2023. *Earth System Science Data*, *15*(12), 5301-5369.

Gaboriau, D. M., Chaste, É., Girardin, M. P., Asselin, H., Ali, A. A., Bergeron, Y., & Hély, C. (2023). Interactions within the climate-vegetation-fire nexus may transform 21st century boreal forests in northwestern Canada. *Iscience*, *26*(6).

Gaboriau, D. M., Remy, C. C., Girardin, M. P., Asselin, H., Hély, C., Bergeron, Y., & Ali, A. A. (2020). Temperature and fuel availability control fire size/severity in the boreal forest of central Northwest Territories, Canada. *Quaternary Science Reviews*, *250*, 106697.

Gajewski, K. (2006). Is arctic palynology a "blunt instrument"? *Geographie Physique et Quaternaire, 60*(2), 95–102. https://doi.org/10.7202/016822ar

Gauthier, S., Bernier, P., Kuuluvainen, T., Shvidenko, A. Z., & Schepaschenko, D. G. (2015). Boreal forest health and global change. *Science*, *349*(6250), 819-822.

Gibson, C., Cottenie, K., Gingras-Hill, T., Kokelj, S. V., Baltzer, J. L., Chasmer, L., & Turetsky, M. R. (2021). Mapping and understanding the vulnerability of northern peatlands to permafrost thaw at scales relevant to community adaptation planning. *Environmental Research Letters*, *16*(5), 055022.

Gibson, C.M., Chasmer, L.E., Thompson, D.K. *et al.* Wildfire as a major driver of recent permafrost thaw in boreal peatlands. *Nat Commun* 9, 3041 (2018). https://doi.org/10.1038/s41467-018-05457-1

Gisnås, K., Westermann, S., Schuler, T. V., Litherland, T., Isaksen, K., Boike, J., & Etzelmüller, B. (2014). A statistical approach to represent small-scale variability of permafrost temperatures due to snow cover. *The Cryosphere*, *8*(6), 2063-2074.

Glew, J. R., Smol, J. P. & Last, W. M. (2001). Sediment Core Collection and Extrusion. In Last, W. M., & Smol, J. P. (eds.), *Tracking Environmental Change Using Lake Sediments. Volume 1: Basin Analysis, Coring, and Chronological Techniques* (pp.73-105). Dordrecht, The Netherlands: Kluwer Academic Publishers.

Glew, J.R. (1988). A portable extruding device for close interval sectioning of unconsolidated core samples. Journal of Paleolimnology, 1(3), 235–239.

González-Pérez, J. A., González-Vila, F. J., Almendros, G., & Knicker, H. (2004). The effect of fire on soil organic matter—a review. *Environment international*, *30*(6), 855-870.

Government of Canada, Natural Resources Canada, Geological Survey of Canada. (2021, August 31). Permafrost, Atlas of Canada, 5th Edition. Natural Resources Canada, Federal Geospatial Platform. https://osdp-psdo.canada.ca/dp/en/search/metadata/NRCAN-FGP-1-d1e2048b-ccff-5852-aaa5-b861bd55c367

Granath, G., Evans, C. D., Strengbom, J., Fölster, J., Grelle, A., Strömqvist, J., & Köhler, S. J. (2020). The impact of wildfire on biogeochemical fluxes and water quality on boreal catchments. *Biogeosciences Discussions*, *2020*, 1-33.

Graneli, W. (2012). Brownification of lakes. In *Encyclopedia of lakes and reservoirs* (pp. 117-119). Springer, Dordrecht.

Greene, D. F., Macdonald, S. E., Haeussler, S., Domenicano, S., Noel, J., Jayen, K., ... & Swift, L. (2007). The reduction of organic-layer depth by wildfire in the North American boreal forest and its effect on tree recruitment by seed. *Canadian Journal of Forest Research*, *37*(6), 1012-1023.

Grimm, E. C. (1987). CONISS: a FORTRAN 77 program for stratigraphically constrained cluster analysis by the method of incremental sum of squares. *Computers & geosciences*, *13*(1), 13-35.

Grogan, P., Burns, T. & Chapin III, F. Fire effects on ecosystem nitrogen cycling in a Californian bishop pine forest. *Oecologia* **122**, 537–544 (2000). https://doi.org/10.1007/s004420050977

Gros, M., Zilkey, D. R., Griffiths, K. T., Pham, J., MacKeigan, P. W., Taranu, Z. E., ... & Gregory-Eaves, I. (2023). Long-term environmental changes in the Canadian boreal zone: Synthesizing temporal trends from lake sediment archives to inform future sustainability. *Environmental Reviews*, *31*(3), 509-526.

Grosbois, G. *et al.* (2023). Land and Freshwater Complex Interactions in Boreal Forests: A Neglected Topic in Forest Management. In: Girona, M.M., Morin, H., Gauthier, S., Bergeron, Y. (eds) Boreal Forests in the Face of Climate Change. Advances in Global Change Research, vol 74. Springer, Cham. https://doi.org/10.1007/978-3-031-15988-6_29

Guiry MD, Guiry GM. 2024. AlgaeBase. World-wide electronic publication, National University of Ireland, Galway. https://www.algaebase.org

Guiry, M. D. (2012). How many species of algae are there?. *Journal of phycology*, *48*(5), 1057-1063.

Gushulak, C. A., & Cumming, B. F. (2020). Diatom assemblages are controlled by light attenuation in oligotrophic and mesotrophic lakes in northern Ontario (Canada). *Journal of Paleolimnology*, *64*, 419-433.

Halsey, L.A., Vitt, D.H. & Zoltai, S.C. Disequilibrium response of permafrost in boreal continental western Canada to climate change. *Climatic Change* 30, 57–73 (1995). https://doi.org/10.1007/BF01093225

Hammer, Ø., Harper, D.A.T., Ryan, P.D. (2001). PAST: Paleontological Statistics software package for education and data analysis. Palaeontologia Electronica 4(1): 9 pp.

Hanes, C. C., Wang, X., Jain, P., Parisien, M. A., Little, J. M., & Flannigan, M. D. (2019). Fire-regime changes in Canada over the last half century. *Canadian Journal of Forest Research*, *49*(3), 256-269.

Hansen, A. M., Kraus, T. E., Pellerin, B. A., Fleck, J. A., Downing, B. D., & Bergamaschi, B. A. (2016). Optical properties of dissolved organic matter (DOM): Effects of biological and photolytic degradation. *Limnology and oceanography*, *61*(3), 1015-1032.

Hanson, P. C., Hamilton, D. P., Stanley, E. H., Preston, N., Langman, O. C., & Kara, E. L. (2011). Fate of allochthonous dissolved organic carbon in lakes: a quantitative approach. *PloS one*, *6*(7), e21884.

Harris, L. I., Richardson, K., Bona, K. A., Davidson, S. J., Finkelstein, S. A., Garneau, M., ... & Ray, J. C. (2022). The essential carbon service provided by northern peatlands. *Frontiers in Ecology and the Environment*, *20*(4), 222-230.

Hayashi, M., Goeller, N., Quinton, W. L., & Wright, N. (2007). A simple heat-conduction method for simulating the frost-table depth in hydrological models. *Hydrological Processes: An International Journal*, *21*(19), 2610-2622.

Haynes, K. M., Connon, R. F., & Quinton, W. L. (2018). Permafrost thaw induced drying of wetlands at Scotty Creek, NWT, Canada. *Environmental Research Letters*, *13*(11), 114001.

Hedges, J. I., and D. C. Mann. 1979. The characterization of plant tissues by their lignin oxidation products. Geochim. Cosmochim. Acta 43: 1803-1807. doi:10.1016/0016-7037(79)90028-0

Heffernan, L., Estop-Aragonés, C., Knorr, K. H., Talbot, J., & Olefeldt, D. (2020). Long-term impacts of permafrost thaw on carbon storage in peatlands: Deep losses offset by surficial accumulation. *Journal of Geophysical Research: Biogeosciences*, *125*(3), e2019JG005501.

Heffernan, L., Kothawala, D. N., & Tranvik, L. J. (2024). Terrestrial dissolved organic carbon in northern permafrost. *The Cryosphere*, *18*(3), 1443-1465.

Heiri O, Lotter AF, Lemcke G. 2001. Loss on ignition as a method for estimating organic and carbonate content in sediments: reproducibility and comparability of results. J Paleolimnol. 25(1):101–110. doi: 10.1023/A:1008119611481.

Helbig, M., Daw, L., Iwata, H., Rudaitis, L., Ueyama, M., & Živković, T. (2024). Boreal forest fire causes daytime surface warming during summer to exceed surface cooling during winter in North America. *AGU Advances*, *5*(5), e2024AV001327.

Helbig, M., Pappas, C., & Sonnentag, O. (2016). Permafrost thaw and wildfire: Equally important drivers of boreal tree cover changes in the Taiga Plains, Canada. *Geophysical Research Letters*, *43*(4), 1598-1606.

Helms, J. R., Stubbins, A., Ritchie, J. D., Minor, E. C., Kieber, D. J., & Mopper, K. (2008). Absorption spectral slopes and slope ratios as indicators of molecular weight, source, and photobleaching of chromophoric dissolved organic matter. *Limnology and oceanography*, *53*(3), 955-969.

Hensgens, G., Laudon, H., Peichl, M., Gil, I. A., Zhou, Q., and Berggren, M. (2020). The role of the understory in litter doc and nutrient leaching in boreal forests. *Biogeochemistry* 149, 87–103. doi: 10.1007/s10533-020-00668-5

Hermanns, Y.M. & Biester, H. (2013). A 17,300-year record of mercury accumulation in a pristine lake in southern Chile. Journal of Paleolimnology, 49, 547–561.

Hessilt, T. D., Abatzoglou, J. T., Chen, Y., Randerson, J. T., Scholten, R. C., Van Der Werf, G., & Veraverbeke, S. (2022). Future increases in lightning ignition efficiency and wildfire occurrence expected from drier fuels in boreal forest ecosystems of western North America. *Environmental Research Letters*, *17*(5), 054008.

Hinkel KM, Hurd JK (2006) Permafrost destabilization and thermokarst following snow fence installation, Barrow, Alaska, USA. Arctic, Antarctic and Alpine Research, 38, 530–539.

Högberg, P., Näsholm, T., Franklin, O., & Högberg, M. N. (2017). *Tamm review: on the nature of the nitrogen limitation to plant growth in Fennoscandian boreal forests. For Ecol Manag 403: 161–185.*

Holgerson, M. A., Richardson, D. C., Roith, J., Bortolotti, L. E., Finlay, K., Hornbach, D. J., ... & Webb, J. R. (2022). Classifying mixing regimes in ponds and shallow lakes. *Water Resources Research*, *58*(7), e2022WR032522.

Holloway, J. E., & Lewkowicz, A. G. (2020). Half a century of discontinuous permafrost persistence and degradation in western Canada. *Permafrost and Periglacial Processes*, *31*(1), 85-96.

Holtvoeth, J., Whiteside, J. H., Engels, S., Freitas, F. S., Grice, K., Greenwood, P., ... & Sepúlveda, J. (2019). The paleolimnologist's guide to compound-specific stable isotope analysis–An introduction to principles and applications of CSIA for Quaternary lake sediments. *Quaternary Science Reviews*, *207*, 101-133.

Horppila, J., Nurminen, L., Rajala, S., & Estlander, S. (2024). Making waves: the sensitivity of lakes to brownification and issues of concern in ecological status assessment. *Water Research*, *249*, 120964.

Hu, F. S., J. I. Hedges, E. S. Gordon, and L. B. Brubaker. 1999. Lignin biomarkers and pollen in postglacial sediments of an Alaskan lake. Geochim. Cosmochim. Acta 63: 1421-1430. doi:10.1016/S0016-7037(99)00100-3

Hu, J., Yu, H., Li, Y., Wang, J., Lv, T., Liu, C., & Yu, D. (2021). Variation in resource allocation strategies and environmental driving factors for different life-forms of aquatic plants in cold temperate zones. *Journal of Ecology*, *109*(8), 3046-3059.

Huang, X., & Rein, G. (2019). Upward-and-downward spread of smoldering peat fire. *Proceedings of the Combustion Institute*, *37*(3), 4025-4033.

Hugelius, G. et al. Estimated stocks of circumpolar permafrost carbon with quantified uncertainty ranges and identified data gaps. *Biogeosciences* **11**, 6573–6593 (2014).

Hugelius, G., Loisel, J., Chadburn, S., Jackson, R. B., Jones, M., MacDonald, G., ... & Yu, Z. (2020). Large stocks of peatland carbon and nitrogen are vulnerable to permafrost thaw. *Proceedings of the National Academy of Sciences*, *117*(34), 20438-20446.

Hutchins, R. H., Tank, S. E., Olefeldt, D., Quinton, W. L., Spence, C., Dion, N., & Mengistu, S. G. (2023). Influence of wildfire on downstream transport of dissolved carbon, nutrients, and mercury in the permafrost zone of Boreal western Canada. *Journal of Geophysical Research: Biogeosciences*, *128*(10), e2023JG007602.

Ibáñez, T. S., Rütting, T., Nilsson, M. C., Wardle, D. A., & Gundale, M. J. (2022). Mid-term effects of wildfire and salvage logging on gross and net soil nitrogen transformation rates in a Swedish boreal forest. *Forest Ecology and Management*, *517*, 120240.

IPCC, 2021: *Climate Change 2021: The Physical Science Basis. Contribution of Working Group I to the Sixth Assessment Report of the Intergovernmental Panel on Climate Change*[Masson-Delmotte, V., P. Zhai, A. Pirani, S.L. Connors, C. Péan, S. Berger, N. Caud, Y. Chen, L. Goldfarb, M.I. Gomis, M. Huang, K. Leitzell, E. Lonnoy, J.B.R. Matthews, T.K. Maycock, T. Waterfield, O. Yelekçi, R. Yu, and B. Zhou (eds.)]. Cambridge University Press, Cambridge, United Kingdom and New York, NY, USA, In press, doi:10.1017/9781009157896.

Ishiwatari, R., S. Yamamoto, and S. Shinoyama. 2006. Lignin and fatty acid records in Lake Baikal sediments over the last 130Kyr: A comparison with pollen records. Org. Geochem. 37: 1787-1802. doi:10.1016/j.orggeochem.2006.10.005

Isidorova, A., Bravo, A. G., Riise, G., Bouchet, S., Björn, E., & Sobek, S. (2016). The effect of lake browning and respiration mode on the burial and fate of carbon and mercury in the sediment of two boreal lakes. *Journal of Geophysical Research: Biogeosciences*, *121*(1), 233-245.

Ito, E. (2001). Application of Stable Isotope Techniquesto Inorganic and Biogenic Carbonates. *Tracking Environmental Change Using Lake Sediments: Physical and geochemical methods*, 351-371.

Iwatani, H., Yasuhara, M., Rosenthal, Y., & Linsley, B. K. (2018). Intermediate-water dynamics and ocean ventilation effects on the Indonesian Throughflow during the past 15,000 years: Ostracod evidence. *Geology*, *46*(6), 567-570.

Jain, P., Barber, Q.E., Taylor, S.W. *et al.* Drivers and Impacts of the Record-Breaking 2023 Wildfire Season in Canada. *Nat Commun* 15, 6764 (2024). https://doi.org/10.1038/s41467-024-51154-7

Jain, P., Wang, X., & Flannigan, M. D. (2017). Trend analysis of fire season length and extreme fire weather in North America between 1979 and 2015. *International journal of wildland fire*, *26*(12), 1009-1020.

Jaman, M. S., Yu, Q., Xu, C., Jamil, M., Ke, Y., Yang, T., ... & Wu, H. (2024). Chronic drought decreased organic carbon content in topsoil greater than intense drought across grasslands in Northern China. *Geoderma*, *443*, 116832.

Jane, S. F., Detmer, T. M., Larrick, S. L., Rose, K. C., Randall, E. A., Jirka, K. J., & McIntyre, P. B. (2024). Concurrent warming and browning eliminate cold-water fish habitat in many temperate lakes. *Proceedings of the National Academy of Sciences*, *121*(2), e2306906120.

Janssen, T.A.J., Jones, M.W., Finney, D. *et al.* Extratropical forests increasingly at risk due to lightning fires. *Nat. Geosci.* **16**, 1136–1144 (2023). https://doi.org/10.1038/s41561-023-01322-z

Jeppesen, E., Leavitt, P., De Meester, L., & Jensen, J. P. (2001). Functional ecology and palaeolimnology: using cladoceran remains to reconstruct anthropogenic impact. *Trends in Ecology & Evolution*, *16*(4), 191-198.

Jiang, G., Ma, R., Duan, H., Loiselle, S. A., Xu, J., & Liu, D. (2014). Remote determination of chromophoric dissolved organic matter in lakes, China. *International Journal of Digital Earth*, *7*(11), 897-915.

Johnston, D. C., Turetsky, M. R., Benscoter, B. W., and Wotton, B. M. (2015). Fuel load, structure, and potential fire behaviour in black spruce bogs. Can. J. For. Res. 45, 888–899. doi: 10.1139/cjfr-2014-0334

Johnston, S. E., Striegl, R. G., Bogard, M. J., Dornblaser, M. M., Butman, D. E., Kellerman, A. M., ... & Spencer, R. G. (2020). Hydrologic connectivity determines dissolved organic matter biogeochemistry in northern high-latitude lakes. *Limnology and Oceanography*, *65*(8), 1764-1780.

Jones, M. C., Grosse, G., Treat, C., Turetsky, M., Anthony, K. W., & Brosius, L. (2023). Past permafrost dynamics can inform future permafrost carbon-climate feedbacks. *Communications Earth & Environment*, *4*(1), 272.

Judd, E. J., Tierney, J. E., Lunt, D. J., Montañez, I. P., Huber, B. T., Wing, S. L., & Valdes, P. J. (2024). A 485-million-year history of Earth's surface temperature. *science*, *385*(6715), eadk3705.

Juggins, S. (2013). Quantitative reconstructions in palaeolimnology: new paradigm or sick science?. *Quaternary Science Reviews*, *64*, 20-32.

Juggins, S. (2023) rioja: Analysis of Quaternary Science Data, R package version (1.0-6). (https://cran.r-project.org/package=rioja).

Juggins, S. (2023) riojaPlot: Stratigraphic diagrams in R, package version (0.1-20). (https://github.com/nsj3/riojaPlot).

Kahlert, M., Rühland, K. M., Lavoie, I., Keck, F., Saulnier-Talbot, E., Bogan, D., ... & Smol, J. P. (2022). Biodiversity patterns of Arctic diatom assemblages in lakes and streams: Current reference conditions and historical context for biomonitoring. *Freshwater Biology*, *67*(1), 116-140.

Kane, D. L., Hinzman, L. D., & Zarling, J. P. (1991). Thermal response of the active layer to climatic warming in a permafrost environment. *Cold Regions Science and Technology*, *19*(2), 111-122.

Karlsson, J., P. Bystrom, J. Ask, P. Ask, L. Persson, M. Jansson. 2009. Light limitation of nutrient-poor lake ecosystems. *Nature* 460: 506–509.

Karst-Riddoch, T. L., Pisaric, M. F., Youngblut, D. K., & Smol, J. P. (2005). Postglacial record of diatom assemblage changes related to climate in an alpine lake in the northern Rocky Mountains, Canada. *Canadian Journal of Botany*, *83*(8), 968-982.

Burd, K., Estop-Aragonés, C., Tank, S. E., & Olefeldt, D. (2020). Lability of dissolved organic carbon from boreal peatlands: interactions between permafrost thaw, wildfire, and season. *Canadian Journal of Soil Science*, *100*(4), 503-515.

Kaur, R., & Sharma, M. (2019). Cereal polysaccharides as sources of functional ingredient for reformulation of meat products: A review. *Journal of Functional Foods*, *62*, 103527.

Kelly, P. T., Solomon, C. T., Weidel, B. C., & Jones, S. E. (2014). Terrestrial carbon is a resource, but not a subsidy, for lake zooplankton. *Ecology*, *95*(5), 1236-1242.

Kelly, P. T., Solomon, C. T., Zwart, J. A., & Jones, S. E. (2018). A framework for understanding variation in pelagic gross primary production of lake ecosystems. *Ecosystems*, *21*, 1364-1376.

Kim, I. W., Timmermann, A., Kim, J. E., Rodgers, K. B., Lee, S. S., Lee, H., & Wieder, W. R. (2024). Abrupt increase in Arctic-Subarctic wildfires caused by future permafrost thaw. *Nature Communications*, *15*(1), 7868.

Knoll, L. B., Williamson, C. E., Pilla, R. M., Leach, T. H., Brentrup, J. A., & Fisher, T. J. (2018). Browning-related oxygen depletion in an oligotrophic lake. *Inland Waters*, *8*(3), 255-263.

Kochtubajda, B., Flannigan, M. D., Gyakum, J. R., Stewart, R. E., & Way, A. (2003, December). Lightning Behaviour in the Northwest Territories, Canada. In *AGU Fall Meeting Abstracts* (Vol. 2003, pp. AE41A-02).

Kokelj, S. V., & Jorgenson, M. T. (2013). Advances in thermokarst research. *Permafrost and Periglacial Processes*, *24*(2), 108-119.

Korhola, A. & Rautio, M. (2001). Cladocera and Other Branchiopod Crustaceans. In Smol, J. P., Birks, H. J. B., & Last, W. M. (eds.), Tracking Environmental Change Using Lake Sediments, Volume 4: Zoological Indicators (pp. 5-41). Dordrecht, The Netherlands: Kluwer Academic Publishers.

Korosi, J. B., Coleman, K. A., Hoskin, G. N., Little, A. J., Stewart, E. M., & Thienpont, J. R. (2022). Paleolimnological perspectives on the shifting geographic template of permafrost landscapes and its implications for Arctic freshwater biodiversity. *Canadian Journal of Fisheries and Aquatic Sciences*, *79*(7), 1162-1172.

Korosi, J. B., McDonald, J., Coleman, K. A., Palmer, M. J., Smol, J. P., Simpson, M. J., & Blais, J. M. (2015). Long-term changes in organic matter and mercury transport to lakes in the sporadic discontinuous permafrost zone related to peat subsidence. *Limnology and Oceanography*, *60*(5), 1550-1561.

Korosi, J.B., Adano, R.C., Do, P.H.P., Hall, R.I., Jeyarajah, J., Stewart, E.M., Wiklund, J.A. and Thienpont, J.R., 2024. Ecosystem impacts of an invasive charophyte (Nitellopsis obtusa) interpreted in a multiple stressor context using paleolimnology. Lake and Reservoir Management, 40(2), pp.132-144.

Korsman T, Nilsson M, Ohman J, Renberg I (1992) Near-infrared reflectance spectroscopy of sediments—a potential method to infer the past pH of lakes. Environ Sci Technol 26:2122–2126

Korsman T. and Birks H.J.B. 1996. Diatom-based water chemistry recontructed from northern Sweden: a comparisson of recontruction techniques. J. Paleolim. 15: 65–77.

Kottek, M., Grieser, J., Beck, C., Rudolf, B., & Rubel, F. (2006). World map of the Köppen-Geiger climate classification updated.

Kozak, N., Ahonen, S. A., Keva, O., Østbye, K., Taipale, S. J., Hayden, B., & Kahilainen, K. K. (2021). Environmental and biological factors are joint drivers of mercury biomagnification in subarctic lake food webs along a climate and productivity gradient. *Science of the Total Environment*, *779*, 146261.

Kragh, T., Sand-Jensen, K., Kristensen, E., Pedersen, O., & Madsen-Østerbye, M. (2022). Removal of chromophoric dissolved organic matter under combined photochemical and microbial degradation as a response to different irradiation intensities. *journal of environmental sciences*, *118*, 76-86.

Krammer K. & Lange-Bertalot H. 1997. Bacillariophyceae 2. Teil: Bacillariaceae, Epithemiaceae, Surirellaceae. Süßwasserflora von Mitteleuropa 2/2. Spektrum Akademischer Verlag, Berlin, Germany.

Krammer K. & Lange-Bertalot H. 1999. Bacillariophyceae 1. Teil: Naviculaceae. Süßwasserflora von Mitteleuropa 2/1. Spektrum Akademisher Verlag, Berlin, Germany.

Krammer K. & Lange-Bertalot H. 2000. Bacillariophyceae 3. Teil: Centrales, Fragilariaceae, Eunotiaceae. Süßwasserflora von Mitteleuropa 2/3. Spektrum Akademischer Verlag, Berlin, Germany.

Krishnaswamy, S., Lal, D., Martin, J.M., & Meybeck, M. (1971). Geochronology of lake sediments. Earth and Planetary Science Letters, 11(1-5), 407-414.

Kritzberg, E. S. (2017). Centennial-long trends of lake browning show major effect of afforestation. *Limnology and Oceanography Letters*, *2*(4), 105-112.

Kritzberg, E. S., Hasselquist, E. M., Škerlep, M., Löfgren, S., Olsson, O., Stadmark, J., ... & Laudon, H. (2020). Browning of freshwaters: Consequences to ecosystem services, underlying drivers, and potential mitigation measures. *Ambio*, *49*, 375-390.

Krzeminski, P., Vogelsang, C., Meyn, T., Köhler, S. J., Poutanen, H., De Wit, H. A., & Uhl, W. (2019). Natural organic matter fractions and their removal in full-scale drinking water treatment under cold climate conditions in Nordic capitals. *Journal of Environmental Management*, *241*, 427-438.

Kubínová, T., & Kyncl, M. (2021, November). Comparison of standard methods for determining the color of water in several countries. In *IOP Conference Series: Earth and Environmental Science* (Vol. 900, No. 1, p. 012018). IOP Publishing.

Kujala, K., Seppälä, M., & Holappa, T. (2008). Physical properties of peat and palsa formation. *Cold Regions Science and Technology*, *52*(3), 408-414.

Kuosmanen, N., Väliranta, M., Piilo, S., Tuittila, E. S., Oksanen, P., & Wallenius, T. (2023). Repeated fires in forested peatlands in sporadic permafrost zone in Western Canada. *Environmental Research Letters*, *18*(9), 094051.

Kurek, M. R., Garcia-Tigreros, F., Wickland, K. P., Frey, K. E., Dornblaser, M. M., Striegl, R. G., ... & Spencer, R. G. (2023). Hydrologic and landscape controls on dissolved organic matter composition across western North American Arctic lakes. *Global Biogeochemical Cycles*, *37*(1), e2022GB007495.

Kurylyk, B. L., Hayashi, M., Quinton, W. L., McKenzie, J. M., & Voss, C. I. (2016). Influence of vertical and lateral heat transfer on permafrost thaw, peatland landscape transition, and groundwater flow. *Water Resources Research*, *52*(2), 1286-1305.

Kurz, W. A., Shaw, C. H., Boisvenue, C., Stinson, G., Metsaranta, J., Leckie, D., ... & Neilson, E. T. (2013). Carbon in Canada's boreal forest—a synthesis. *Environmental Reviews*, *21*(4), 260-292.

Kyaschenko, J., Ovaskainen, O., Ekblad, A., Hagenbo, A., Karltun, E., Clemmensen, K. E., & Lindahl, B. D. (2019). Soil fertility in boreal forest relates to root-driven nitrogen retention and carbon sequestration in the mor layer. *New Phytologist*, *221*(3), 1492-1502.

Lacis, A. A., Schmidt, G. A., Rind, D., & Ruedy, R. A. (2010). Atmospheric CO2: Principal control knob governing Earth's temperature. *Science*, *330*(6002), 356-359.

Laird, K. R., Li, S., Gushulak, C. A., Moir, K. E., Wang, Y., Leavitt, P. R., & Cumming, B. F. (2023). Influence of cultural eutrophication, climate, and landscape connectivity on 3 Kawartha lakes (Ontario, Canada) since the early 1800s. *Lake and Reservoir Management*, *39*(2), 120-140.

Landau, S., & Ster, I. C. (2010). Cluster analysis: overview. *Á Á*, *11*(x12), x1p.

Lange-Bertalot, H., Hofmann, G., Werum, M., Kelly, M., & Cantonati, M. (2017). *Freshwater benthic diatoms of Central Europe: over 800 common species used in ecological assessment* (Vol. 942, pp. 1-908). Schmitten-Oberreifenberg: Koeltz Botanical Books.

Lapierre, J. F., Guillemette, F., Berggren, M., & Del Giorgio, P. A. (2013). Increases in terrestrially derived carbon stimulate organic carbon processing and CO2 emissions in boreal aquatic ecosystems. *Nature communications*, *4*(1), 2972.

Last, W.M. Textural analysis of lake sediments. Smol, J.P., Birks, H.J. and Last, W.M. eds., 2002. *Tracking environmental change using lake sediments: Volume 2: Physical and Geochemical Methods*. (Vol. 2 pp. 41-83).

Lavonen, E. E., Gonsior, M., Tranvik, L. J., Schmitt-Kopplin, P., & Köhler, S. J. (2013). Selective chlorination of natural organic matter: identification of previously unknown disinfection byproducts. *Environmental science & technology*, *47*(5), 2264-2271.

Le Costaouëc, T., Unamunzaga, C., Mantecon, L., & Helbert, W. (2017). New structural insights into the cell-wall polysaccharide of the diatom Phaeodactylum tricornutum. *Algal research*, *26*, 172-179.

Lear, C. H., Anand, P., Blenkinsop, T., Foster, G. L., Gagen, M., Hoogakker, B., ... & Zalasiewicz, J. (2021). Geological Society of London Scientific Statement: what the geological record tells us about our present and future climate. *Journal of the Geological Society*, *178*(1), jgs2020-239.

Leech, D. M., Pollard, A. I., Labou, S. G., & Hampton, S. E. (2018). Fewer blue lakes and more murky lakes across the continental US: Implications for planktonic food webs. *Limnology and Oceanography*, *63*(6), 2661-2680.

Legendre, P., & Gallagher, E. D. (2001). Ecologically meaningful transformations for ordination of species data. *Oecologia*, *129*, 271-280.

Legleiter, C. J., Lawrence, R. L., Fonstad, M. A., Marcus, W. A., & Aspinall, R. (2003). Fluvial response a decade after wildfire in the northern Yellowstone ecosystem: a spatially explicit analysis. *Geomorphology*, *54*(3-4), 119-136.

Lei, M., Cui, Y., Ni, J., Zhang, G., Li, Y., Wang, H., ... & Zhou, L. (2022). Temporal evolution of the hydromechanical properties of soil-root systems in a forest fire in China. *Science of the Total Environment*, *809*, 151165.

Lei, Y., Wang, Y., Qin, F., Liu, J., Feng, P., Luo, L., ... & Jiang, S. (2021). Diatom assemblage shift driven by nutrient dynamics in a large, subtropical reservoir in southern China. *Journal of Cleaner Production*, *317*, 128435.

Li, A., Aubeneau, A. F., King, T., Cory, R. M., Neilson, B. T., Bolster, D., & Packman, A. I. (2019). Effects of vertical hydrodynamic mixing on photomineralization of dissolved organic carbon in arctic surface waters. *Environmental Science: Processes & Impacts*, *21*(4), 748-760.

Li, W., Yang, M., Wang, B., & Liu, C. Q. (2022). Regulation strategy for nutrient-dependent carbon and nitrogen stoichiometric homeostasis in freshwater phytoplankton. *Science of the Total Environment*, *823*, 153797.

Liang, J. et al. Co-limitation towards lower latitudes shapes global forest diversity gradients. *Nat. Ecol. Evol.* 6, 1423–1437 (2022).

Liebmann, P., Bárta, J., Vogel, C. *et al.* Permafrost degradation and its consequences for carbon storage in soils of Interior Alaska. *Biogeochemistry* **167**, 199–223 (2024). https://doi.org/10.1007/s10533-024-01132-4

Lim, D. S., Smol, J. P., & Douglas, M. S. (2007). Diatom assemblages and their relationships to lakewater nitrogen levels and other limnological variables from 36 lakes and ponds on Banks Island, NWT, Canadian Arctic. *Hydrobiologia*, *586*, 191-211.

Lindbladh, M., Oswald, W. W., Foster, D. R., Faison, E. K., Hou, J., & Huang, Y. (2007). A late-glacial transition from Picea glauca to Picea mariana in southern New England. *Quaternary Research*, *67*(3), 502-508.

Loisel, J. et al. A database and synthesis of northern peatland soil properties and Holocene carbon and nitrogen accumulation. *Holocene* **24**, 1028–1042 (2014).

Lotter, A. F., & Bigler, C. (2000). Do diatoms in the Swiss Alps reflect the length of ice-cover?. Aquatic Sciences, 62(2), 125-141.

Lynch, J. P., Strock, C. F., Schneider, H. M., Sidhu, J. S., Ajmera, I., Galindo-Castañeda, T., ... & Hanlon, M. T. (2021). Root anatomy and soil resource capture. *Plant and Soil*, *466*(1), 21-63.

Maavara, T., Logozzo, L., Stubbins, A., Aho, K., Brinkerhoff, C., Hosen, J., & Raymond, P. (2021). Does photomineralization of dissolved organics matter in temperate rivers?. *Journal of Geophysical Research: Biogeosciences*, *126*(7), e2021JG006402.

Mack, M. C., Walker, X. J., Johnstone, J. F., Alexander, H. D., Melvin, A. M., Jean, M., & Miller, S. N. (2021). Carbon loss from boreal forest wildfires offset by increased dominance of deciduous trees. *Science*, *372*(6539), 280-283.

Mackay, J. R. (1998). Pingo growth and collapse, Tuktoyaktuk Peninsula area, western Arctic coast, Canada: A long-term field study. *Géographie physique et Quaternaire*, *52*(3), 271-323.

Makoto, K., & Koike, T. (2021). Charcoal ecology: Its function as a hub for plant succession and soil nutrient cycling in boreal forests. *Ecological Research*, *36*(1), 4-12.

Malviya, S., Scalco, E., Audic, S., Vincent, F., Veluchamy, A., Poulain, J., ... & Bowler, C. (2016). Insights into global diatom distribution and diversity in the world's ocean. *Proceedings of the National Academy of Sciences*, *113*(11), E1516-E1525.

Massey, R., Rogers, B. M., Berner, L. T., Cooperdock, S., Mack, M. C., Walker, X. J., & Goetz, S. J. (2023). Forest composition change and biophysical climate feedbacks across boreal North America. *Nature Climate Change*, *13*(12), 1368-1375.

Maynard, D. G., Paré, D., Thiffault, E., Lafleur, B., Hogg, K. E., & Kishchuk, B. (2014). How do natural disturbances and human activities affect soils and tree nutrition and growth in the Canadian boreal forest?. *Environmental Reviews*, *22*(2), 161-178.

Mayner, K. M., Moore, P. A., Wilkinson, S. L., Gage, H. J., & Waddington, J. M. (2024). Differential Post-Fire Vegetation Recovery of Boreal Plains Bogs and Margins. *Wetlands*, *44*(4), 44.

Mayzel, B., Aram, L., Varsano, N., Wolf, S. G., & Gal, A. (2021). Structural evidence for extracellular silica formation by diatoms. *Nature communications*, *12*(1), 4639.

Mazoyer, F., Laurion, I., & Rautio, M. (2022). The dominant role of sunlight in degrading winter dissolved organic matter from a thermokarst lake in a subarctic peatland. *Biogeosciences*, *19*(17), 3959-3977.

McClymont, A. F., Hayashi, M., Bentley, L. R., & Christensen, B. S. (2013). Geophysical imaging and thermal modeling of subsurface morphology and thaw evolution of discontinuous permafrost. *Journal of Geophysical Research: Earth Surface*, *118*(3), 1826-1837.

McLauchlan, K. K., Higuera, P. E., Miesel, J., Rogers, B. M., Schweitzer, J., Shuman, J. K., ... & Watts, A. C. (2020). Fire as a fundamental ecological process: Research advances and frontiers. *Journal of Ecology*, *108*(5), 2047-2069.

Meyer-Jacob, C., Labaj, A. L., Paterson, A. M., Edwards, B. A., Keller, W. B., Cumming, B. F., & Smol, J. P. (2020). Re-browning of Sudbury (Ontario, Canada) lakes now approaches pre-acid deposition lake-water dissolved organic carbon levels. *Science of the Total Environment*, *725*, 138347.

Meyer-Jacob, C., Michelutti, N., Paterson, A. M., Cumming, B. F., Keller, W., & Smol, J. P. (2019). The browning and re-browning of lakes: Divergent lake-water organic carbon trends linked to acid deposition and climate change. *Scientific reports*, *9*(1), 16676.

Meyers, P. A. (2003). Applications of organic geochemistry to paleolimnological reconstructions: a summary of examples from the Laurentian Great Lakes. *Organic geochemistry*, *34*(2), 261-289.

Meyers, P. A., & Lallier-Vergès, E. (1999). Lacustrine sedimentary organic matter records of Late Quaternary paleoclimates. *Journal of Paleolimnology*, *21*(3), 345-372.

Meyers, P. A., & Teranes, J. L. (2001). Sediment organic matter. *Tracking environmental change using lake sediments: physical and geochemical methods*, 239-269.

Michelutti, N., Blais, J. M., Cumming, B. F., Paterson, A. M., Rühland, K., Wolfe, A. P., & Smol, J. P. (2010). Do spectrally inferred determinations of chlorophyll a reflect trends in lake trophic status?. *Journal of Paleolimnology*, *43*, 205-217.

Miller, K. G., Wright, J. D., Browning, J. V., Kulpecz, A., Kominz, M., Naish, T. R., ... & Sosdian, S. (2012). High tide of the warm Pliocene: Implications of global sea level for Antarctic deglaciation. *Geology*, *40*(5), 407-410.

Mischke, S., Aichner, B., Diekmann, B., Herzschuh, U., Plessen, B., Wünnemann, B., & Zhang, C. (2010). Ostracods and stable isotopes of a late glacial and Holocene lake record from the NE Tibetan Plateau. *Chemical Geology*, *276*(1-2), 95-103.

Moazeni, S., & Cerda, A. (2024). The Impacts of Forest Fires on Watershed Hydrological Response. A review. *Trees, Forests and People*, 100707.

Mohammed, W. J., MacDonald, L. A., Wolfe, B. B., & Hall, R. I. (2021). Use of artificial-substrate samplers to identify relations between periphytic diatom community composition and hydro-limnological conditions in shallow lakes of Old Crow Flats, Yukon Territory (Canada). *Hydrobiologia*, *848*(19), 4551-4567.

Monson, R. K., Lipson, D. L., Burns, S. P., Turnipseed, A. A., Delany, A. C., Williams, M. W., & Schmidt, S. K. (2006). Winter forest soil respiration controlled by climate and microbial community composition. *Nature*, *439*(7077), 711-714.

Monteith, D. T., Stoddard, J. L., Evans, C. D., De Wit, H. A., Forsius, M., Høgåsen, T., ... & Vesely, J. (2007). Dissolved organic carbon trends resulting from changes in atmospheric deposition chemistry. *Nature*, *450*(7169), 537-540.

Mormul, R.P., J. Ahlgren, M.K. Ekvall, L.A. Hansson, and C. Brönmark. 2012. Water brownification may increase the invasibility of a submerged non-native macrophyte. *Biological Invasions* 14: 2091–2099.

Moyle, M., & Boyle, J. F. (2021). A method for reconstructing past lake water phosphorus concentrations using sediment geochemical records. *Journal of Paleolimnology*, *65*(4), 461-478.

Mroz, G. D., Jurgensen, M. F., Harvey, A. E., & Larsen, M. J. (1980). Effects of fire on nitrogen in forest floor horizons. *Soil Science Society of America Journal*, *44*(2), 395-400.

Nagy, S. S. (2011). Collecting, cleaning, mounting, and photographing diatoms. In *The diatom world* (pp. 1-18). Dordrecht: Springer Netherlands.

Neelin, J. D., Battisti, D. S., Hirst, A. C., Jin, F. F., Wakata, Y., Yamagata, T., & Zebiak, S. E. (1998). ENSO theory. *Journal of Geophysical Research: Oceans*, *103*(C7), 14261-14290.

Nilsson, M. B., Dåbakk, E., Korsman, T., & Renberg, I. (1996). Quantifying relationships between near-infrared reflectance spectra of lake sediments and water chemistry. *Environmental Science & Technology*, *30*(8), 2586-2590.

Nunes, J. P., Doerr, S. H., Sheridan, G., Neris, J., Santín, C., Emelko, M. B., ... & Keizer, J. (2018). Assessing water contamination risk from vegetation fires: Challenges, opportunities and a framework for progress. *Hydrological Processes*, *32*(5), 687-694.

Obu, J. (2021). How much of the earth's surface is underlain by permafrost?. *Journal of Geophysical Research: Earth Surface*, *126*(5), e2021JF006123.

Ogden, E. L., Cumming, S. G., Smith, S. L., Turetsky, M. R., & Baltzer, J. L. (2023). Permafrost thaw induces short-term increase in vegetation productivity in northwestern Canada. *Global Change Biology*, *29*(18), 5352-5366.

Oksanen J, Simpson G, Blanchet F, Kindt R, Legendre P, Minchin P, O'Hara R, Solymos P, Stevens M, Szoecs E, Wagner H, Barbour M, Bedward M, Bolker B, Borcard D, Carvalho G, Chirico M, De Caceres M, Durand S, Evangelista H, FitzJohn R, Friendly M, Furneaux B, Hannigan G, Hill M, Lahti L, McGlinn D, Ouellette M, Ribeiro Cunha E, Smith T, Stier A, Ter Braak C, Weedon J (2024). _vegan: Community Ecology Package_. R package version 2.6-6.1, <https://CRAN.R-project.org/package=vegan>.

Olefeldt, D., Devito, K. J., & Turetsky, M. R. (2013). Sources and fate of terrestrial dissolved organic carbon in lakes of a Boreal Plains region recently affected by wildfire. *Biogeosciences*, *10*(10), 6247-6265.

Olefeldt, D., Heffernan, L., Jones, M. C., Sannel, A. B. K., Treat, C. C., & Turetsky, M. R. (2021). Permafrost thaw in northern peatlands: rapid changes in ecosystem and landscape functions. *Ecosystem collapse and climate change*, 27-67.

O'Neill, H. B., Wolfe, S. A., & Duchesne, C. (2019). New ground ice maps for Canada using a paleogeographic modelling approach. *The cryosphere*, *13*(3), 753-773.

Oni, S. K., Futter, M. N., Bishop, K., Köhler, S. J., Ottosson-Löfvenius, M., & Laudon, H. (2013). Long-term patterns in dissolved organic carbon, major elements and trace metals in boreal headwater catchments: trends, mechanisms and heterogeneity. *Biogeosciences*, *10*(4), 2315-2330.

Osterkamp TE (2007) Characteristics of the recent warming of permafrost in Alaska. Journal of Geophysical Research – Earth Surface, 112, F02S02. DOI: 10.1029/ 2006JF000578.

Pan, Y., Birdsey, R.A., Phillips, O.L. *et al.* The enduring world forest carbon sink. *Nature* 631, 563–569 (2024). https://doi.org/10.1038/s41586-024-07602-x

Park, J., Moon, M., Green, T., Kang, M., Cho, S., Lim, J., & Kim, S. J. (2024). Impact of tree species composition on fire resistance in temperate forest stands. *Forest Ecology and Management*, *572*, 122279.

Patterson, W.P., Smith, G.R. (2001). Fish. In: Smol, J.P., Birks, H.J.B., Last, W.M. (eds) Tracking Environmental Change Using Lake Sediments. Developments in Paleoenvironmental Research, vol 4. Springer, Dordrecht. https://doi.org/10.1007/0-306-47671-1_9

Paul, M. J., LeDuc, S. D., Lassiter, M. G., Moorhead, L. C., Noyes, P. D., & Leibowitz, S. G. (2022). Wildfire induces changes in receiving waters: A review with considerations for water quality management. *Water Resources Research*, *58*(9), e2021WR030699.

Payette, S., Couillard, P. L., Frégeau, M., Laflamme, J., & Lavoie, M. (2022). The velocity of postglacial migration of fire-adapted boreal tree species in eastern North America. *Proceedings of the National Academy of Sciences*, *119*(43), e2210496119.

Peet, R. K. (1974). The measurement of species diversity. *Annual review of ecology and systematics*, 285-307.

Pellegrini, A. F., Ahlström, A., Hobbie, S. E., Reich, P. B., Nieradzik, L. P., Staver, A. C., ... & Jackson, R. B. (2018). Fire frequency drives decadal changes in soil carbon and nitrogen and ecosystem productivity. *Nature*, *553*(7687), 194-198.

Pelletier, N., Chételat, J., Blarquez, O., & Vermaire, J. C. (2020). Paleolimnological assessment of wildfire-derived atmospheric deposition of trace metal (loid) s and major ions to subarctic lakes (Northwest Territories, Canada). *Journal of Geophysical Research: Biogeosciences*, *125*(8), e2020JG005720.

Pelletier, N., Talbot, J., Olefeldt, D., Turetsky, M., Blodau, C., Sonnentag, O., & Quinton, W. L. (2017). Influence of Holocene permafrost aggradation and thaw on the paleoecology and carbon storage of a peatland complex in northwestern Canada. *The Holocene*, *27*(9), 1391-1405.

Perkins, M. J., McDonald, R. A., van Veen, F. F., Kelly, S. D., Rees, G., & Bearhop, S. (2014). Application of nitrogen and carbon stable isotopes (δ15N and δ13C) to quantify food chain length and trophic structure. *PloS one*, *9*(3), e93281.

Permafrost Subcommittee: 1988, Glossary of permafrost and related ground-ice terms, Associate Committee on Geotechnical Research, National Research Council of Canada, Ottawa, Technical Memorandum No. 142, 156 pp.

Peros, M. C., & Gajewski, K. (2009). Pollen-based reconstructions of late Holocene climate from the central and western Canadian Arctic. *Journal of Paleolimnology*, *41*(1), 161-175.

Perovich, D. K., Light, B., Eicken, H., Jones, K. F., Runciman, K., & Nghiem, S. V. (2007). Increasing solar heating of the Arctic Ocean and adjacent seas, 1979–2005: Attribution and role in the ice-albedo feedback. *Geophysical Research Letters*, *34*(19).

Peszek, Ł., Zgrundo, A., Noga, T., Kochman-Kędziora, N., Poradowska, A., Rybak, M., ... & Lee, J. (2021). The influence of drought on diatom assemblages in a temperate climate zone: A case study from the Carpathian Mountains, Poland. *Ecological Indicators*, *125*, 107579.

Peter, S., Isidorova, A., & Sobek, S. (2016). Enhanced carbon loss from anoxic lake sediment through diffusion of dissolved organic carbon. *Journal of Geophysical Research: Biogeosciences*, *121*(7), 1959-1977.

Philippsen, B. The freshwater reservoir effect in radiocarbon dating. *herit sci* **1**, 24 (2013). https://doi.org/10.1186/2050-7445-1-24

Piao, S., Zhang, X., Chen, A., Liu, Q., Lian, X., Wang, X., ... & Wu, X. (2019). The impacts of climate extremes on the terrestrial carbon cycle: A review. *Science China Earth Sciences*, *62*(10), 1551-1563.

Pielou, E.C. (1966). The measurement of diversity in different types of biological collections. *Journal of Theoretical Biology, 13*, pp. 131–144. doi:10.1016/0022-5193(66)90013-0.

Pilla, R. M., Williamson, C. E., Zhang, J., Smyth, R. L., Lenters, J. D., Brentrup, J. A., ... & Fisher, T. J. (2018). Browning-related decreases in water transparency lead to long-term increases in surface water temperature and thermal stratification in two small lakes. *Journal of Geophysical Research: Biogeosciences*, *123*(5), 1651-1665.

Pithan, F., & Mauritsen, T. (2014). *Arctic amplification dominated by temperature feedbacks in contemporary climate models, Nat. Geosci., 7, 181–184*.

Popović, Z., Bojović, S., Marković, M., & Cerdà, A. (2021). Tree species flammability based on plant traits: A synthesis. *Science of the Total Environment*, *800*, 149625.

Posit team (2023). RStudio: Integrated Development Environment for R. Posit Software, PBC, Boston, MA. URL http://www.posit.co/.

Post, E., Alley, R. B., Christensen, T. R., Macias-Fauria, M., Forbes, B. C., Gooseff, M. N., ... & Wang, M. (2019). The polar regions in a 2 C warmer world. *Science advances*, *5*(12), eaaw9883.

Potapov, P., Hansen, M. C., Laestadius, L., Turubanova, S., Yaroshenko, A., Thies, C., ... & Esipova, E. (2017). The last frontiers of wilderness: Tracking loss of intact forest landscapes from 2000 to 2013. *Science advances*, *3*(1), e1600821.

Poulíčková, A., Špačková, J., Kelly, M.G. *et al.* Ecological variation within *Sellaphora* species complexes (Bacillariophyceae): specialists or generalists?. *Hydrobiologia* **614**, 373–386 (2008). https://doi.org/10.1007/s10750-008-9521-y

Preston, C. M., & Schmidt, M. W. (2006). Black (pyrogenic) carbon: a synthesis of current knowledge and uncertainties with special consideration of boreal regions. *Biogeosciences*, *3*(4), 397-420.

Price, D. T., Alfaro, R. I., Brown, K. J., Flannigan, M. D., Fleming, R. A., Hogg, E. H., ... & Venier, L. A. (2013). Anticipating the consequences of climate change for Canada's boreal forest ecosystems. *Environmental Reviews*, *21*(4), 322-365.

Pugh, E. A., Olefeldt, D., Leader, S. N., Hokanson, K. J., & Devito, K. J. (2021). Characteristics of dissolved organic carbon in Boreal Lakes: high spatial and inter-annual variability controlled by landscape attributes and wet-dry periods. *Water Resources Research*, *57*(11), e2021WR030021.

Qu, Q., Xu, H., Xu, L., You, C., Tan, B., Li, H., ... & Wang, M. (2025). Forest thinning effects on soil carbon stocks and dynamics: Perspective of soil organic carbon sequestration rates. *CATENA*, *250*, 108759.

Quinton, W. L., Hayashi, M., & Chasmer, L. E. (2009). Peatland hydrology of discontinuous permafrost in the Northwest Territories: overview and synthesis. *Canadian Water Resources Journal*, *34*(4), 311-328.

Quinton, W., Berg, A., Braverman, M., Carpino, O., Chasmer, L., Connon, R., ... & Sonnentag, O. (2018). A synthesis of three decades of eco-hydrological research at Scotty Creek, NWT, Canada. *Hydrology and Earth System Sciences Discussions*, *2018*, 1-36.

R Core Team (2024). _R: A Language and Environment for Statistical Computing_. R Foundation for Statistical Computing, Vienna, Austria. <https://www.R-project.org/>.

Räike, A., Taskinen, A., Härkönen, L. H., Kortelainen, P., & Lepistö, A. (2024). Browning from headwaters to coastal areas in the boreal region: Trends and drivers. *Science of the Total Environment*, *927*, 171959.

Randsalu-Wendrup, L., Conley, D. J., Carstensen, J., & Fritz, S. C. (2016). Paleolimnological records of regime shifts in lakes in response to climate change and anthropogenic activities. *Journal of Paleolimnology 56*, 1 – 14

Rankinen, K., Junttila, V., Futter, M., Cano Bernal, J. E., Butterfield, D., & Holmberg, M. (2023). Quantification of the effect of environmental changes on the brownification of Lake Kukkia in southern Finland. *Ambio*, *52*(11), 1834-1846.

Rantanen, M., Karpechko, A.Y., Lipponen, A. *et al.* The Arctic has warmed nearly four times faster than the globe since 1979. *Commun Earth Environ* 3, 168 (2022). https://doi.org/10.1038/s43247-022-00498-3

Redden, D., Trueman, B. F., Dunnington, D. W., Anderson, L. E., & Gagnon, G. A. (2021). Chemical recovery and browning of Nova Scotia surface waters in response to declining acid deposition. *Environmental Science: Processes & Impacts*, *23*(3), 446-456.

Reid, K.A., Day, N.J., Alfaro-Sánchez, R. *et al.* Black spruce (*Picea mariana*) seed availability and viability in boreal forests after large wildfires. *Annals of Forest Science* 80, 4 (2023). https://doi.org/10.1186/s13595-022-01166-4

Reinthal, P. N., Cohen, A. S., & Dettman, D. L. (2011). Fish fossils as paleo-indicators of ichthyofauna composition and climatic change in Lake Malawi, Africa. *Palaeogeography, Palaeoclimatology, Palaeoecology*, *303*(1-4), 126-132.

Renaudin, M., Laforest-Lapointe, I., & Bellenger, J. P. (2022). Unraveling global and diazotrophic bacteriomes of boreal forest floor feather mosses and their environmental drivers at the ecosystem and at the plant scale in North America. *Science of The Total Environment*, *837*, 155761.

Ritson, J. P., Graham, N. J. D., Templeton, M. R., Clark, J. M., Gough, R., & Freeman, C. (2014). The impact of climate change on the treatability of dissolved organic matter (DOM) in upland water supplies: A UK perspective. *Science of the Total Environment*, *473*, 714-730.

Hoffman, R. S. (1958). The meaning of the word" taiga.". *Ecology*, *39*(3), 540–541. https://doi.org/10.2307/1931768

Robertson, C., Pelletier, N., Smol, J.P. *et al.* Chironomid-based paleotemperature reconstruction of the North Slave Region (Northwest Territories, Canada) during the Late Holocene. *J Paleolimnol* (2025). https://doi.org/10.1007/s10933-025-00364-0

Robinson, C. H. (2001). Cold adaptation in Arctic and Antarctic fungi. *New phytologist*, *151*(2), 341-353.

Rodriguez-Cardona, B. M., Coble, A. A., Wymore, A. S., Kolosov, R., Podgorski, D. C., Zito, P., ... & McDowell, W. H. (2020). Wildfires lead to decreased carbon and increased nitrogen concentrations in upland arctic streams. *Scientific Reports*, *10*(1), 8722.

Rodríguez-Cardona, B. M., Houle, D., Couture, S., Lapierre, J. F., & del Giorgio, P. A. (2023). Long-term trends in carbon and color signal uneven browning and terrestrialization of northern lakes. *Communications Earth & Environment*, *4*(1), 338.

Rose, N. (2002). Fly-Ash Particles. In: Last, W.M., Smol, J.P. (eds) Tracking Environmental Change Using Lake Sediments. Developments in Paleoenvironmental Research, vol 2. Springer, Dordrecht. https://doi.org/10.1007/0-306-47670-3_12

Roseacute;n, P., Hall, R., Korsman, T., & Renberg, I. (2000). Diatom transfer-functions for quantifying past air temperature, pH and total organic carbon concentration from lakes in northern Sweden. *Journal of Paleolimnology*, *24*(2), 109-123.

Rosén, P. (2005). Total organic carbon (TOC) of lake water during the Holocene inferred from lake sediments and near-infrared spectroscopy (NIRS) in eight lakes from northern Sweden. *Biogeochemistry*, *76*, 503-516.

Rosén, P., Cunningham, L., Vonk, J., and Karlsson, J. (2009). Effects of climate on organic carbon and the ratio of planktonic to benthic primary producers in a subarctic lake during the past 45 years. *Limnol. Oceanogr.* 54, 1723–1732. doi: 10.4319/lo.2009.54.5.1723

Rouillard, A., Rosén, P., Douglas, M. S., Pienitz, R., & Smol, J. P. (2011). A model for inferring dissolved organic carbon (DOC) in lakewater from visible-near-infrared spectroscopy (VNIRS) measures in lake sediment. *Journal of Paleolimnology*, *46*, 187-202.

Round, F.E., Crawford, R.M. and Mann, D.G. (1990) The Diatoms. Biology and Morphology of the Genera. *Cambridge University Press, Cambridge, 747 pp.*

Rühland, K. M., Paterson, A. M., & Smol, J. P. (2015). Lake diatom responses to warming: reviewing the evidence. *Journal of paleolimnology*, *54*(1), 1-35.

Rühland, K., & Smol, J. P. (2005). Diatom shifts as evidence for recent Subarctic warming in a remote tundra lake, NWT, Canada. *Palaeogeography, Palaeoclimatology, Palaeoecology, 226*(1-2), 1-16.

Rühland, K., Paterson, A. M., & Smol, J. P. (2008). Hemispheric-scale patterns of climate-related shifts in planktonic diatoms from North American and European lakes. Global Change Biology, 14(11), 2740-2754.

Rühland, K., Priesnitz, A., & Smol, J. P. (2003). Paleolimnological evidence from diatoms for recent environmental changes in 50 lakes across Canadian Arctic treeline. *Arctic, antarctic, and alpine research*, *35*(1), 110-123.

Ryan, K. A., Adler, T., Chalmers, A. T., Perdrial, J., Sebestyen, S., Shanley, J. B., & Stubbins, A. (2023). Optical properties of dissolved organic matter in throughfall and stemflow vary across tree species and season in a temperate headwater forest. *Biogeochemistry*, *164*(1), 53-72.

Rybak, M., Kochman-Kędziora, N., & Pęczuła, W. (2020). Diversity of the Rhopalodiaceae Diatoms (Bacillariophyta) on Macrophytes of Different Architecture in Small and Shallow Oxbow Lakes (SE Poland). *Journal of Ecological Engineering*, *21*(5), 164-173.

Rydberg, J., Klaminder, J., Rosén, P., & Bindler, R. (2010). Climate driven release of carbon and mercury from permafrost mires increases mercury loading to sub-arctic lakes. Science of The Total Environment, 408(20), 4778-4783. doi:10.1016/j.scitotenv.2010.06.056.

Saha, J., Price, C., Plotnik, T., & Guha, A. (2023). Are thunderstorms linked to the rapid Sea ice loss in the Arctic?. *Atmospheric Research*, *294*, 106988.

Sanchez-Cabeza, J. A., & Ruiz-Fernández, A. C. (2012). 210Pb sediment radiochronology: an integrated formulation and classification of dating models. *Geochimica et Cosmochimica Acta*, *82*, 183-200.

Sanchez-Garcia, C., Santín, C., Neris, J., Sigmund, G., Otero, X. L., Manley, J., ... & Doerr, S. H. (2023). Chemical characteristics of wildfire ash across the globe and their environmental and socio-economic implications. *Environment International*, *178*, 108065.

Sankey, T. T., Tango, L., Tatum, J., & Sankey, J. B. (2024). Forest fire, thinning, and flood in wildland-urban interface: UAV and lidar-based estimate of natural disaster impacts. *Landscape Ecology*, *39*(3), 58.

Santín, C., Doerr, S. H., Preston, C. M., & González-Rodríguez, G. (2015). Pyrogenic organic matter production from wildfires: a missing sink in the global carbon cycle. *Global Change Biology*, *21*(4), 1621-1633.

Sariyildiz, T. (2008). Effects of gap-size classes on long-term litter decomposition rates of beech, oak and chestnut species at high elevations in Northeast Turkey. *Ecosystems*, *11*(6), 841-853.

Saros, J. E., Arp, C. D., Bouchard, F., Comte, J., Couture, R. M., Dean, J. F., ... & Vincent, W. F. (2022). Sentinel responses of Arctic freshwater systems to climate: linkages, evidence, and a roadmap for future research. *Arctic Science*, *9*(2), 356-392.

Saros, J. E., Hazuková, V., Northington, R. M., Huston, G. P., Lamb, A., Birkel, S., ... & McGowan, S. (2025). Abrupt transformation of west Greenland lakes following compound climate extremes associated with atmospheric rivers. *Proceedings of the National Academy of Sciences*, *122*(4), e2413855122.

Saros, J. E., Northington, R. M., Anderson, D. S., & Anderson, N. J. (2016). A whole-lake experiment confirms a small centric diatom species as an indicator of changing lake thermal structure. *Limnology and Oceanography Letters*, *1*(1), 27-35.

Saros, J. E., Stone, J. R., Pederson, G. T., Slemmons, K. E., Spanbauer, T., Schliep, A., ... & Engstrom, D. R. (2012). Climate-induced changes in lake ecosystem structure inferred from coupled neo-and paleoecological approaches. *Ecology*, *93*(10), 2155-2164.

Saunders, C. (2008). Charge separation mechanisms in clouds. *Planetary Atmospheric Electricity*, 335-353.

Sayedi, S. S., Abbott, B. W., Thornton, B. F., Frederick, J. M., Vonk, J. E., Overduin, P., ... & Frei, R. J. (2020). Subsea permafrost carbon stocks and climate change sensitivity estimated by expert assessment. *Environmental Research Letters*, *15*(12), 124075.

Sazonova, T. S., Romanovsky, V. E., Walsh, J. E., & Sergueev, D. O. (2004). Permafrost dynamics in the 20th and 21st centuries along the East Siberian transect. *Journal of Geophysical Research: Atmospheres*, *109*(D1).

Schmid, A. M. M. (1987). Wall morphogenesis in centric diatoms. In *Algal development: molecular and cellular aspects* (pp. 34-41). Berlin, Heidelberg: Springer Berlin Heidelberg.

Scholten, R. C., Jandt, R., Miller, E. A., Rogers, B. M., & Veraverbeke, S. (2021). Overwintering fires in boreal forests. *Nature*, *593*(7859), 399-404.

Seekell, D. A., Lapierre, J. F., Ask, J., Bergström, A. K., Deininger, A., Rodríguez, P., & Karlsson, J. (2015). The influence of dissolved organic carbon on primary production in northern lakes. *Limnology and Oceanography*, *60*(4), 1276-1285.

Sepúlveda-Zúñiga, E. A., Villacís, L. A., Maidana, N. I., Sagredo, E., & Moreno, P. I. (2024). Paleolimnology of Lago Pichilaguna over the past~ 12,600 years based on a fine-resolution diatom record, northwestern Patagonia (41° S). *Quaternary Science Reviews*, *339*, 108835.

Serreze, M. C., & Barry, R. G. (2011). Processes and impacts of Arctic amplification: A research synthesis. *Global and planetary change*, *77*(1-2), 85-96.

Shabbar, A., & Khandekar, M. (1996). The impact of el Nino-Southern oscillation on the temperature field over Canada: Research note. *Atmosphere-Ocean*, *34*(2), 401-416.

Shabbar, A., Bonsal, B., & Khandekar, M. (1997). Canadian precipitation patterns associated with the Southern Oscillation. *Journal of Climate*, *10*(12), 3016-3027.

Shakesby, R. A., & Doerr, S. H. (2006). Wildfire as a hydrological and geomorphological agent. *Earth-Science Reviews*, *74*(3-4), 269-307.

Shannon, C.E. (1948). A mathematical theory of communication. *The Bell System Technical Journal, 27*, pp. 379-423.

Sharpe, M., Hwang, H., Schroeder, D., Ryu, S. R., & Lieffers, V. J. (2017). Prescribed fire as a tool to regenerate live and dead serotinous jack pine (Pinus banksiana) stands. *International Journal of Wildland Fire*, *26*(6), 478-484.

Shen, Y., Tian, D., Hou, J., Wang, J., Zhang, R., Li, Z., ... & Niu, S. (2021). Forest soil acidification consistently reduces litter decomposition irrespective of nutrient availability and litter type. *Functional Ecology*, *35*(12), 2753-2762.

Sherbo, B. A., Tonin, J., Paterson, M. J., Hann, B. J., Kozak, J., & Higgins, S. N. (2023). The effects of terrestrial dissolved organic matter on phytoplankton biomass and productivity in boreal lakes. *Freshwater Biology*, *68*(12), 2109-2119.

Shulski, M., and G. Wendler, 2007: *The Climate of Alaska*. University of Alaska Press, 216 pp.

Simpson G (2024). _gratia: Graceful ggplot-Based Graphics and Other Functions for GAMs Fitted using mgcv_. R package version 0.9.0, <https://gavinsimpson.github.io/gratia/>.

Simpson, E.H. (1949). Measurement of diversity. *Nature, 163*, pp. 688. doi:10.1038/163688a0

Škerlep, M., Nehzati, S., Johansson, U., Kleja, D. B., Persson, P., & Kritzberg, E. S. (2022). Spruce forest afforestation leading to increased Fe mobilization from soils. *Biogeochemistry*, *157*(3), 273-290.

Škerlep, M., Steiner, E., Axelsson, A. L., & Kritzberg, E. S. (2020). Afforestation driving long-term surface water browning. *Global Change Biology*, *26*(3), 1390-1399.

Smith, H. G., Sheridan, G. J., Lane, P. N., Nyman, P., & Haydon, S. (2011). Wildfire effects on water quality in forest catchments: A review with implications for water supply. *Journal of Hydrology*, *396*(1-2), 170-192.

Smith, M. W. (1975). Microclimatic influences on ground temperatures and permafrost distribution, Mackenzie Delta, Northwest Territories. *Canadian Journal of Earth Sciences*, *12*(8), 1421-1438.

Smith, V. H., Tilman, G. D., & Nekola, J. C. (1999). Eutrophication: Impacts of excess nutrient inputs on freshwater, marine, and terrestrial ecosystems. In *Environmental Pollution* (Vol. 100, pp. 179–196). Elsevier Ltd. https://doi.org/10.1016/S0269-7491(99)00091-3

Smol, J. P. (1981). Problems associated with the use of "species diversity" in paleolimnological studies. *Quaternary Research*, *15*(2), 209-212.

Smol, J. P. (2008). *Pollution of lakes and rivers: a paleoenvironmental perspective*. John Wiley & Sons.

Smol, J. P. (2016). Arctic and Sub-Arctic shallow lakes in a multiple-stressor world: a paleoecological perspective. *Hydrobiologia*, *778*, 253-272.

Smol, J. P. (2019). Under the radar: long-term perspectives on ecological changes in lakes. *Proceedings of the Royal Society B*, *286*(1906), 20190834.

Smol, J. P., & Douglas, M. S. (2007). From controversy to consensus: making the case for recent climate change in the Arctic using lake sediments. *Frontiers in Ecology and the Environment*, *5*(9), 466-474.

Smol, J. P., Cumming, B. F., Dixit, A. S., & Dixit, S. S. (1998). Tracking recovery patterns in acidified lakes: a paleolimnological perspective. *Restoration Ecology*, *6*(4), 318-326.

Smol, J. P., Wolfe, A. P., Birks, H. J. B., Douglas, M. S., Jones, V. J., Korhola, A., ... & Weckström, J. (2005). Climate-driven regime shifts in the biological communities of arctic lakes. *Proceedings of the National Academy of Sciences*, *102*(12), 4397-4402.

Smol, J.P., Birks, H.J. and Last, W.M. (2002). Using biology to study long-term environmental change. Smol, J.P., Birks, H.J. & Last, W.M. (2002). *Tracking environmental change using lake sediments: Volume 3: Terrestrial, Algal, and Siliceous Indicators*. (Vol. 3 pp. 1 – 5).

Sobek, S., Tranvik, L. J., Prairie, Y. T., Kortelainen, P., & Cole, J. J. (2007). Patterns and regulation of dissolved organic carbon: An analysis of 7,500 widely distributed lakes. *Limnology and oceanography*, *52*(3), 1208-1219.

Solomon, C. T., Jones, S. E., Weidel, B. C., Buffam, I., Fork, M. L., Karlsson, J., ... & Saros, J. E. (2015). Ecosystem consequences of changing inputs of terrestrial dissolved organic matter to lakes: current knowledge and future challenges. *Ecosystems*, *18*, 376-389.

Souza-Alonso, P., Prats, S.A., Merino, A. *et al.* Fire enhances changes in phosphorus (P) dynamics determining potential post-fire soil recovery in Mediterranean woodlands. *Sci Rep* **14**, 21718 (2024). https://doi.org/10.1038/s41598-024-72361-8

Spaulding SA, Potapova MG, Bishop IW, Lee SS, Gasperak TS, Jovanoska E, Furey PC, Edlund MB. 2021. Diatoms.org: supporting taxonomists, connecting communities. Diatom Res. 36(4):291–304

Spence, C., Norris, M., Bickerton, G., Bonsal, B. R., Brua, R., Culp, J. M., ... & Wolfe, S. A. (2020). The Canadian water resource vulnerability index to permafrost thaw (CWRVIPT). *Arctic Science*, *6*(4), 437-462.

Spencer, R. G., Aiken, G. R., Wickland, K. P., Striegl, R. G., & Hernes, P. J. (2008). Seasonal and spatial variability in dissolved organic matter quantity and composition from the Yukon River basin, Alaska. *Global Biogeochemical Cycles*, *22*(4).

Stager, J. C., Sporn, L. A., Johnson, M., & Regalado, S. (2015). Of paleo-genes and perch: What if an "alien" is actually a native?. *PLoS One*, *10*(3), e0119071.

Statistics Canada (2021). *2021 Census – Boundary Files* [Data set]. Government of Canada. https://www12.statcan.gc.ca/census-recensement/2021/geo/sip-pis/boundary-limites/index2021-eng.cfm?year=21

Štefková, E. (2006). Epilithic diatoms of mountain lakes of the Tatra Mountains (Slovakia). *Biologia*, *61*(18), S101-S108.

Stetler, J. T., Knoll, L. B., Driscoll, C. T., & Rose, K. C. (2021). Lake browning generates a spatiotemporal mismatch between dissolved organic carbon and limiting nutrients. *Limnology and Oceanography Letters*, *6*(4), 182-191.

Stocks, B. J., Mason, J. A., Todd, J. B., Bosch, E. M., Wotton, B. M., Amiro, B. D., ... & Skinner, W. R. (2002). Large forest fires in Canada, 1959–1997. *Journal of Geophysical Research: Atmospheres*, *107*(D1), FFR-5.

Strock, K. E., Theodore, N., Gawley, W. G., Ellsworth, A. C., & Saros, J. E. (2017). Increasing dissolved organic carbon concentrations in northern boreal lakes: Implications for lake water transparency and thermal structure. *Journal of Geophysical Research: Biogeosciences*, *122*(5), 1022-1035.

Strong, W. L., & Roi, G. L. (1983). Root-system morphology of common boreal forest trees in Alberta, Canada. *Canadian Journal of Forest Research*, *13*(6), 1164-1173.

Stuecker, M. F., Bitz, C. M., Armour, K. C., Proistosescu, C., Kang, S. M., Xie, S. P., ... & Jin, F. F. (2018). Polar amplification dominated by local forcing and feedbacks. *Nature Climate Change*, *8*(12), 1076-1081.

Su, W. Q., Tang, C., Lin, J., Yu, M., Dai, Z., Luo, Y., ... & Xu, J. (2022). Recovery patterns of soil bacterial and fungal communities in Chinese boreal forests along a fire chronosequence. *Science of the Total Environment*, *805*, 150372.

Sugisaki, S., Buylaert, J. P., Murray, A. S., Harada, N., Kimoto, K., Okazaki, Y., ... & Nogi, Y. (2012). High resolution optically stimulated luminescence dating of a sediment core from the southwestern Sea of Okhotsk. *Geochemistry, Geophysics, Geosystems*, *13*(5).

Sutheimer, C. M., Meunier, J., Hotchkiss, S. C., Rebitzke, E., & Radeloff, V. C. (2021). Historical fire regimes of North American hemiboreal peatlands. *Forest Ecology and Management*, *498*, 119561.

Taipale, S. J., Kahilainen, K. K., Holtgrieve, G. W., & Peltomaa, E. T. (2018). Simulated eutrophication and browning alters zooplankton nutritional quality and determines juvenile fish growth and survival. *Ecology and Evolution*, *8*(5), 2671-2687.

Taipale, S. J., Vuorio, K., Strandberg, U., Kahilainen, K. K., Järvinen, M., Hiltunen, M., ... & Kankaala, P. (2016). Lake eutrophication and brownification downgrade availability and transfer of essential fatty acids for human consumption. *Environment International*, *96*, 156-166.

Takahashi, K., & Martínez, A. G. (2019). The very strong coastal El Niño in 1925 in the far-eastern Pacific. *Climate Dynamics*, *52*(12), 7389-7415.

Taylor, J., Fay, M., Williams, R. L., Wilbur, S. B., McClure, P. R., Zaccaria, K., ... & Citra, M. J. (2017). Toxicological profile for toluene.

Taylor, W. G. (1998). *Effect of El Nino Southern Oscillation (ENSO) on British Columbia and Yukon winter weather*. Aquatic and Atmospheric Science Division, Pacific and Yukon Region, Environment Canada.

Terrier, A., Girardin, M. P., Périé, C., Legendre, P., & Bergeron, Y. (2013). Potential changes in forest composition could reduce impacts of climate change on boreal wildfires. *Ecological Applications*, *23*(1), 21-35.

Thieme, L., Graeber, D., Hofmann, D., Bischoff, S., Schwarz, M. T., Steffen, B., ... & Siemens, J. (2019). Dissolved organic matter characteristics of deciduous and coniferous forests with variable management: different at the source, aligned in the soil. *Biogeosciences*, *16*(7), 1411-1432.

Thienpont, J. R., O'Hagan, C., Kokelj, S. V., Hoskin, G. N., Pisaric, M. F., Smol, J. P., ... & Korosi, J. B. (2025). A Framework for Understanding the Impacts of Thaw-Driven Disturbance Regimes on Northern Lakes. *Permafrost and Periglacial Processes*, *36*(1), 137-150.

Thienpont, J. R., Ruehland, K. M., Pisaric, M. F., Kokelj, S. V., Kimpe, L. E., Blais, J. M., & Smol, J. P. (2013). Biological responses to permafrost thaw slumping in Canadian Arctic lakes. *Freshwater Biology*, *58*(2), 337-353.

Thrane, J. E., Hessen, D. O., & Andersen, T. (2014). The absorption of light in lakes: negative impact of dissolved organic carbon on primary productivity. *Ecosystems*, *17*(6), 1040-1052.

Tichá, A., Vondrák, D., Moravcová, A., Chiverrell, R., & Kuneš, P. (2023). Climate-related soil saturation and peatland development may have conditioned surface water brownification at a central European lake for millennia. *Science of The Total Environment*, *858*, 159982.

Ting, M., Kushnir, Y., Seager, R., & Li, C. (2009). Forced and internal twentieth-century SST trends in the North Atlantic. *Journal of Climate*, *22*(6), 1469-1481.

Tiwari, T., Sponseller, R.A. & Laudon, H. The emerging role of drought as a regulator of dissolved organic carbon in boreal landscapes. *Nat Commun* **13**, 5125 (2022). https://doi.org/10.1038/s41467-022-32839-3

Tranvik, L. J., Downing, J. A., Cotner, J. B., Loiselle, S. A., Striegl, R. G., Ballatore, T. J., ... & Weyhenmeyer, G. A. (2009). Lakes and reservoirs as regulators of carbon cycling and climate. *Limnology and oceanography*, *54*(6part2), 2298-2314.

Treat, C. C., & Jones, M. C. (2018). Near-surface permafrost aggradation in Northern Hemisphere peatlands shows regional and global trends during the past 6000 years. *The Holocene*, *28*(6), 998-1010.

Treat, C. C., Jones, M. C., Camill, P., Gallego-Sala, A., Garneau, M., Harden, J. W., ... & Väliranta, M. (2016). Effects of permafrost aggradation on peat properties as determined from a pan-Arctic synthesis of plant macrofossils. *Journal of Geophysical Research: Biogeosciences*, *121*(1), 78-94.

Tsuyuzaki, S., Narita, K., Sawada, Y., & Kushida, K. (2014). The establishment patterns of tree seedlings are determined immediately after wildfire in a black spruce (Picea mariana) forest. *Plant ecology*, *215*, 327-337.

Turetsky, M. R., Abbott, B. W., Jones, M. C., Anthony, K. W., Olefeldt, D., Schuur, E. A., ... & McGuire, A. D. (2020). Carbon release through abrupt permafrost thaw. *Nature Geoscience*, *13*(2), 138-143.

Turetsky, M. R., Bond-Lamberty, B., Euskirchen, E., Talbot, J., Frolking, S., McGuire, A. D., & Tuittila, E. S. (2012). The resilience and functional role of moss in boreal and arctic ecosystems. *New Phytologist*, *196*(1), 49-67.

Turetsky, M. R., Kane, E. S., Harden, J. W., Ottmar, R. D., Manies, K. L., Hoy, E., & Kasischke, E. S. (2011). Recent acceleration of biomass burning and carbon losses in Alaskan forests and peatlands. *Nature Geoscience*, *4*(1), 27–31. https://doi.org/10.1038/ngeo1027

Turunen, J., & Aroviita, J. (2024). Influence of water color and catchment lake cover on stream macroinvertebrate communities: Ecological insights into browning effects. *Water Research*, *250*, 121048.

Vaikutienė, G., Skipitytė, R., Mažeika, J., Martma, T., Garbaras, A., Barisevičiūtė, R., & Remeikis, V. (2017). Environmental changes induced by human activities in the Northern

Curonian Lagoon (Eastern Baltic): diatoms and stable isotope data. *Estonian journal of earth sciences.*, *66*(2), 93-108.

Van de Vijver, B., Peeters, V., Hansen, I., Ballings, P., & de Haan, M. (2024). Five new species in the genus Staurosirella (Bacillariophyta) from European freshwater habitats. *PhytoKeys*, *242*, 139.

Vance, D. E., & Vance, J. E. (1985). Biochemistry of lipids and membranes. *(No Title)*.

Varotsos, C. A., Franzke, C. L., Efstathiou, M. N., & Degermendzhi, A. G. (2014). Evidence for two abrupt warming events of SST in the last century. *Theoretical and Applied Climatology*, *116*(1), 51-60.

Velez MI, Salgado J, Brenner M, Hooghiemstra H, Escobar J, Boom A, Bird B, Curtis JH, Temoltzin-Loranca Y, Patino LF, Gonzalez-Arango C. 2021. Novel responses of diatoms in neotropical mountain lakes to indigenous and post-European occupation. Anthropocene. 34:1–13.

Veraverbeke, S., Rogers, B. M., Goulden, M. L., Jandt, R. R., Miller, C. E., Wiggins, E. B., & Randerson, J. T. (2017). Lightning as a major driver of recent large fire years in North American boreal forests. *Nature Climate Change*, *7*(7), 529-534.

Viereck, L. A. (1975). Forest ecology of the Alaska taiga.

Viereck, L. A., Werdin-Pfisterer, N. R., Adams, P. C., & Yoshikawa, K. (2008). Effect of wildfire and fireline construction on the annual depth of thaw in a black spruce permafrost forest in interior Alaska: a 36-year record of recovery. In *In: Kane, Douglas L.; Hinkel, Kenneth*

M., eds. Proceedings of the Ninth International Conference on Permafrost; June 29-July 3, 2008; Fairbanks, AK: 1845-1850..

Vitt, D. H., Halsey, L. A., & Zoltai, S. C. (1994). The bog landforms of continental western Canada in relation to climate and permafrost patterns. *Arctic and Alpine Research*, *26*(1), 1-13.

Vitt, D. H., Halsey, L. A., & Zoltai, S. C. (2000). The changing landscape of Canada's western boreal forest: the current dynamics of permafrost. Canadian Journal of Forest Research, 30(2), 283-287

Vonk, J. E., Tank, S. E., Bowden, W. B., Laurion, I., Vincent, W. F., Alekseychik, P., ... & Wickland, K. P. (2015). Reviews and syntheses: Effects of permafrost thaw on Arctic aquatic ecosystems. *Biogeosciences*, *12*(23), 7129-7167.

Vonk, J. E., Tank, S. E., & Walvoord, M. A. (2019). Integrating hydrology and biogeochemistry across frozen landscapes. *Nature Communications*, *10*(1), 5377.

Walker, I. R. (2001). Midges: Chironomidae and related diptera. *Tracking Environmental Change Using Lake Sediments: Volume 4: Zoological Indicators*, 43-66.

Walker, X. J., Baltzer, J. L., Bourgeau-Chavez, L., Day, N. J., Dieleman, C. M., Johnstone, J. F., ... & Mack, M. C. (2020). Patterns of ecosystem structure and wildfire carbon combustion across six ecoregions of the North American boreal forest. *Frontiers in Forests and Global Change*, *3*, 87.

Walker, X. J., Rogers, B. M., Baltzer, J. L., Cumming, S. G., Day, N. J., Goetz, S. J., ... & Mack, M. C. (2018). Cross-scale controls on carbon emissions from boreal forest megafires. *Global Change Biology*, *24*(9), 4251-4265.

Wallace, M. B., Wax, A., Roberts, D. N., & Graf, R. N. (2009). Reflectance spectroscopy. *Gastrointestinal endoscopy clinics of North America*, *19*(2), 233-242.

Wällstedt, T., Björkvald, L., & Gustafsson, J. P. (2010). Increasing concentrations of arsenic and vanadium in (southern) Swedish streams. *Applied Geochemistry*, *25*(8), 1162-1175.

Walsh, J. E. (2014). Intensified warming of the Arctic: Causes and impacts on middle latitudes. *Global and Planetary Change*, *117*, 52-63.

Wang, C., Wang, H., Kuang, X., & Guo, G. (2021). Life stages and morphological variations of Limnocythere inopinata (Crustacea, Ostracoda) from Lake Jiang-Co (northern Tibet): a bioculture experiment. *ZooKeys*, *1011*, 25.

Wang, D., Zang, S., Wu, X., Ma, D., Li, M., Chen, Q., ... & Zhang, N. (2021). Soil organic carbon stabilization in permafrost peatlands. *Saudi Journal of Biological Sciences*, *28*(12), 7037-7045.

Wang, X., Thompson, D. K., Marshall, G. A., Tymstra, C., Carr, R., & Flannigan, M. D. (2015). Increasing frequency of extreme fire weather in Canada with climate change. *Climatic Change*, *130*, 573-586.

Wang, Y., Hogg, E. H., Price, D. T., Edwards, J., & Williamson, T. (2014). Past and projected future changes in moisture conditions in the Canadian boreal forest. *The Forestry Chronicle*, *90*(5), 678-691.

Wang, Y., Liu, S., Wang, J., Yao, Y., Chen, Y., Xu, Q., ... & Chen, N. (2022). Diatom biodiversity and speciation revealed by comparative analysis of mitochondrial genomes. *Frontiers in plant science*, *13*, 749982.

Wang, Z., Wang, Z., Zou, Z. *et al.* Severe Global Environmental Issues Caused by Canada's Record-Breaking Wildfires in 2023. *Adv. Atmos. Sci.* 41, 565–571 (2024). https://doi.org/10.1007/s00376-023-3241-0

Watson, V. T., & Medeiros, A. S. (2021). The value of paleolimnology in reconstructing and managing ecosystem vulnerability: a systematic map. *Facets*, *6*(1), 517-536.

Watts, A.C., Kobziar, L.N. Smoldering Combustion and Ground Fires: Ecological Effects and Multi-Scale Significance. *fire ecol* **9**, 124–132 (2013). https://doi.org/10.4996/fireecology.0901124

Wauthy, M., Rautio, M., Christoffersen, K. S., Forsström, L., Laurion, I., Mariash, H. L., ... & Vincent, W. F. (2018). Increasing dominance of terrigenous organic matter in circumpolar freshwaters due to permafrost thaw. *Limnology and Oceanography Letters*, *3*(3), 186-198.

Weckström, K., Weckström, J., Wischnewski, J., Davidson, T. A., Lauridsen, T. L., Landkildehus, F., ... & Jeppesen, E. (2023). Unlocking environmental archives in the Arctic—insights from modern diatom-environment relationships in lakes and ponds across Greenland. *Frontiers in Ecology and Evolution*, *11*, 1177638.

Wei, X., Hayes, D. J., & Fernandez, I. (2021). Fire reduces riverine DOC concentration draining a watershed and alters post-fire DOC recovery patterns. *Environmental Research Letters*, *16*(2), 024022.

Weir, J. M. H., Johnson, E. A., & Miyanishi, K. (2000). Fire frequency and the spatial age mosaic of the mixed-wood boreal forest in western Canada. *Ecological Applications*, *10*(4), 1162-1177.

Weyhenmeyer, G. A., Prairie, Y. T., & Tranvik, L. J. (2014). Browning of boreal freshwaters coupled to carbon-iron interactions along the aquatic continuum. *PloS one*, *9*(2), e88104.

Whitman, T., Whitman, E., Woolet, J., Flannigan, M. D., Thompson, D. K., & Parisien, M. A. (2019). Soil bacterial and fungal response to wildfires in the Canadian boreal forest across a burn severity gradient. *Soil Biology and Biochemistry*, *138*, 107571.

Wickham H, François R, Henry L, Müller K, Vaughan D (2023). _dplyr: A Grammar of Data Manipulation_. R package version 1.1.4, <https://CRAN.R-project.org/package=dplyr>.

Wickham, H. ggplot2: Elegant Graphics for Data Analysis. Springer-Verlag New York, 2016.

Wik, M., & Renberg, I. (1996). Environmental records of carbonaceous fly-ash particles from fossil-fuel combustion: A summary. *Journal of Paleolimnology*, *15*, 193-206.

Wilkenskjeld, S., Miesner, F., Overduin, P. P., Puglini, M., & Brovkin, V. (2021). Strong Increase of Thawing of Subsea Permafrost in the 22nd Century Caused by Anthropogenic Climate Change. *The Cryosphere Discussions*, *2021*, 1-18.

Wilkinson, S. L., Moore, P. A., & Waddington, J. M. (2019). Assessing drivers of cross-scale variability in peat smoldering combustion vulnerability in forested boreal peatlands. *Frontiers in Forests and Global Change*, *2*, 84.

Williams, J. W., Blois, J. L., & Shuman, B. N. (2011). Extrinsic and intrinsic forcing of abrupt ecological change: case studies from the late Quaternary. *Journal of Ecology*, *99*(3), 664-677.

Williams, J. W., Shuman, B. N., Webb III, T., Bartlein, P. J., & Leduc, P. L. (2004). Late-Quaternary vegetation dynamics in North America: scaling from taxa to biomes. *Ecological Monographs*, *74*(2), 309-334.

Williamson, C. E., Overholt, E. P., Pilla, R. M., Leach, T. H., Brentrup, J. A., Knoll, L. B., ... & Moeller, R. E. (2015). Ecological consequences of long-term browning in lakes. *Scientific reports*, *5*(1), 18666.

Williamson, C. E., Saros, J. E., Vincent, W. F., & Smol, J. P. (2009). Lakes and reservoirs as sentinels, integrators, and regulators of climate change. *Limnology and oceanography*, *54*(6part2), 2273-2282.

Williamson, C., Overholt, E., Pilla, R. *et al.* Ecological consequences of long-term browning in lakes. *Sci Rep* 5, 18666 (2016). https://doi.org/10.1038/srep18666

Wolf, K. D., Higuera, P. E., Davis, K. T., & Dobrowski, S. Z. (2021). Wildfire impacts on forest microclimate vary with biophysical context. *Ecosphere*, *12*(5), e03467.

Wood, S. N. (2017). *Generalized additive models: an introduction with R*. chapman and hall/CRC. doi:10.1201/9781315370279.

Wright, N., Hayashi, M., & Quinton, W. L. (2009). Spatial and temporal variations in active layer thawing and their implication on runoff generation in peat-covered permafrost terrain. *Water Resources Research*, *45*(5).

Wright, S. N., Thompson, L. M., Olefeldt, D., Connon, R. F., Carpino, O. A., Beel, C. R., & Quinton, W. L. (2022). Thaw-induced impacts on land and water in discontinuous permafrost: A review of the Taiga Plains and Taiga Shield, northwestern Canada. *Earth-Science Reviews*, *232*, 104104.

Xing, Y., Cheng, L., Zheng, L., Wu, H., Tan, Q., Wang, X., & Tian, Q. (2024). Brownification increases the abundance of microorganisms related to carbon and nitrogen cycling in shallow lakes. *Environmental Research*, *257*, 119243.

Yang, X. Y., Fyfe, J. C., & Flato, G. M. (2010). The role of poleward energy transport in Arctic temperature evolution. *Geophysical Research Letters*, *37*(14).

Yoshikawa, K., Bolton, W. R., Romanovsky, V. E., Fukuda, M., & Hinzman, L. D. (2003). Impacts of wildfire on the permafrost in the boreal forests of Interior Alaska (DOI 10.1029/2001JD000438). *JOURNAL OF GEOPHYSICAL RESEARCH-ALL SERIES-*, *108*(1; SECT 4), FFR-4.

Zastruzny, S. F., Ingeman-Nielsen, T., Zhang, W., & Elberling, B. (2023). Accelerated permafrost thaw and increased drainage in the active layer: Responses from experimental surface alteration. *Cold Regions Science and Technology*, *212*, 103899.

Zepernick, B. N., Chase, E. E., Denison, E. R., Gilbert, N. E., Truchon, A. R., Frenken, T., ... & Wilhelm, S. W. (2024). Declines in ice cover are accompanied by light limitation responses and community change in freshwater diatoms. *The ISME Journal*, *18*(1), wrad015.

Zhao, Y. (2024). New insight into and characterization of DOC, DON and CDOM for urban waters in the lower reaches of the Yellow River, China. *Science of the Total Environment*, *914*, 169828.

Zibulski, R., Herzschuh, U., Pestryakova, L. A., Wolter, J., Müller, S., Schilling, N., ... & Tian, F. (2013). River flooding as a driver of polygon dynamics: modern vegetation data and a millennial peat record from the Anabar River lowlands (Arctic Siberia). *Biogeosciences*, *10*(8), 5703-5728.

Zoltai, S. C. (1993). Cyclic development of permafrost in the peatlands of northwestern Alberta, Canada. *Arctic and Alpine Research*, *25*(3), 240-246.

Zoltai, S. C., & Tarnocai, C. (1975). Perennially frozen peatlands in the western Arctic and Subarctic of Canada. *Canadian Journal of Earth Sciences*, *12*(1), 28-43.